

Scott Polar Research Institute
University of Cambridge



**UNIVERSITY OF
CAMBRIDGE**



i

“Marine-terminating outlet glacier response to hydrological mechanisms:

A comparative study at Store Glestcher and Rink Isbrae, Uummannaq Bay, West Greenland”

Helena Nathan-King

Newnham College

Dr. Poul Christoffersen

MPhil Polar Studies

June 2015

19999 words

This dissertation is submitted for the degree of Master of Philosophy



Declaration of Originality

I declare that this thesis is entirely my own work, and includes nothing that is the outcome of work done in collaboration with others, except where clearly acknowledged in the text or Acknowledgements. It has not been submitted in whole or in part for a degree at this or any other University. This thesis does not exceed 20,000 words, excluding Figures and their captions, Tables and their captions, Cover Page, Declaration, Acknowledgements, References, and Lists of Contents, Figures, Tables, and Mathematical Notation.

Helena Nathan-King

June 2015

Abstract

The dynamics of marine-terminating outlet glaciers on the Greenland Ice Sheet are of crucial importance with their principal role in draining the ice sheet. Much work has focused on determining the processes and mechanisms influencing their flow, with most focus on terminus processes, whilst little attention has been paid to the effects of hydrological processes via surface runoff and supraglacial lake drainage. There has been increasing evidence for the influence of enhanced meltwater inputs on impacting short term velocity at marine-terminating outlet glaciers with contrasting responses at individual glaciers. This study uses a remote sensing approach to characterise supraglacial lakes and their volumes at Store Gletscher and Rink Isbrae, two marine-terminating outlet glaciers in West Greenland, to assess the influence of such processes on their flow, providing an effective comparison due to their contrasting geometries, despite similar environmental controls. At Store there is evidence of a strong influence of hydrological mechanisms on its summer velocity variability, supporting observations in previous work with a transition to efficient drainage. However, the opposite is identified at Rink. This difference is suggested to be caused by Rink's lower capacity for lake formation with a steeper hypsometry and narrower ablation area compared to Store, reflecting the primary controls of surface topography and surface runoff volume on lake formation. These conclusions reveal the possible significant influence of hydrological mechanisms on flow at marine-terminating margins, whilst also indicating a probable range of responses at different glaciers dependent on glacier-specific factors.

Acknowledgements

Firstly, I would like to thank my supervisor, Dr. Poul Christoffersen, for his advice and support throughout the production of this thesis, and also throughout the academic year. I would also like to thank Dr. Neil Arnold and Dr. Alison Banwell for generously providing me with their lake detection algorithm, and MATLAB advice, without which I would not be able to complete this project. I also want to thank Andrew Williamson and Joe Todd for their helpful advice and support along the way. An additional thank you also goes to David Edey for helping me through some of my coding crises.

On a personal level, I am indebted to my parents for their generous funding and support throughout my time at Cambridge, without whom none of this would be possible. Finally, a big thank you to all who work at the Scott Polar Research Institute for keeping me entertained throughout the year, particularly the MPhils.

I am incredibly grateful to have been given the opportunity to study the Greenland Ice Sheet in more detail than I had ever hoped to. The photograph on the title page (taken by me on a plane to the USA in July 2010) is a real testament to my 15 year old self who was so keen to get into glaciology, spending much of the journey with a camera glued to the window when flying over Greenland. So a huge thank you to everyone mentioned here who has made it all possible.

Contents	Page no.
Declaration of Originality	iii
Abstract	iv
Acknowledgements	v
List of figures	ix
List of tables	xii
1.0 Introduction	1
1.1 Overview	1
1.2 Supraglacial lakes	2
1.2.1 Monitoring of supraglacial lakes	3
1.2.2 Recent trends	4
1.3 Hydrological mechanisms and ice sheet flow	4
1.3.1 'Alpine-style response'	5
1.4 Marine-terminating outlet glaciers	7
1.4.1 Processes and mechanisms of flow	7
1.4.2 Hydrological mechanisms and marine-terminating outlet dynamics	9
1.4.3 Glacier-specific factors	11
2.0 Project	12
2.1 Study site	12
2.2 Rationale, aims, and objectives	14
3.0 Methodology	16
3.1 Analysis of supraglacial lakes	16
3.1.1 Data acquisition and processing	16
3.1.2 Hydrological catchment delineation	17
3.1.3 Lake boundaries and area	19
3.1.4 Lake depth and volume	20
3.2 Velocity data	22

3.0 Results	24
3.1 Supraglacial lakes	24
3.1.1 Lake detection: Overview	24
3.1.2 A comparison of the lake systems of Store and Rink	26
3.1.3 Lake system evolution at Store and Rink	31
3.1.4 Supraglacial lake drainage events	34
3.2 Seasonal change in ice flow	39
3.3 Supraglacial lakes and velocity change	44
3.3.1 Trends through time	44
3.3.2 Trends through space	46
3.4 Results summary	51
3.4.1 Supraglacial lake evolution	51
3.4.2 Velocity change	51
3.4.3 Supraglacial lake drainage and velocity	52
4.0 Discussion	52
4.1 Comparing and contrasting the supraglacial lake systems at Store and Rink	52
4.2 Hydrological controls on the flow of marine-terminating outlet glaciers	55
4.2.1 Hydrology and ice flow at Store	55
4.2.2 Hydrology and ice flow at Rink	57
4.3 Reconciling contrasting flow regimes of Store and Rink	63
5.0 Study limitations	65
5.1 Theoretical	65
5.2 Methodological	66
5.2.1 Landsat-7	66
5.2.2 Lake detection algorithm	67
5.2.3 Hydrological catchment delineation	68
5.3 Velocity data	68
5.3.1 Temporal resolution	68

5.3.2 Spatial coverage	69
6.0 Conclusion	69
6.1 Future research	71
Reference list	72

List of Figures

Figure	Description	Page no.
1	Schematic diagram showing the balance of forces in subglacial channel development Source: Schoof (2010) page 803	6
2	Graphs indicating different modes of marine-terminating outlet glacier response to surface runoff. Source: Moon <i>et al.</i> (2014) page 7211	10
3	Location map of study site at Uummannaq Bay	12
4	A comparison of the hypsometries of Store (a) and Rink (b)	13
5	A comparison of summer velocity change at Store (a) and Rink (b)	14
6	Landsat imagery before (a) and after (b) scan-line removal	16
7	Hydrological catchment output at Store	18
8	Hydrological catchment output at Rink	19
9	Flowchart of the key stages in the lake detection and depth estimation algorithm	19
10	Illustration of the impacts of floating ice on the lake detection algorithm output	25
11	Example lake detection algorithm output at Store (a-b) outlining key areas of interest (c-d)	27
12	Example lake detection algorithm output at Rink (a-b) outlining key areas of interest (c-d)	28
13	Evolution of lakes at higher elevations at Store	29
14	Boxplot diagrams comparing the supraglacial lake systems observed at Store and Rink in figures 11 and 12	30
15	Bar graphs comparing mean total area (a) and mean total volume (b) each year 2009-2012 at Store and Rink	31
16	Graphs comparing lake volumes at Store at different elevations in the first half (a) and second half (b) of the melt season	32

17	Graphs comparing lake volumes at Rink at different elevations in the first half (a) and second half (b) of the melt season	33
18	Supraglacial lake drainage events identified at Store 2009-2012	36
19	Supraglacial lake drainage events identified at Rink 2009-2012	37
20	Bar graphs showing the percentage total drainage each year 2009-2012 within different elevation bands at Store (a) and Rink (b)	38
21	Absolute velocity at Store and Rink in summer (a) and winter (b)	39
22	Summer velocity difference maps at Store 2009-2012	40
23	Summer velocity difference maps at Rink 2009-2012	41
24	Winter velocity difference maps at Store 2009-2012	42
25	Winter velocity difference maps at Rink 2009-2012	43
26	Percentage change in mean velocity compared to supraglacial lake volumes at Store (a) and Rink (b)	44
27	Comparison between supraglacial lake drainage events and velocity in time at Store	45
28	Comparison between supraglacial lake drainage events and velocity in time at Rink	45
29	Comparison between supraglacial lake drainage events and velocity change in space at Store	47
30	Localised velocity change corresponding to lake drainage events identified at Store in 2009 and 2010	48
31	Comparison between supraglacial lake drainage events and velocity change in space at Rink	49
32	Localised velocity change corresponding to lake drainage events identified at Rink 2009, 2011, and 2012	50

33	Comparison between the locations of supraglacial lake drainage events and ice thickness changes at Store (a) and Rink (b)	60
34	Scatter plots indicating how ice thickness varies with drainage volume at the locations of individual drainage events at Store (a) and Rink (b)	61

List of tables

Table	Description	Page no.
1	Table of results of the lake detection algorithm at Store	24
2	Table of results of the lake detection algorithm at Rink	26
3	Summary table of supraglacial lake drainage events at Store 2009-2012	34
4	Summary table of supraglacial lake drainage events at Rink 2009-2012	34
5	Summary table of the relationship between minimum, mean, and maximum ice thickness at the locations of drainage events at Store and Rink	61

1.0 Introduction

1.1 Overview

Mass loss from the Greenland Ice Sheet (GrIS) is concentrated along the coastal margins with the drainage of marine-terminating outlet glaciers predominantly via calving (Vaughan *et al.*, 2013). However, with enhanced rates of flow (>50%) since the 1990s at these glaciers (Rignot and Kanagaratnam, 2006), this could have a profound influence on sea level rise. Already, the GrIS contributes to half of present sea level rise, suggesting that enhanced flow at these margins under a warming climate will further impact global sea levels (Joughin *et al.*, 2004). Indeed, recent trends have revealed that the contribution of Greenland's mass loss to rate sea level rise increased from 0.21 mmyr^{-1} 1993-2003 to 0.5 mmyr^{-1} 2003-2007 (Rignot *et al.*, 2011). It is therefore crucial to better understand the processes governing the flow of marine-terminating outlet glaciers.

So far most work on marine-terminating outlet glacier stability has focused on the influence of terminus perturbations on calving (Joughin *et al.*, 2008a), associated with warmer oceans (e.g. Holland *et al.*, 2008) and sea ice variability (e.g. Todd and Christoffersen, 2014). However, there has been less research on the effects of increasing surface melt on the flow of marine-terminating outlet glaciers, contributing to poor understanding of these mechanisms on influencing their stability. Most research of this process is based on land-terminating regions, where supraglacial lake drainage and surface runoff have been identified to directly influence ice flow (Zwally *et al.*, 2002; Parizek and Alley, 2004; Das *et al.*, 2008).

Recently, however there have been indications of marine-terminating outlet glaciers responding readily to supraglacial lake drainage and surface runoff in a similar manner to land-terminating portions of the ice sheet (Howat *et al.*, 2010; Moon *et al.*, 2014). Therefore, with current trends of supraglacial lakes forming at increasingly higher elevations (Howat *et al.*, 2013; Leeson *et al.*, 2014), and the potential impact of this on marine-terminating outlet glacier stability, it will be crucial to better understand the effects of this process on marine-terminating outlet glacier dynamics (Joughin *et al.*, 2008a). Furthermore, asynchronous trends observed between marine-terminating outlet glaciers despite exposure to similar mechanisms are thought to pertain to glacier-specific factors, identifying the need to compare the response of different glaciers (Moon and Joughin, 2008).

This study assesses the influence of supraglacial lake drainage on marine-terminating outlet glacier flow. This relationship is assessed at two glaciers, Store Gletscher and Rink Isbrae, terminating in the same fjord in West Greenland. Lake evolution, volume and drainage are characterised at both glaciers and compared with velocity change to assess the relationship between these factors in an attempt to improve understand of marine-terminating outlet glacier response to hydrological mechanisms.

1.2 Supraglacial lakes

0.5% of the surface of the GrIS is made up by supraglacial lakes storing surface runoff, whilst remaining surface runoff is unconfined, percolating through moulins and surface crevasses (Chu, 2013). Supraglacial lakes form at the beginning of the melt season in May, with surface runoff pooling in impermeable surface depressions (Chu, 2013). Lake numbers peak by the end of June (McMillan *et al.*, 2007), after which some lakes begin to drain (Das *et al.*, 2008). This generates what is known as the spring event (Das *et al.*, 2008), whereby greater lubrication of the bed enhances ice flow with basal sliding (e.g. Zwally *et al.*, 2002; Parizek and Alley, 2004).

Every melt season, supraglacial lakes are observed to form in the same locations to similar extents (Fitzpatrick *et al.*, 2014), reflecting primary control of surface topography on lake shape and distribution (Echelmeyer *et al.*, 1991; Arnold *et al.*, 2014). Indeed, lakes at higher elevations also grow to form larger lakes overall, associated with shallower slopes allowing for greater ponding capacity, identifying an additional direct influence of surface topography on lake morphology and distribution (Sundal *et al.*, 2009; Liang *et al.*, 2012). Consequently, shallower surfaces will introduce greater capacity for ponding for supraglacial lake formation.

Lake distribution and morphology is also determined by surface runoff volume (Leeson *et al.*, 2012; Sundal *et al.*, 2009; Sneed and Hamilton, 2007). Surface runoff volume is dependent on the size of the ablation area, and on air temperature, which is by extension a function of elevation, timing, and latitude (McMillan *et al.*, 2007). Lakes at lower elevations are observed to form and drain first, with a more intense 'slow fill rapid drain' cycle where temperatures are warmer at the beginning of the melt season (Fitzpatrick *et al.*, 2014). This trend then occurs at progressively higher elevations throughout the melt season (McMillan *et al.*, 2007; Sneed and Hamilton, 2007). By contrast, lakes at higher elevations form and drain over longer periods later in the melt season, pertaining to a less intense 'slow fill rapid drain' cycle with lower rates of warming (Sneed and Hamilton, 2007;

Sundal *et al.*, 2009; Fitzpatrick *et al.*, 2014). At lower latitudes, this pattern is also identified to occur earlier in the melt season, with a decline in air temperature of -0.78°C per latitude (Steffen and Box, 2001).

1.2.1 Monitoring of supraglacial lakes

Supraglacial lakes on the GrIS have been extensively monitored using a variety of techniques (Lüthje *et al.*, 2006; McMillan *et al.*, 2007; Sundal *et al.*, 2009; Liang *et al.*, 2012). At local scales, this has involved direct observations of the evolution of individual lakes providing detailed observations of lake drainage mechanisms (e.g. Das *et al.*, 2008; Doyle *et al.*, 2013). However, employment of satellite imagery to track lakes over multiple years has allowed for a more synoptic understanding of lake formation and evolution (e.g. Fitzpatrick *et al.*, 2014; Box and Ski, 2007).

Box and Ski (2007) first developed a method to classify lakes in satellite imagery using MODIS imagery. Indeed, the high temporal resolution of MODIS imagery with data acquired at daily intervals allows for detailed lake monitoring throughout the melt season, a significant breakthrough in improving supraglacial lake observations (e.g. Sundal *et al.*, 2009; Liang *et al.*, 2012; Howat *et al.*, 2013). This method has since been adapted for use with other satellite imagery, such as Landsat-7 (Banwell *et al.*, 2014) with additional newly adapted methods using a normalised difference water index to classify water-filled areas (Fitzpatrick *et al.*, 2014).

Lake volumes have been estimated using a number of methods, including positive degree-day models to estimate surface runoff, combined with digital elevation models to predict lake distribution and volume (McMillan *et al.*, 2007). Empirical remote-sensing techniques have also been employed, using field-calibrated algorithms with known lake depths (Fitzpatrick *et al.*, 2014). Of particular note, however, is the use of radiance-transfer models to estimate lake depths, using the Beer-Lambert Law, whereby the intensity of green band reflectance diminishes progressively with depth (Sneed and Hamilton, 2007). Although originally applied using ASTER (Sneed and Hamilton, 2007), this method has since been effectively adapted for use with Landsat-7 (Banwell *et al.*, 2014), allowing for more detailed analysis of lake depths with Landsat's higher spatial resolution.

1.2.2 Recent trends

Inland expansion of supraglacial lakes has been observed to occur at varying portions of the GrIS (Howat *et al.*, 2013; Leeson *et al.*, 2014). This has been associated with increasing elevations of the snowline over the past two decades with temperature rise increasing the summer melt extent (Braithwaite *et al.*, 1994). Consequently, this has generated concerns over further inland expansion with temperatures predicted to continue rising (Howat *et al.*, 2013; Leeson *et al.*, 2014).

Despite this trend, the extent of its continuation depends on the conditions of the firn at higher elevations, with a thicker and more permeable firn identified here, providing unsuitable conditions for ponding (Sneed and Hamilton, 2007). However, the recent observed trends appear significant with a 53 km inland migration of the lake line over 40 years (Howat *et al.*, 2013; Leeson *et al.*, 2014), whilst the elevation band containing the highest proportion of total supraglacial lake volume increases each year (Sole *et al.*, 2011). This trend is also associated with drainage events occurring at progressively higher elevations each year, particularly during warmer years (Liang *et al.*, 2012).

However, despite the trend at higher elevations, less variability is expected at lower elevations due to the first-order control of surface topography with lakes already forming in any suitable locations. Therefore, it is instead suggested that at lower elevations there could be an intensification of drainage frequency (Lüthje *et al.*, 2006; Fitzpatrick *et al.*, 2014). This increasing frequency of drainage events at lower elevations combined with greater occurrence of drainage at higher elevations, therefore presents potentially damaging consequences for GrIS stability (Das *et al.*, 2008; Zwally *et al.*, 2002), revealing the need for continued monitoring of supraglacial lakes.

1.3 Hydrological mechanisms and ice sheet flow

Ice flows through a combination of internal ice deformation, basal sliding, and subglacial deformation (Joughin *et al.*, 2008a). Multiple studies, predominantly in West Greenland, have demonstrated a strong relationship between daily surface runoff and ice flow variability whereby increased meltwater at the bed enhances basal sliding with basal lubrication (e.g. Zwally *et al.*, 2002; Shepherd *et al.*, 2009 Palmer *et al.*, 2011). However, in addition to surface runoff, the widespread seasonal drainage of supraglacial lakes provides the strongest mechanism for increasing basal lubrication via high volume meltwater pulses to the bed with moulin formation (Van der Veen, 2007). Indeed,

supraglacial lake drainage provides a mechanism for which meltwater is able to propagate through >1 km thick ice on the GrIS, allowing large meltwater pulses to reach the bed (Zwally *et al.*, 2002; Parizek and Alley, 2004; Das *et al.*, 2008). Therefore, despite containing a very low proportional quantity of total surface runoff (Chu, 2013), drainage of supraglacial lakes provides a significant mechanism for generating intensified basal sliding to impact ice flow.

Fracture mechanics provides the mechanism for a hydraulic connection to be made, whereby water-filled crevasses beneath a supraglacial lake penetrate to the bed under high pressure generated by the high lake volumes forming a moulin (Weertman, 1973; Van der Veen, 2007). Once drainage is initiated, water-filled crevasses propagate rapidly downward at rates dependent on meltwater volume maintaining filled crevasses (Alley *et al.*, 2005; Das *et al.*, 2008). Das *et al.* (2008) observed this process at two supraglacial lakes in West Greenland where the lakes initially drained slowly at the onset of fracture propagation (1.5 cmhr^{-1}) followed by rapid drainage (12 mhr^{-1}) once a full connection to the bed was made. In addition to hydrofracture, it is also possible for lakes to drain at slower rates via overspill into nearby moulins (Danielson and Sharp, 2013; Poinar *et al.*, 2015).

When drainage occurs via either mechanism, combined with inputs from daily surface runoff, the enhanced meltwater input causes basal water pressures to exceed the capacity of the subglacial drainage network; this is identified by hydraulic jacking causing surface uplift (Iken *et al.*, 1983; Das *et al.*, 2008). The increase in basal water pressure causes enhanced basal sliding at the bed due to greater lubrication, enhancing ice flow. Consequently, during high melt years (Ettema *et al.*, 2009), when there is greater frequency of supraglacial lake drainage events (Fitzpatrick *et al.*, 2014; Leeson *et al.*, 2014), higher mean annual velocities have been observed (Zwally *et al.*, 2002; Parizek and Alley, 2004; Shepherd *et al.*, 2009). This relationship was originally proposed by Zwally *et al.* (2002) at the ice sheet interior at Swiss Camp, West Greenland, where they conclude that with greater melt predicted with future warming, drainage event frequency will continue to increase, increasing the long term instability of the GrIS.

1.3.1 'Alpine-style' response

More recently, however, research has suggested that rather than causing an increase in mean annual velocity (Zwally *et al.*, 2002), higher surface runoff and greater frequency of supraglacial lake drainage at the GrIS instead generates a stabilising effect, with very little change to mean annual velocity (van de Wal *et al.*, 2008; Van der Veen, 2007; Sundal *et*

al., 2011). Instead, with drainage to the bed in the melt season, large short term velocity increases associated with higher rates of basal sliding are followed by abrupt declines in velocity in midsummer indicating higher velocity variability (~30%) rather than long term velocity increases (Sundal *et al.*, 2011). Consequently, there could be a long term stabilising effect of enhanced surface runoff (van de Wal *et al.*, 2008).

The theoretical understanding of this relates to processes observed at smaller alpine-glaciers (e.g. Iken and Bindschadler, 1986; Iken *et al.*, 1983). Efficiency of the subglacial drainage network is determined by a transient balance between water pressure and ice-overburden pressure, known as effective pressure (Rothlisberger, 1972; Kamb, 1987). Therefore, the system continually readjusts through channel size modification towards efficiency dependent meltwater flux to the bed (Schoof, 2010).

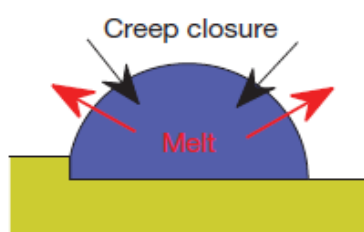


Figure 1: A schematic diagram of the forces acting on channel development in a subglacial drainage network. The red arrows indicate conduit-widening by melting of the walls with frictional-heating. The black arrows indicate creep-closure opposing channel-widening. The balance of forces is dependent on effective pressure with varying basal water pressures. When creep-closure > wall melt, conduit closure is promoted with no channel development. When creep-closure < wall melt, channel widening is promoted with channel development. Source: Schoof (2010) page 803

At the onset of the melt season, subglacial drainage is characterised by inefficient distributed cavities where water pressure is insufficient to promote conduit-widening, with higher rates of creep closure and basal sliding; in figure 1, the black arrows therefore exceed the red arrows (Schoof, 2010). With additional meltwater inputs to the bed, basal water pressures increase, breaching drainage capacity and enhancing basal sliding rates (Iken, 1981; Schoof, 2010). However, with higher rates of frictional-heating caused by higher discharge with turbulent flow, conduit-widening is promoted, whereby melting of the walls begins to exceed creep closure (the red arrows exceed the black arrows (fig.1)), to develop a channelised network. This process is also enhanced along a steeper hydraulic potential (Schoof, 2010).

This occurs until the channels increase to a size of sufficient capacity for higher water pressures, causing the system to collapse into an efficient network with lower basal water pressures, reducing basal sliding rates (Rothlisberger, 1972; Kamb, 1987). Consequently, the sensitivity of ice flow to additional melt inputs is reduced, preventing further enhanced

ice flow (Schoof, 2010). This therefore provides a mechanism for velocity decrease with increasing melt. By the end of the melt season, however, surface runoff wains and therefore drainage volume at the bed lowers to insufficient volumes for maintaining an efficient channelised network (Schoof, 2010). Consequently, creep closure rates exceed conduit widening rates causing a transition to inefficient drainage once again, allowing for basal sliding causing a net increase in winter velocities (Schoof, 2010).

Due to the >1 km thick ice at the GrIS, this process should not be plausible due to such thick ice creating conditions for greater conduit closure (Schoof, 2010; Bartholomew *et al.*, 2011). However, dye-tracing experiments at land-terminating portions of the ice sheet have revealed that it is a plausible explanation whereby large outbursts of subglacial melt exits the glacier after a transition to efficient drainage, indicating a subsequent reduction in pressure after enhanced ice flow (Bartholomew *et al.*, 2008; Bartholomew *et al.*, 2011; Bartholomew *et al.*, 2012; Cowton *et al.*, 2013). The ability for this process to operate at >1 km thick ice is explained by supraglacial lake drainage events providing sufficiently high volume meltwater fluxes to generate high enough rates of conduit widening for channelisation (Bartholomew *et al.*, 2011), identifying the importance of supraglacial lake drainage events in modulating ice flow (Das *et al.*, 2008).

Due to no observations at the bed allowing for direct analysis of the basal drainage network at the GrIS (Hoffman *et al.*, 2011; Andersen *et al.*, 2011), the 'alpine-style' response has therefore been used as an analogue to explain a lack of observed long term increase in mean annual velocities with high surface melt at the GrIS (van de Wal *et al.*, 2008; Sundal *et al.*, 2011). However, the ice dynamic response to this process is also governed by the rapidity of the transition to efficient drainage, dependent on glacier-specific factors, identifying the need to assess this relationship in a number of regions before drawing generalised conclusions (Sundal *et al.*, 2011).

1.4 Marine-terminating outlet glaciers

1.4.1 Processes and mechanisms of flow

Despite current understanding of the influence of hydrological mechanisms on GrIS ice flow, research on this relationship has focused predominantly on land-terminating portions of the ice sheet with little emphasis on marine terminating outlet glaciers (Vieli *et al.*, 2004). So far, research has shown that the latter exhibit less sensitivity to basal sliding changes with varying meltwater input, with low seasonal variability in flow (Echelmeyer

and Harrison, 1990). This is suggested due to enhanced basal water pressures all year round caused by greater rates of frictional heating generating continuous high melt conditions (Iken, 1981). Indeed, melt-induced speed-ups are estimated to influence velocity at marine-terminating outlet glaciers by <10-15% relative to >50-100% at land terminating portions inland (Echelmeyer and Harrison, 1990; Joughin *et al.*, 2008a). Consequently, the idea of supraglacial lake drainage and surface runoff influencing ice flow is undermined relative to other processes (Joughin *et al.*, 2008a).

Instead, ice flow variability at marine-terminating outlet glaciers has most often been related to terminus position, dependent on calving rates (Thomas, 2004). Force imbalances at the terminus generate stress-failures instigating calving which reduces buttressing, causing retreat (Benn *et al.*, 2007). This generates higher ice flow rates, with a signature of decreasing velocity change with distance from the terminus (Thomas, 2004; Walter *et al.*, 2012). Such force imbalances are generated by two main processes: firstly, when the terminus is forced above a critical height of flotation pushing the glacier out of buoyant equilibrium (Vieli and Nick, 2011; O'Leary and Christoffersen, 2013), and secondly via a loss of terminus backstress generating a force imbalance to instigate calving (Amundson *et al.*, 2010).

For the first mechanism, the main driver of terminus thinning is submarine melt of the calving front by the relatively warm ocean at the terminus, generating force imbalances for calving, providing a mechanism for long term velocity increase (Holland *et al.*, 2008; Straneo *et al.*, 2010). Intermediate warming of subtropical waters (STW) around Greenland of 2°C 1994-2004 (Holland *et al.*, 2008) coincides with many of the observed trends, with increases in ice flow of >50% in the 1990s, until 2006. Enhanced submarine melt over this period is suggested to have contributed to this trend whereby STW spreading onto the continental shelf coincided with a weaker subpolar gyre caused by a switch to a weak negative North Atlantic Oscillation in 1996 (Christoffersen *et al.*, 2011). Submarine melt is also enhanced by convection driven meltwater plumes (Jenkins, 2011) whereby buoyant subglacial meltwater ejected from the terminus enters the fjord to form a rising plume at the calving front, encouraging a compensatory inflow of warmer STW at depth, enhancing submarine melt (Motyka *et al.*, 2011).

For the second mechanism, the seasonal sea ice melange has been demonstrated to modulate calving rates throughout the year by varying the level of buttressing at the terminus, providing a seasonal control on velocity (Amundson *et al.*, 2010; Todd and

Christoffersen, 2014). Sea ice melange is a rigid mixture of sea ice and icebergs coalescing at the terminus (Joughin *et al.*, 2008b). During the winter when it is strongest, the melange exerts a backstress (30-60kpa) on the terminus against ice flow, preventing force imbalances and crevasse propagation (Amundson *et al.*, 2010; Walter *et al.*, 2012). However, upon its break-up early in the melt season, the loss of backstress generates a force imbalance at the terminus promoting crevasse propagation and calving (Amundson *et al.*, 2010). This has been identified at a number of marine-terminating outlet glaciers, including Store Gletscher in West Greenland (Todd and Christoffersen, 2014), and Kangerdlugssuaq Glacier in Southeast Greenland (Seale *et al.*, 2011).

1.4.2 Hydrological mechanisms and marine-terminating outlet dynamics

Regardless of the significant influence of terminus processes on affecting ice flow, there is increasing evidence to suggest that hydrological processes similar to those operating at land-terminating portions of the ice sheet could have a strong influence on the flow of marine-terminating outlet glaciers (Howat *et al.*, 2010; Moon *et al.*, 2014; Sole *et al.*, 2011; Andersen *et al.*, 2010; Csatho *et al.*, 2014), albeit with lower magnitude responses overall (Sole *et al.*, 2011; Shepherd *et al.*, 2009). Previous research suggesting little significant response to hydrological processes have mostly been focused near the termini, where calving is likely to be the most significant contributor to velocity change (e.g. Joughin *et al.*, 2008a), masking any hydrological influence (Sole *et al.*, 2011). Therefore, the relative importance of hydrological processes and calving are poorly understood with inappropriate separation of both processes in previous studies (Andersen *et al.*, 2011).

Observations of significant velocity change coinciding with supraglacial lake drainage events have been identified to occur at marine-terminating outlet glaciers. Joughin *et al.* (1996) first identified a possible link between supraglacial lake drainage and marine-terminating outlet glacier flow at Ryder Glacier, North Greenland. Using satellite interferometry, they identified a 400% velocity increase over 7 weeks, coinciding with a drainage event. A similar observation was made more recently in a survey of glaciers at Uummannaq Bay, West Greenland, where a number of outlet glaciers were identified to experience a midsummer velocity slowdown (Howat *et al.*, 2010). The strongest evidence was at Store Gletscher, whereby a 30-60% midsummer velocity decrease coincided with supraglacial lake drainage (Howat *et al.*, 2010), exhibiting the stabilising influence with enhanced varying water pressures (van de Wal *et al.*, 2008; Bartholomew *et al.*, 2010).

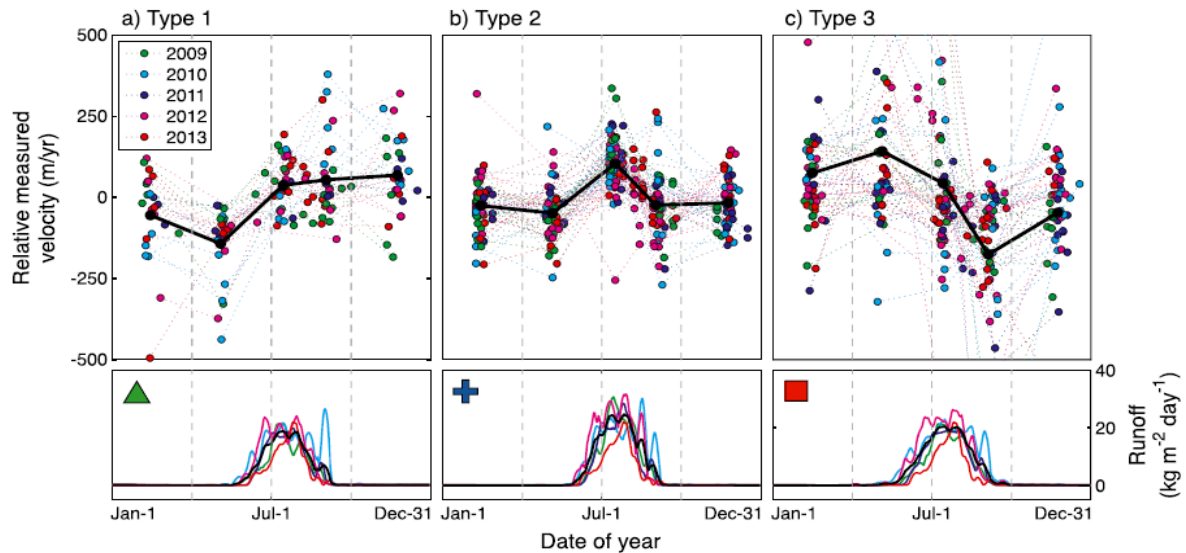


Figure 2: The results presented by Moon *et al.* (2014) (page 7211) comparing relationships of 55 marine-terminating outlet glacier velocity to surface runoff identifying three types of response to surface runoff.: Type 1 glaciers experience velocity increase into the winter after surface runoff wains, type 2 glaciers experience increasing velocity throughout summer followed by a decline in winter as surface runoff wains, and type 3 glaciers experience a sharp drop in velocity during the melt season before experiencing a gradual increase in velocity in winter. The top panel represents the velocity values acquired using InSAR (m/yr) for glaciers exhibiting dominant modes of response for years 2009-2013. The mean velocity for all years at each point of the year is also indicated by the black line. The bottom panel represents runoff as estimated using RACMO2.3 ($\text{kg m}^{-2} \text{ day}^{-1}$), indicating the results for the same observation period 2009-2013, with mean values indicated by the black line.

Similar relationships have also been identified between surface runoff and ice flow at marine-terminating outlet glaciers. Most recently, in a survey of 55 marine-terminating outlet glaciers around Greenland, Moon *et al.* (2014) compared relationships between surface runoff and ice velocity, identifying three glacier ‘types’ (fig.2). “Type 1” are glaciers responding more readily to terminus position with velocity remaining high until late winter; “Type 2” are glaciers experiencing a velocity decrease towards the end of the melt season associated with no transition to efficient drainage; and “Type 3” are glaciers experiencing an abrupt midsummer slowdown followed by rebound in winter, consistent to a switch to efficient drainage. In another ice sheet-wide survey, Csatho *et al.* (2014) suggest that spatial and temporal variability in ice thickness changes up-ice at marine-terminating outlet glaciers is likely to relate to widespread hydrological processes, with ice thickening corresponding to velocity decreases with a switch to efficient drainage. However, this trend is not identified at all glaciers, with some exhibiting more prominent dynamic thinning than thickening.

At local scales, Sundal *et al.* (2013) identified a relationship between velocity and surface runoff at Kangerdlugssuaq, Southeast Greenland, whereby velocity increases of <15% were observed in June after surface runoff increase, followed by velocity decrease. Furthermore, the peak in velocity did not dissipate upstream as expected for velocity change induced by terminus processes (Thomas, 2004). At Kangiata Nunata Sermia,

Southwest Greenland, Sole *et al.* (2011) identified maximum rates of surface uplift coinciding with 1-15 day speedup events followed by 10% velocity decreases. Throughout the observation period, the calving front maintained the same position, whilst surface uplift indicates no significant longitudinal stretching (Thomas, 2004), suggesting the velocity change was unlikely related to terminus position (Nick *et al.*, 2009).

1.4.3 Glacier-specific factors

Despite the evidence presented for marine-terminating outlet glacier response to hydrological processes, individual glaciers are likely to exhibit contrasting sensitivities due to glacier-specific factors (Meier and Post, 1987; Carr *et al.*, 2013). Indeed, different marine-terminating glaciers within the same proximity have been observed to respond differently to the same processes despite being subject to similar environmental controls (Howat *et al.*, 2010; Moon *et al.*, 2014), with glacier-specific factors likely pertaining to asynchronous trends observed around Greenland (Moon and Joughin, 2008). Indeed, the results of Moon *et al.* (2014) and Csatho *et al.* (2014) identify how marine-terminating glaciers can respond so differently to hydrological processes, whilst Howat *et al.* (2010) demonstrated the range of dynamics observed between 11 glaciers all terminating within Uummannaq Bay. Furthermore, the ice-dynamic response to enhanced meltwater inputs will depend on the rate at which a transition is made to efficient drainage (Sundal *et al.*, 2011; Moon *et al.*, 2014) which is likely to be influenced by glacier-specific factors.

A number of glacier-specific factors are identified to influence the way marine-terminating outlet glaciers respond to terminus processes (e.g. Carr *et al.*, 2013; Meier and Post, 1987). Bed topography and basal pinning points are identified to generate non-linear responses to terminus perturbations; for example, retreat into overdeepenings creates unprecedented retreat by producing a force which must be balanced upstream through intensified longitudinal stress gradients (Meier and Post, 1987; Howat *et al.*, 2007), whilst pinning points prevent unprecedented retreat from occurring (Carr *et al.*, 2013). Secondly, fjord geometry and glacier shape can create force imbalances influencing terminus stability (Enderlin *et al.*, 2013; Pfeffer, 2007). For example, in narrower fjords, perturbations at the terminus will be dampened by the strong influence of lateral resistive stresses relative to basal stresses (Pfeffer, 2007). Consequently, it is likely that glacier-specific factors will act to influence marine-terminating outlet glacier response to hydrological processes as well.

2.0 Project

2.1 Study site

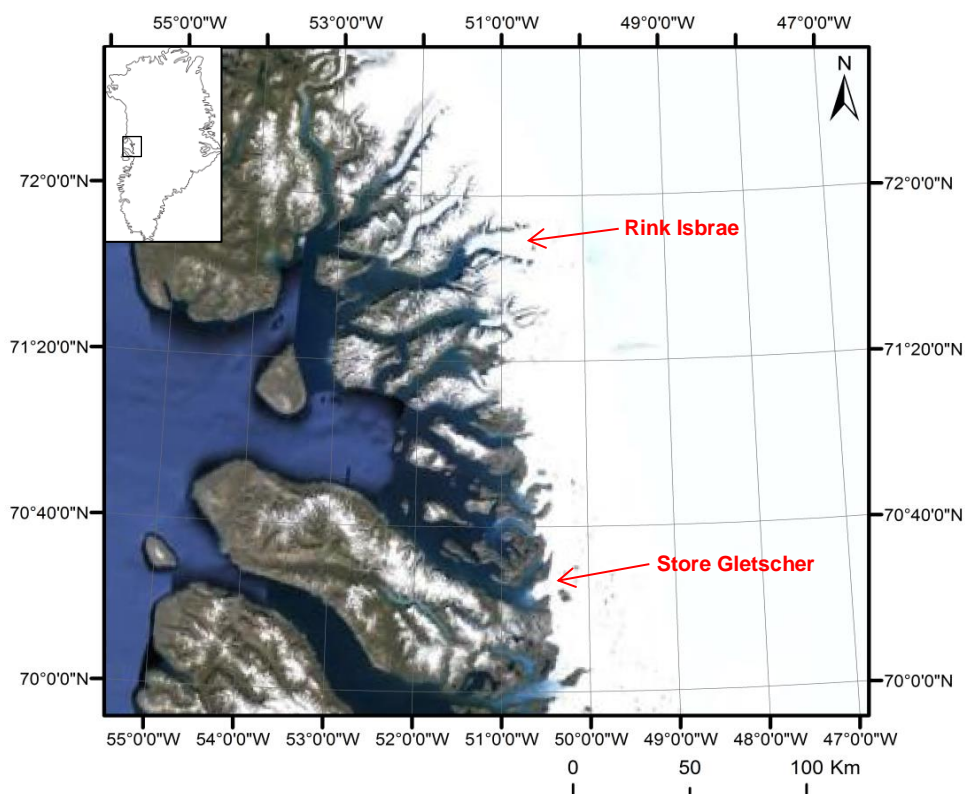


Figure 3: Study site location map at Uummannaq Bay, West Greenland. The two marine-terminating outlet glaciers of interest, Store Gletscher and Rink Isbrae, are highlighted by the red arrows. The base map imagery is Landsat imagery courtesy of the USGS and Google Earth.

Uummannaq Bay is a fjord system located in West Greenland (fig.3), comprising of 11 major marine-terminating outlet glaciers, including Store Gletscher, henceforth referred to as Store, and Rink Isbrae, henceforth referred to as Rink (Howat *et al.*, 2010). This region has also experienced temperature increases of 2°C since the early 1990s potentially impacting the stability of its glaciers (Howat *et al.*, 2010). Furthermore, due to its over-deepened glacial trough, it is also widely exposed to warm subtropical water, influencing submarine melt rates and terminus stability (Chauché *et al.*, 2014). However, despite all glaciers being subject to the same environmental conditions and trends, within a region ~250km north to south, significant differences in glacier dynamics have been observed (Howat *et al.*, 2010; Moon *et al.*, 2014), proposed to relate to the contrasting geometries and topographical settings of individual glaciers (Howat *et al.*, 2010; Carr *et al.*, 2013). For example, Rink is more uniformly exposed to intermediate subtropical waters at >500 m depths due to its terminus being grounded at 750 m, compared to 500 m at Store, making Rink more susceptible to submarine melt (Holland *et al.*, 2008; Chauché *et al.*, 2014). This

therefore demonstrates one of the many ways glacier-specific factors can influence their sensitivities.

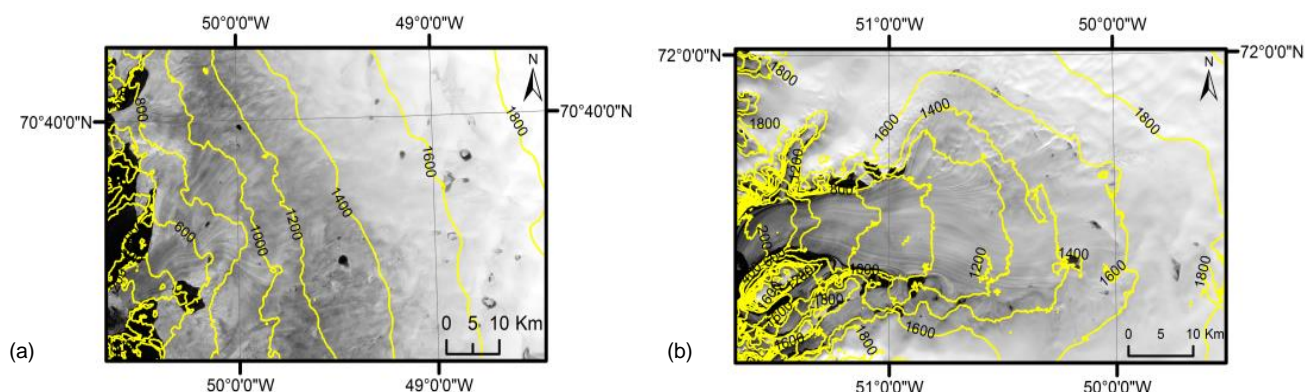


Figure 4: Elevation contours in yellow (extracted from the GIMP DEM (Howat *et al.*, 2014)) at Store (a) and Rink (b) demonstrating the contrasting hypsometry of both glaciers. Landsat imagery from 20th August 2012 at Store and 27th August 2012 at Rink, are used.

Store (70°23'N 50°34'W) (fig.3) drains an area of 34000km² from the northeast into Ikerasak Fjord, a tributary of Uummannaq Bay (Rignot *et al.*, 2008; Todd and Christoffersen, 2014). Store has an estimated annual discharge of 14-18 km³ (Weidick and Bennike, 2007), with a 5 km wide terminus, wide ablation area, and low hypsometric profile as indicated by the elevation contours in figure 4 (a). It experiences seasonal oscillations of ~200 m, although is relatively stable maintaining a similar position (± 1.5 km) for 40 years (Weidick, 1995; Howat *et al.*, 2010). Recent work on Store has demonstrated a strong influence of the seasonal sea ice melange on controlling calving rates through generating a buttressing effect on the terminus in winter through to May, after which melange removal coincides with rapid retreat, before the melange reforms the following winter (Todd and Christoffersen, 2014). Originally, Store was considered to experience little variability in seasonal velocity, based on measurements taken ~30 km from the ice front (Joughin *et al.*, 2008a). However, Howat *et al.* (2010) have identified 30-60% velocity variation during the summer with suggestions that this trend relates to hydrological mechanisms (Howat *et al.*, 2010).

Rink (71°78'N 51°68'W) also drains into Uummannaq Bay, ~150 km to the north of Store (fig.3). It drains an area of ~40000km² from the northeast, with a 5.5 km wide terminus, and an estimated annual discharge of 11-17 km³ (Weidick and Bennike, 2007). Contrasting to Store, Rink's hypsometric profile is much steeper, shown by the elevation contours in figure 4 (b), with a narrower ablation area. Rink advances in winter before extensive retreat until mid-July with substantial velocity increases during this retreat (~25%), and ~1 km terminus oscillations, the largest of all glaciers in this region (Schild

and Hamilton, 2013); consequently Rink is considered to be relatively unstable (Howat *et al.*, 2010). These trends are considered to be dominated by changes in ice front position with varying calving rates modulated by the summer disintegration of its floating tongue (Howat *et al.*, 2010). However, relative to Store, Rink experiences less inter-seasonal velocity variability, with no equivalent midsummer slowdown identified (Howat *et al.*, 2010).

2.2 Rationale, aims and objectives

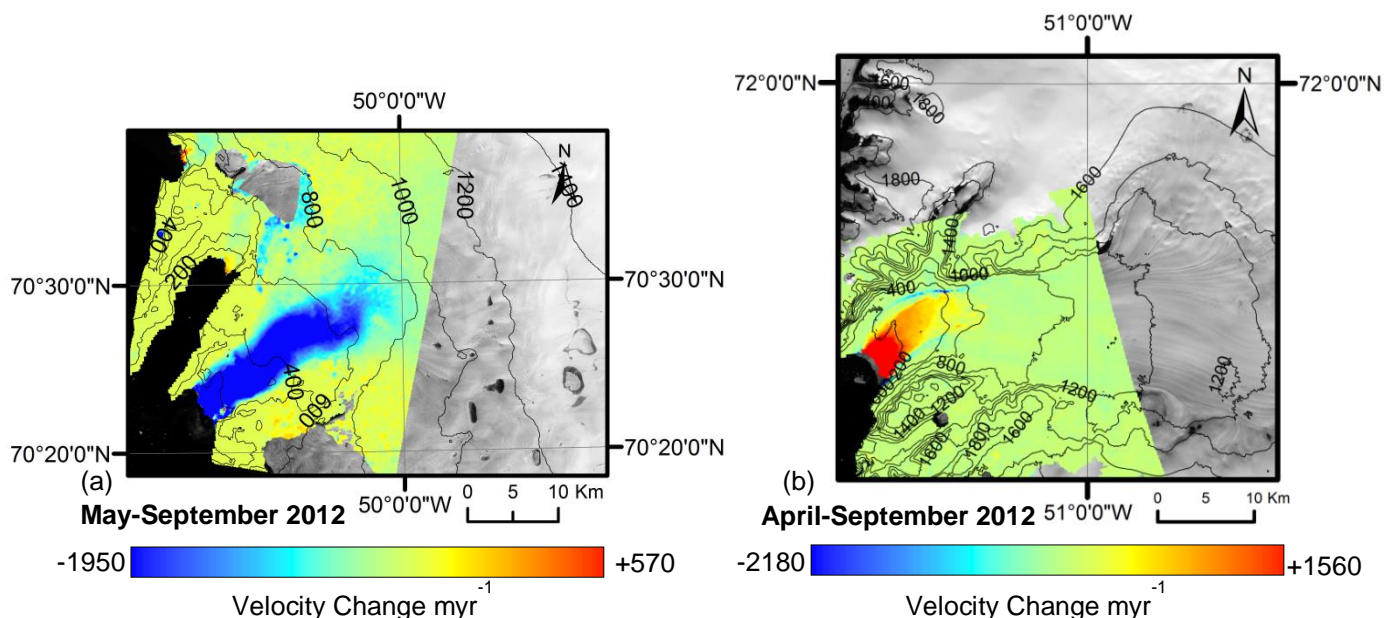


Figure 5: MeASURES InSAR velocity data (Joughin *et al.*, 2011) revealing opposite trends in summer velocity change in 2012, based on available acquisition dates (May-September at Store, April-September at Rink). Note that the scales on the colour bars differ. The colour bars reveal the absolute change in velocity in myr^{-1} , with blue indicating a net decrease in velocity and red indicating a net increase in velocity. The data are superimposed onto Landsat imagery acquired on 21st August 2009 at Store and 26th August 2009 at Rink. Elevation data are extracted from the GIMP DEM (Howat *et al.*, 2014).

Store and Rink are two similar-sized marine-terminating outlet glaciers draining into a common fjord system in West Greenland (fig.3). However, despite being exposed to similar environmental factors separated by only $\sim 150\text{km}$, both glaciers experience contrasting flow regimes. This difference is illustrated in figure 5 for Store (a) and Rink (b) during the summer in 2012, whereby Store experiences a net decrease in velocity, and Rink a net increase (Joughin *et al.*, 2011). Therefore, it is likely that glacier-specific factors play an important role (Meier and Post, 1987).

Research at Store has indicated a possible influence of varying meltwater input to the basal drainage network with supraglacial lake drainage events in the summer (Howat *et al.*, 2010), with the net velocity decrease in summer (fig.5) associated with a transient switch to efficient drainage (Schoof, 2010). In contrast, Rink does not exhibit the same

trend, with net velocity increase in summer (fig.5), suggesting a different response to varying basal water pressure.

With supraglacial lake drainage providing a mechanism to transport additional meltwater to the bed (van der Veen, 2007), it is possible that contrasting supraglacial lake drainage trends at Store and Rink could pertain to these differences. Therefore, understanding these processes at both glaciers is vital to understand their contrasting responses, with wider implications for marine-terminating outlet glacier stability.

Additionally, with recent increasing temperature trends (Hanna *et al.*, 2014; Howat *et al.*, 2010) connected to higher rates of surface runoff production (Ettema *et al.*, 2009), it is likely that the supraglacial lake systems at these glaciers have evolved steadily becoming increasingly extensive (Liang *et al.*, 2012; Howat *et al.*, 2013) representing a possible threat for the future stability of the GrIS (Zwally *et al.*, 2002). Therefore, if supraglacial lake drainage does impact ice flow for either of these glaciers, responsible for draining 7% and 8% of the central western sector of the GrIS, these trends could have significant consequences for the future of the GrIS (Vaughan *et al.*, 2013; IPCC, 2013).

The aim of this research is to characterise the supraglacial lake systems of Store and Rink in a comparative study, with a particular focus on lake volumes, to evaluate the potential effects of supraglacial lake drainage on seasonal dynamics of marine terminating outlet glaciers via the following objectives:

1. Estimate lake volumes within the hydrological catchments of Store and Rink
2. Obtain estimates of velocity change at Store and Rink
3. Compare lake volume change and supraglacial lake drainage to velocity changes at Store and Rink

Relating supraglacial lake volumes to velocity change rather than total surface runoff is justified by the lakes themselves generating the most significant pulses of meltwater to the bed (Van der Veen, 2007), providing the most prominent routing of meltwater to the bed for impacting ice flow rather than lower volume daily inputs of surface runoff. Furthermore, the added ability of pinpointing individual lake drainage events in time and space allows for more direct comparison of additional meltwater inputs to velocity change.

The main hypothesis to guide this study is that due to Store's lower hypsometric profile and wider ablation area, Store develops a more extensive and dynamic supraglacial lake network with a higher volume and frequency of drainage events (Liang *et al.*, 2012),

increasing Store's sensitivity to varying basal water pressures, explaining the observed differences in summer velocity change in figure 5 for Store and Rink.

3.0 Methodology

3.1 Analysis of supraglacial lakes

3.1.1 Data acquisition and processing

Landsat-7 ETM+ 'Level 1 Product' imagery (with a spatial resolution of 30m) was downloaded from the Earth Explorer website at <http://earthexplorer.usgs.gov/> for both Store and Rink glaciers during the period covering the melt season 1st May-30th September for years 2009 through to 2012 (however generally September imagery did not contain any lakes and therefore have not been used). These years were selected due to limitations on available velocity data outlined later (Joughin *et al.*, 2011). Only images with minimal cloud cover, and minimal snow cover were selected to avoid missing any lakes obscured by either cloud or snow.

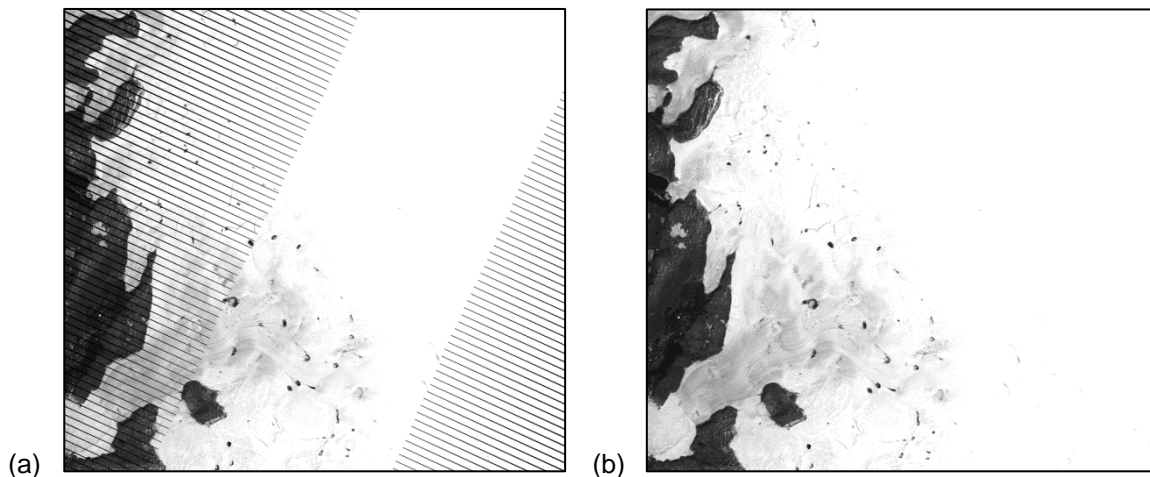


Figure 6: The results of inverse distance weighting interpolation in removing the scan-lines caused by the failure of the scan-line corrector on 31st May 2003 (USGS, 2013) are shown, using the 10th June 2012 acquisition. (a) is the raw image containing the scan-lines of 'no data', and (b) is the output after interpolation has been applied.

Due to the failure of the scan-line corrector on 31st May 2003, all images were affected by data loss due to scan-lines (fig.6), making up 22% of each image acquisition (USGS, 2013). In order to reduce the error in subsequent analysis due to this data loss, inverse distance weighting interpolation was conducted in Quantum GIS (QGIS) to 'fill' the scan-lines. Using the 'translate' function in QGIS to turn the scan-line pixels into 'no data' values, it was possible to interpolate around these areas, taking the weighted average of pixels around each 'no data' pixel. An example result of this process is shown in figure 6, illustrating the image before interpolation (a) and after interpolation (b). Despite generating

some uncertainty, particularly at the edges of each acquisition where the scan-lines are thickest, the use of interpolation improves the overall quality of each image, yielding more accurate results in subsequent analysis.

All images were cropped to the same extent using Multispec, with a ~5000 km² area for Store and a ~4000 km² area for Rink. To avoid ‘non-ice’ areas being classified as lakes, such as the coast, nunataks, and the ocean, the 30 m resolution GIMP ice mask (Howat *et al.*, 2014) was used to identify these areas as ‘no-data’ values in analysis. The 30 m mask was selected over the 15 m or 90 m mask to match the resolution of the Landsat imagery, also at 30 m, thus not requiring further processing.

3.1.2 Hydrological catchment delineation

The boundaries of the hydrological catchments of Store and Rink were estimated to exclude any regions of the ice surface whereby lakes forming in these locations are unlikely to impact the dynamic response of either glacier (Fitzpatrick *et al.*, 2014). A theoretical hydraulic potential to determine the direction of water flow was generated using equation 1 (Shreve, 1985):

$$-\nabla\phi h = -p_i g(S + 0.09 B) \quad (1)$$

where p_i is overburden ice pressure, g is gravity, S is the surface elevation, and B is bed elevation. 0.09 is a coefficient representing an approximate value for $\frac{p_w}{p_i} - 1$, so that the bed slope gradient is required to be approximately 11 times greater than the surface slope gradient for water to flow down the bed slope potential, representing the dominant control of the surface slope on water flow (Shreve, 1985; Cuffey and Paterson, 2010). Although in previous work a flotation fraction was used to delineate the hydrological catchment based on ice discharge (e.g. Banwell *et al.*, 2013), this was not used so that the catchment area was maximised to incorporate all potential lakes influencing flow with drainage within the proximity of each glacier. The potential surface was generated through combining the GIMP surface DEM at a 90m resolution (S) downloaded at <http://research.bpcrc.osu.edu/GDG/gimpdem.php> via the Byrd Polar and Climate Research Centre courtesy of Howat *et al.* (2014), and Icebridge BedMachine bed elevation data (B), downloaded at <http://nsidc.org/data/docs/daac/icebridge/idbmg4/index.html> via the National Snow and Ice Data Centre website (NSDIC), courtesy of Morlighem *et al.*, (2014). The surface DEM was produced using a combination of ASTER and SPOT-5

elevation data, whilst the bed topography DEM comprises of estimates based on mass conservation data 1993-2014 derived by airborne and satellite radar.

The generated potential surface was analysed using hydrological tools in ArcGIS to delineate the hydrological catchment. The ‘fill’ tool was used to identify the surface depressions where water is likely to collect. This was followed by ‘flow direction’ to plot the vectors of water flow across the surface, using the ‘flow accumulation’ tool to identify where the water was likely to accumulate within the identified depressions based on the estimated flow vectors. The catchment was then delineated using ‘watershed’, by first manually selecting a pour point for water flow near the glacier terminus using ‘snap pour point’, finally producing a raster of the catchment. The Landsat imagery was subsequently inspected to assess the likely accuracy of the output by identifying stream flow direction (Fitzpatrick *et al.*, 2014). The final outputs are presented in figures 7 and 8.

The catchments were resampled to 30 m pixel resolution to match Landsat-7 resolution, and a mask generated by assigning a value of 0 to non-catchment pixels, and a value of 1 to catchment pixels. The masks were then incorporated into the lake detection algorithm.

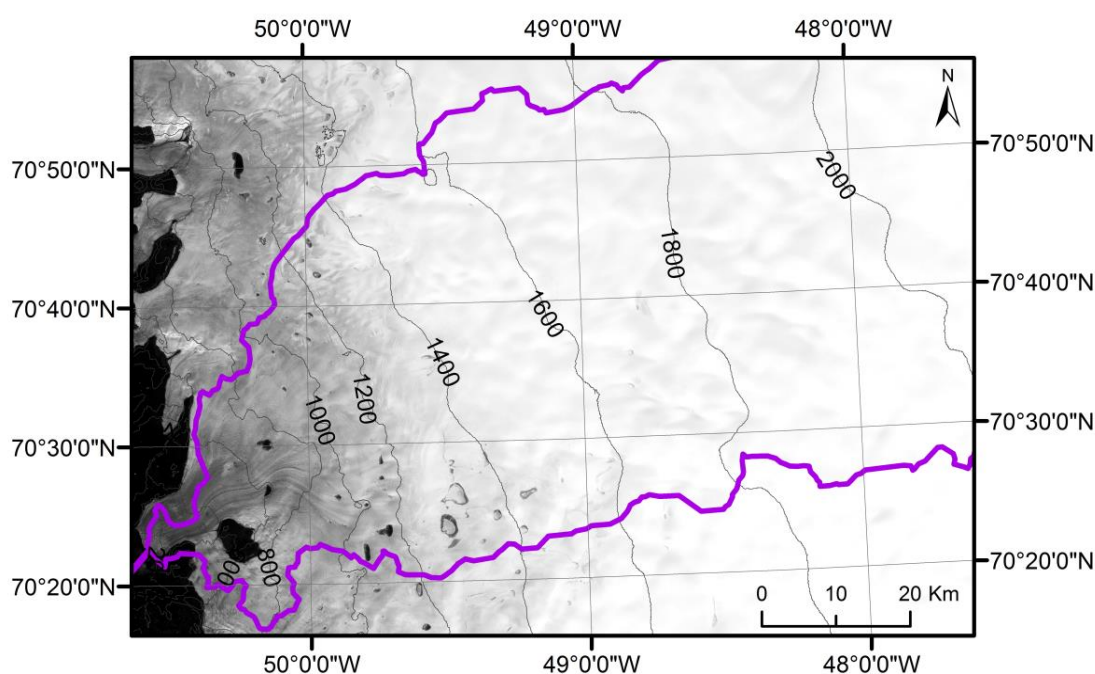


Figure 7: The results of the delineation of the hydrological catchment (n purple) at Store superimposed onto the 21st August 2009 Landsat-7 image acquisition. The map is projected in Polar Stereographic Grid EPSG code 3413 (as for all remaining figures), and the elevation data demarcated by elevation contours at 200m intervals is extracted from the GIMP ice mask (Howat *et al.*, 2014).

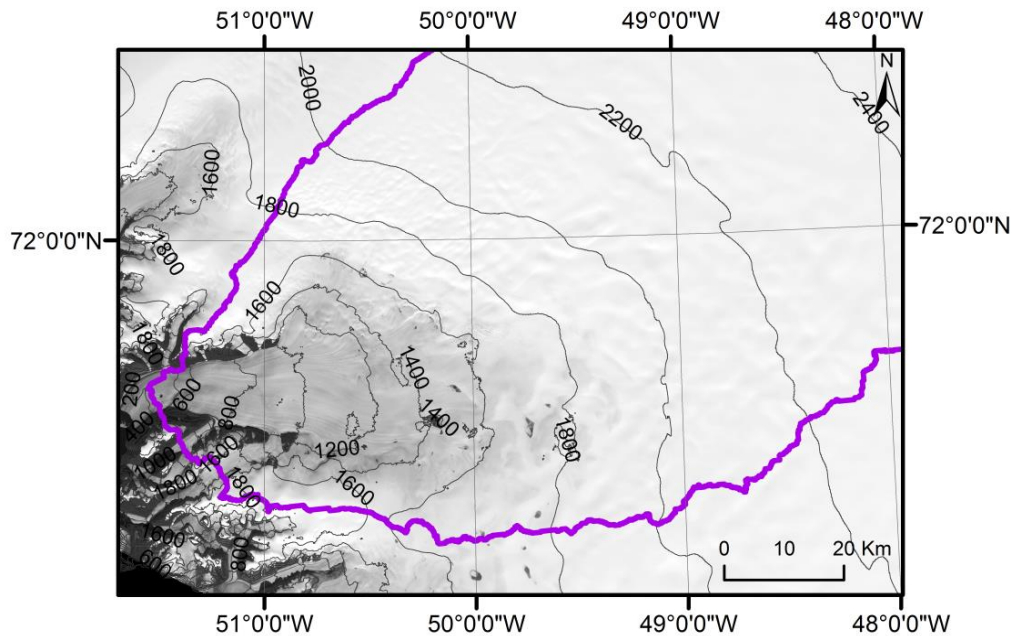


Figure 8: The results of the delineation of the hydrological catchment (n purple) at Rink superimposed onto the 27th August 2012 Landsat-7 image acquisition. The map is projected in Polar Stereographic Grid EPSG code 3413 (as for all remaining figures), and the elevation data demarcated by elevation contours at 200m intervals is extracted from the GIMP ice mask (Howat *et al.*, 2014).

3.1.3 Lake boundaries and area

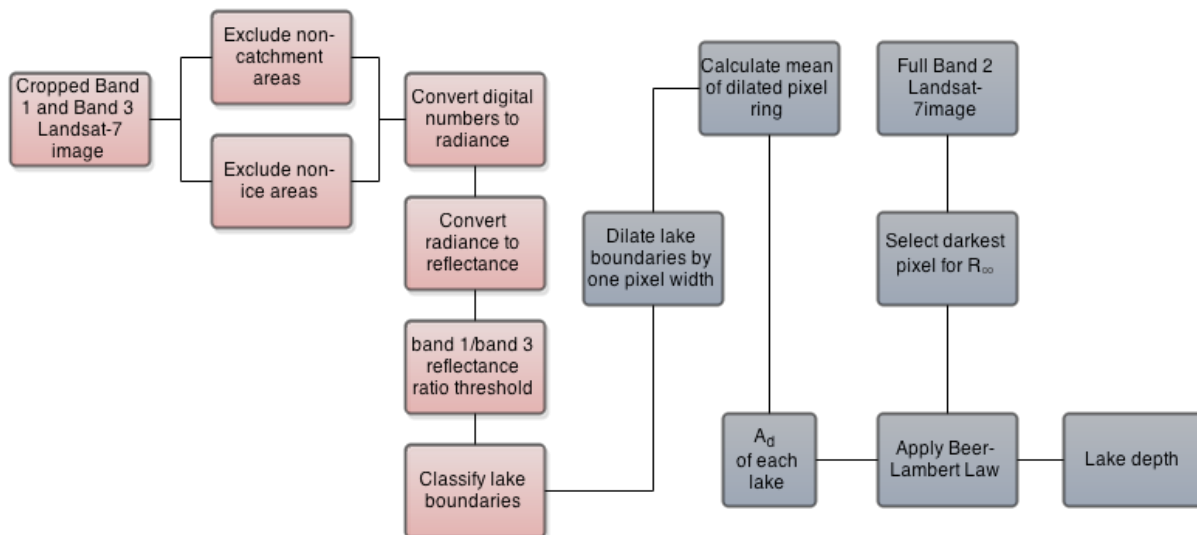


Figure 9: A flowchart outlining the key steps in determining lake depths from the scan-line-corrected Landsat imagery. The methods for determining lake boundaries and area, following the approach of Box and Ski (2007), are highlighted in red. The methods for determining lake depth, following the approach of Sneed and Hamilton (2007), are highlighted in blue.

The lake detection algorithm (provided by Dr. Neil Arnold and Dr. Alison Banwell) was used to determine lake boundaries on a lake-by-lake basis relying on band reflectance ratios (Box and Ski, 2007; Liang *et al.*, 2012), with methods used summarised in red in figure 9. Although the original method designed by Box and Ski (2007) used MODIS imagery, it has since been adapted for use with Landsat-7 imagery (Banwell *et al.*, 2014),

successfully validated by Arnold *et al.* (2014) to analyse lakes at Paakitsoq, West Greenland, and Banwell *et al.* (2014) also at Paakitsoq, and the Larsen B Ice Shelf, Antarctica, demonstrating its capability in operating well in highly contrasting environments. Previous methods of lake classification have relied on less accurate methods of manual digitisation (McMillan *et al.*, 2007 using ASTER), and partially-automated approaches using a normalised difference water index (Fitzpatrick *et al.*, 2014 using MODIS). However, for this study, the band reflectance threshold approach by Box and Ski (2007) will be followed.

Lake boundaries were identified by classifying all non-masked pixels as 'bare ice' or 'water-filled' (Box and Ski, 2007). Using the 'Level 1 Product' Metadata for each image, the digital numbers of bands 1 (blue; 450-515nm) and 3 (red; 630-690nm) were converted to radiance, and from radiance to reflectance (Chander *et al.*, 2009). A band1/band3 (blue/red) reflectance ratio threshold was individually selected for each image to classify every pixel as either 'bare ice' or 'water-filled'. Towards the centre of lakes, where water is deepest, the relative quantity of blue reflectance is greater, thus requiring a relatively low blue/red threshold to be classified as 'water-filled'. However, for shallower regions towards lake edges, the relative quantity of blue reflectance decreases, and therefore a lower blue/red threshold does not classify the shallowest pixels as 'water-filled'. Consequently, for accurate lake boundary delineation, the threshold was carefully selected with manual inspection of the original Landsat image.

Box and Ski (2007) recommend a blue/red reflectance ratio threshold between 1.05 and 1.25 based on empirical data of known lake areas in West Greenland. However, Banwell *et al.* (2014) use a value of 1.4; this identifies the need to experiment with different threshold values for each image. For this study, threshold values between 1.35 and 1.45 were generally deemed most appropriate to match the original imagery, similar to Banwell *et al.* (2014), and values within this range were therefore used for lake classification. Once a threshold was determined for each image, the 'bwboundaries' function in MATLAB was used to demarcate lake boundaries on a lake-by-lake basis.

3.1.4 Lake depth and volume

The depths of each pixel within lake boundaries were determined through estimating lake-bottom albedo using the Beer-Lambert Law in a radiative transfer function (Sneed and Hamilton, 2007), with the methods used summarised in blue in figure 9. Although originally based on satellite imagery alone, this method has since been validated with *in situ*

measurements (Sneed and Hamilton, 2011). Sneed and Hamilton (2007) originally used the VNIR1 ASTER band with wavelengths of 520-600nm. However with band 2 (green) Landsat-7 imagery having similar wavelengths (525-605m), this method has been shown to work well using Landsat-7 and has since been adapted (Banwell *et al.*, 2014). Previous methods of lake depth estimation have relied on positive degree day models to quantify likely surface meltwater volume (McMillan *et al.*, 2007) and also the relationship of band 1 reflectance reducing exponentially with depth (Box and Ski, 2007). However, for this study, the radiative transfer model designed by Sneed and Hamilton (2007) is followed.

The Beer-Lambert law describes the attenuation of radiation through the water column, with a reduction in reflectance strength at progressively increasing depths (Ingle and Crouch, 1988). The law is applied using the following equation:

$$I(z, \lambda) = I(0, \lambda)e^{-(K_\lambda)(z)} \quad (2)$$

where $I(z, \lambda)$ is the water-leaving spectral intensity at a given depth, $I(0, \lambda)$ is the spectral intensity identified at 0 m depth, K_λ is the spectral attenuation, and z is depth. Equation (3) is the same law however rearranged to represent an equation for depth estimation (z) in terms of reflectance (Philpot, 1989):

$$z = \frac{[\ln(A_d - R_\infty) - \ln(R_w - R_\infty)]}{-g} \quad (3)$$

where A_d is the bottom albedo (reflectance), R_∞ is the reflectance of optically deep water (i.e. no bottom albedo), R_w is the reflectance of the pixel of interest, and g is determined by:

$$g \approx K_d + aD_u \quad (4)$$

where K_d is the diffuse attenuation coefficient for downwelling light, a is the beam absorption coefficient, and D_u is an upwelling light distribution function (Mobley, 1994). Bottom albedo (A_d) was determined by dilating the lake boundary by a width of one pixel around each lake and taking the mean reflectance value of this pixel ring. With these pixels representing regions barely covered with water, they theoretically provide a reflectance value for the bottom substrate of each lake. Sneed and Hamilton (2007) originally only identified a single value of A_d for each image, thus applying the same value to every lake in a single image. However, the algorithm has since been adapted to

estimate a unique A_d for every lake (Banwell *et al.*, 2014) improving the overall accuracy of depths estimated at each lake. For R_∞ , the darkest pixel was selected from each image to represent the reflectance of optically deep water, selecting an ocean pixel value from the uncropped band 2 image, taking care to avoid shallower pixels near the shoreline or pixels masked by floating ice due to their inappropriately high reflectance (Sneed and Hamilton, 2011).

In addition to the above methods, the original lake detection algorithm of Box and Ski (2007) has since been adapted by Banwell *et al.* (2014) to mask out regions of floating ice to avoid the effects of calculating negative lake depths with higher reflectance values of ice relative to water improving the clarity of the results.

Lake volumes of each identified lake were estimated by finding the sum of pixel depths within each lake boundary, and multiplying by pixel size (0.0009 km²; 30 m resolution), giving an estimate of volume in km³. Additional parameters, such as mean depth ('meanintensity') and maximum depth ('maxintensity') for each lake were also estimated using the 'regionprops' function in MATLAB.

3.2 Velocity data

The 'MeASURES' programme (Making Earth System Data Records for Use in Research Environments) provide open-source velocity maps for selected sites around Greenland 2009-2012 (Joughin *et al.*, 2011). The velocity maps were generated through a combination of InSAR (interferometric synthetic aperture radar) and speckle-tracking techniques (Joughin *et al.*, 2011; Joughin, 2002). Both methods have greatly impacted research in polar environments (Nathan-King, 2014, *unpublished*), especially for assessing ice sheet dynamics and flow (e.g. Palmer *et al.*, 2011). Velocity is measured by estimating the displacement between two SAR images acquired in the same orbit using retained phase and amplitude information, and the known temporal baseline and geometry of each acquisition. Any displacement caused by topographic change is removed using a digital elevation model (Rees, 2013). Speckle-tracking methods are used to fill regions of missing data by tracking individual speckles produced by backscatter of the image acquisitions (Joughin, 2002).

For this study, the sites containing Store (W70.55N), and Rink (W71.65N) were used, downloaded freely at http://nsidc.org/data/docs/measures/nsidc0481_joughin/index.html via the NSIDC courtesy of the MeASURES programme (Joughin *et al.*, 2011). The data

were acquired using the TerraSAR-X satellite with images taken at 11 day intervals at various points 2009-2012. The raw data, downloaded in big-endian IEEE floating point format, was converted into a readable matrix using the 'fread' function in MATLAB. To give an impression of how velocity changes through time at Store and Rink, velocity difference over the summer and winter periods using the available dates were then determined by calculating the difference between absolute velocities of two InSAR acquisitions. Mean estimates of velocity were also acquired along a flow-line transect of each glacier.

Ahlstrøm *et al.* (2013) have produced continuous velocity records of Store and Rink via *in situ* GPS, downloaded freely at http://doi.geus.dk/seasonal_velocities/ via the Geological Survey of Denmark and Greenland courtesy of Ahlstrøm *et al.* (2013). Both datasets cover most of 2009-2011, within the observation period of this study. However, due to the GPS receiver being advected down ice, advection effects have occurred due to moving towards faster portions of the glacier, limiting their use for analysis.

3.0 Results

3.1 Supraglacial lakes

3.1.1 Lake detection: Overview

Store

Year	Date	Misclassified/ negative lakes	No. Lakes	Mean lake area (m ²)	Max Depth (m)	Total Volume (km ³)
2009	24 May	1	16	0.034	4.56	0.00640
	18 June	0	53	0.14	7.57	0.0189
	29 July	1	63	0.34	12.43	0.0578
	5 August	2	81	0.33	7.93	0.0806
	21 August	0	52	0.31	7.86	0.0478
2010	29 May	0	80	0.11	8.21	0.0174
	14 June	1	74	0.15	7.40	0.0171
	21 June	1	79	0.20	9.40	0.0420
	15 August	83	63	0.30	8.66	0.0440
2011	15 June	1	131	0.09	7.74	0.0148
	1 July	0	122	0.19	9.06	0.0562
	3 July	0	101	0.20	8.91	0.0471
	2 August	3	125	0.23	8.90	0.0654
2012	10 June	0	76	0.22	9.05	0.0450
	17 June	1	100	0.22	9.89	0.0654
	20 August	2	83	0.37	10.18	0.0864

Table 1: Summary of the results of the lake detection algorithm at Store, signifying the number of misclassified and negative lakes, the number of lakes excluding misclassified and negative lakes, mean lake area (m²), maximum lake depth (m), and total lake volume (km³). Images impacted by heavy cloud cover and/or cropping of the northeast catchment due to acquisition geometry are highlighted in red.

The lake detection algorithm was successfully run for 16 image acquisitions at Store, with their results displayed in table 1. Four images were subject to data loss at higher elevations in the northeast corner of the catchment due to the geometry of the acquisition (identified in red in table 1) however they are still included in analysis where appropriate due to valuable data acquired elsewhere in the catchment. Generally, the algorithm proved successful in classifying lakes correctly, with minimal misclassifications which were subsequently removed (apart from 15th August 2011 which was subject to extensive cloud cover >2000 m of the catchment, however beyond the lake limit of any other image). The estimated bottom albedo (A_d) ranged between 0.35 and 0.77 with a mean of 0.61.

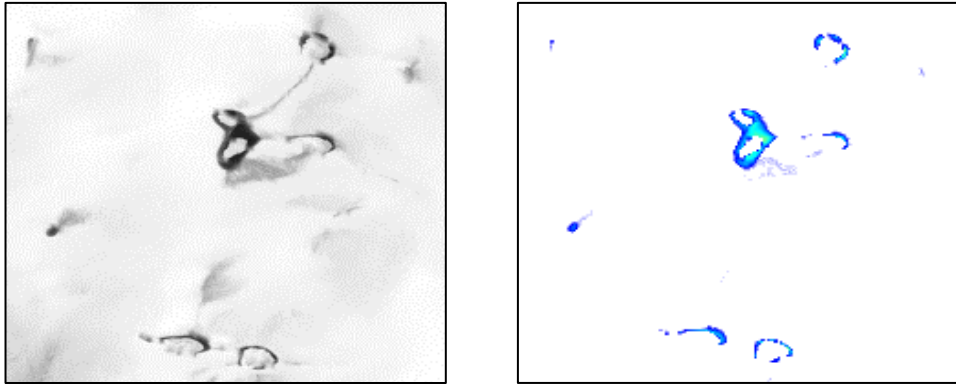


Figure 10: Example portion of the catchment at Store demonstrating the impact of floating ice on the Landsat imagery on the output of the lake detection algorithm, resulting in data loss by masking water-filled areas. The example is taken from the 20th August 2012 image acquisition

A mean total of 81.2 lakes were detected throughout the observation period for Store. The mean estimated total lake area was 0.21 m² with a mean estimated maximum lake depth of 8.61m; maximum overall lake depth occurred on 29th July 2009 (12.43 m). Total estimated lake volume generally increases throughout the melt season (with 2009 as an exception where volume decreases 5th-21st August), and inter-annually with the greatest volume occurring on 20th August 2012 (0.0864 km³). However, due to the presence of floating ice on the surface of lakes, water-filled areas were often masked by 'bare ice' (such as those shown in figure 10 for 20th August 2012); consequently, estimated lake volumes underestimate the true value, and thus represent minimum values for volume.

For Rink, 15 images were successfully analysed, with the results are summarised in table 2. The period June-August is generally well covered for all years, apart from 2011 where there are no suitable images available after 30th May. Therefore, 2011 has been omitted from some analysis. Only two of the analysed images were subject to missing data in the northeast corner of the catchment due to the geometry of the image acquisition (identified in red in table 2), however once again both images provide valuable data for lakes lower in the catchment. In general, 1-4 non-flooded pixels were misclassified as lakes or acquired negative values. The value for bottom albedo (A_d) for each lake varied between 0.21 and 0.76, with an overall mean of 0.60.

Rink

Year	Date	Misclassified/ negative lakes	No. Lakes	Mean lake area (m ²)	Max Depth (m)	Total Volume (km ³)
2009	9 July	1	70	0.13	7.15	0.0197
	18 July	0	102	0.14	7.99	0.0276
	26 August	0	61	0.15	6.77	0.0116
2010	18 May	0	23	0.07	2.94	0.000920
	5 July	1	59	0.18	8.59	0.0298
	12 July	2	47	0.20	8.64	0.0280
	13 August	2	75	0.13	7.57	0.0195
2011	21 May	2	30	0.14	2.88	0.00199
	30 May	2	27	0.14	2.62	0.00159
	1 July	3	45	0.13	6.69	0.0122
2012	30 May	2	25	0.15	3.29	0.00188
	1 June	12	86	0.07	3.87	0.00330
	17 July	2	64	0.22	7.79	0.0328
	26 July	2	61	0.21	9.55	0.0327
	27 August	4	47	0.24	9.06	0.0297

Table 2: Summary of the results of the lake detection algorithm at Rink, signifying the number of misclassified and negative lakes, the number of lakes minus misclassified and negative lakes, mean lake area (m²), maximum lake depth (m), and total lake volume (km³). Images impacted by heavy cloud cover and/or cropping of the northeast catchment due to acquisition geometry are highlighted in red.

A mean total of 54.8 lakes were detected for all images at Rink, with a mean estimated total lake area of 0.15 m². The mean maximum estimated lake depth was 6.36 m, with a maximum overall lake depth of 9.55 m on 26th July 2012. However some lakes were also impacted by floating ice as at Store. Contrasting to Store, for all years the estimated lake volume decreases between the final two acquisitions, with a peak in July followed by a decline in August.

3.1.2 A comparison of the lake systems of Store and Rink

For all years at both glaciers, it is clear that lakes form in the same locations to similar extents each year, with no major changes in morphology. However, analysis of the lake systems at Store and Rink reveal contrasting characteristics between each site both spatially and temporally. Examples are presented in figures 11 and 12 for Store and Rink respectively, to illustrate the different features observed for 21st June 2010 at Store and 5th July 2010 at Rink. These image acquisitions were selected due to both images best representing the greatest range of supraglacial lake characteristics, whilst also occurring at a similar points of the melt season.

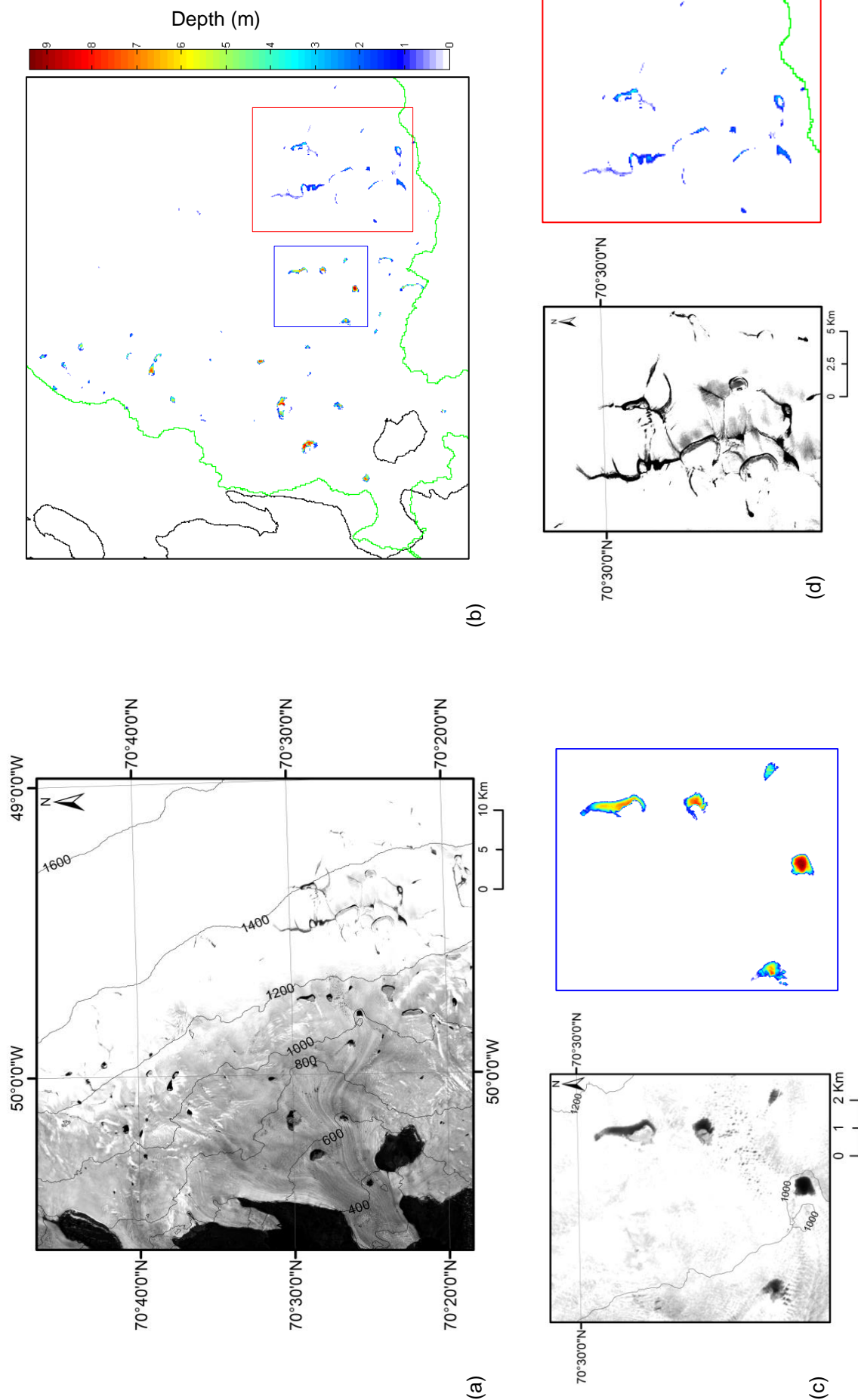


Figure 11: Example output at Store for 21 June 2010. The top panel compares the original Landsat image with elevation contours extracted from the GIMP DEM (Howat *et al.*, 2014) (a) with the output from the lake detection and depth estimation algorithm (b). The colour bar represents depths in meters on a pixel-by-pixel basis. On the bottom panel, (c) identifies a region in the catchment outlined in blue in (b) with the output (using the same colour bar as in (b)), and (d) identifies a region in the catchment outlined in red in (b) (using the same colour bar as in (b)). Note the impact in (d) of choosing a reflectance ratio threshold most effective for the image as a whole on identifying water-filled pixels in shallower areas, resulting in some data loss.

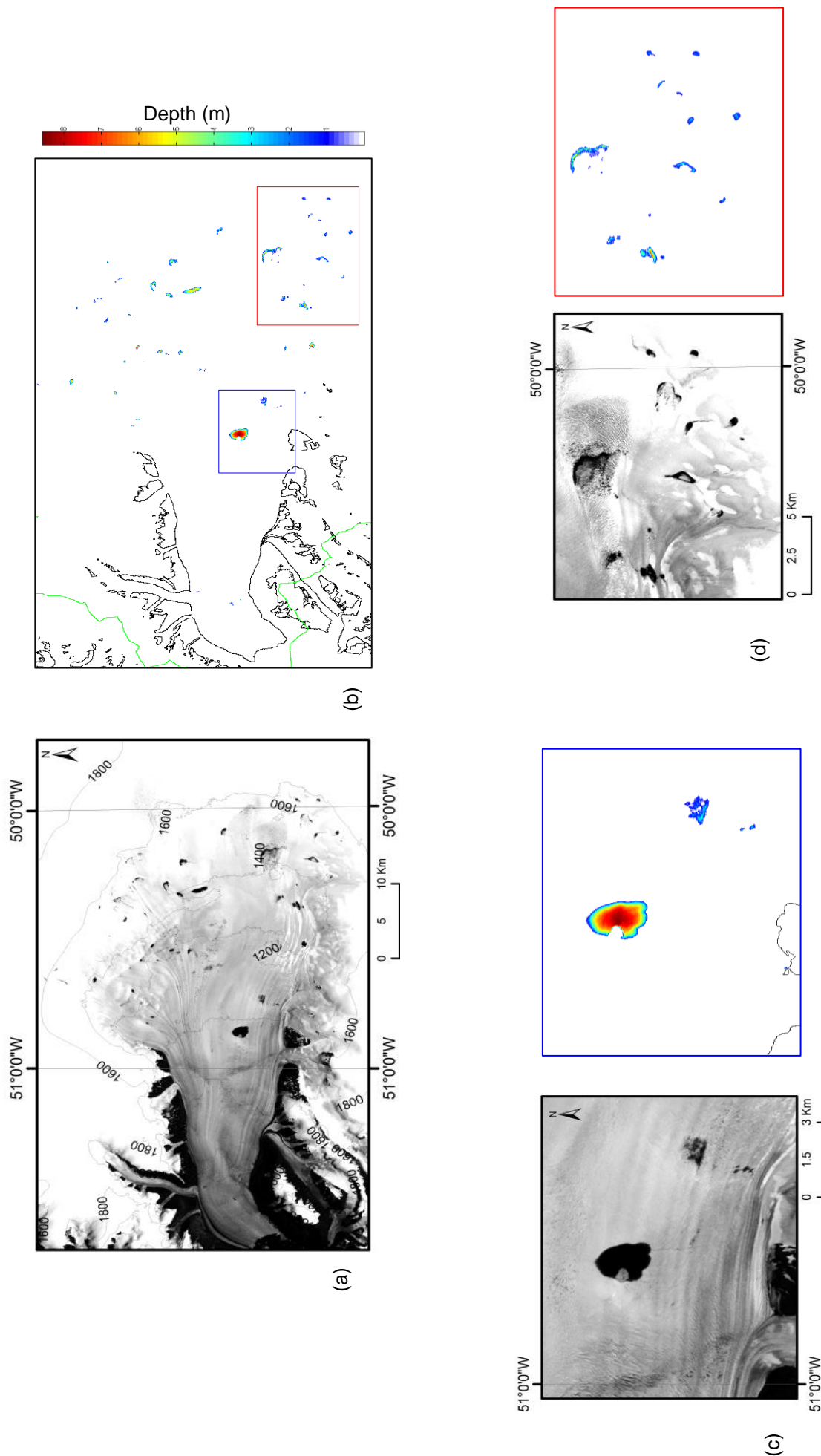


Figure 12: Example output at Rink for 5th July 2010. The top panel compares the original Landsat image with elevation contours extracted from the GIMP DEM (Howat *et al.*, 2014) (a) with the output from the lake detection and depth estimation algorithm (b). The colour bar represents depths in meters on a pixel-by-pixel basis. On the bottom panel, (c) identifies a region in the catchment outlined in blue in (b) with the output (using the same colour bar as in (b)), and (d) identifies a region in the catchment outlined in red in (b) (using the same colour bar as in (b)). Note the impact in (d) of choosing a reflectance ratio threshold most effective for the image as a whole on identifying water-filled pixels in shallower areas, resulting in some data loss.

Within these examples, 79 supraglacial lakes are identified at Store between elevations of 200-1600 m. 57 lakes were identified at Rink, however, Rink's supraglacial lakes generally form at higher elevations, between >800-1600 m. Furthermore, the percentage area covered by lakes at Store relative to the rest of the catchment (0.0059%) is double that of Rink (0.0035%). With regards to lake morphology, from both examples, it is clear that the lakes at Store exhibit a far wider range of lake morphology relative to Rink.

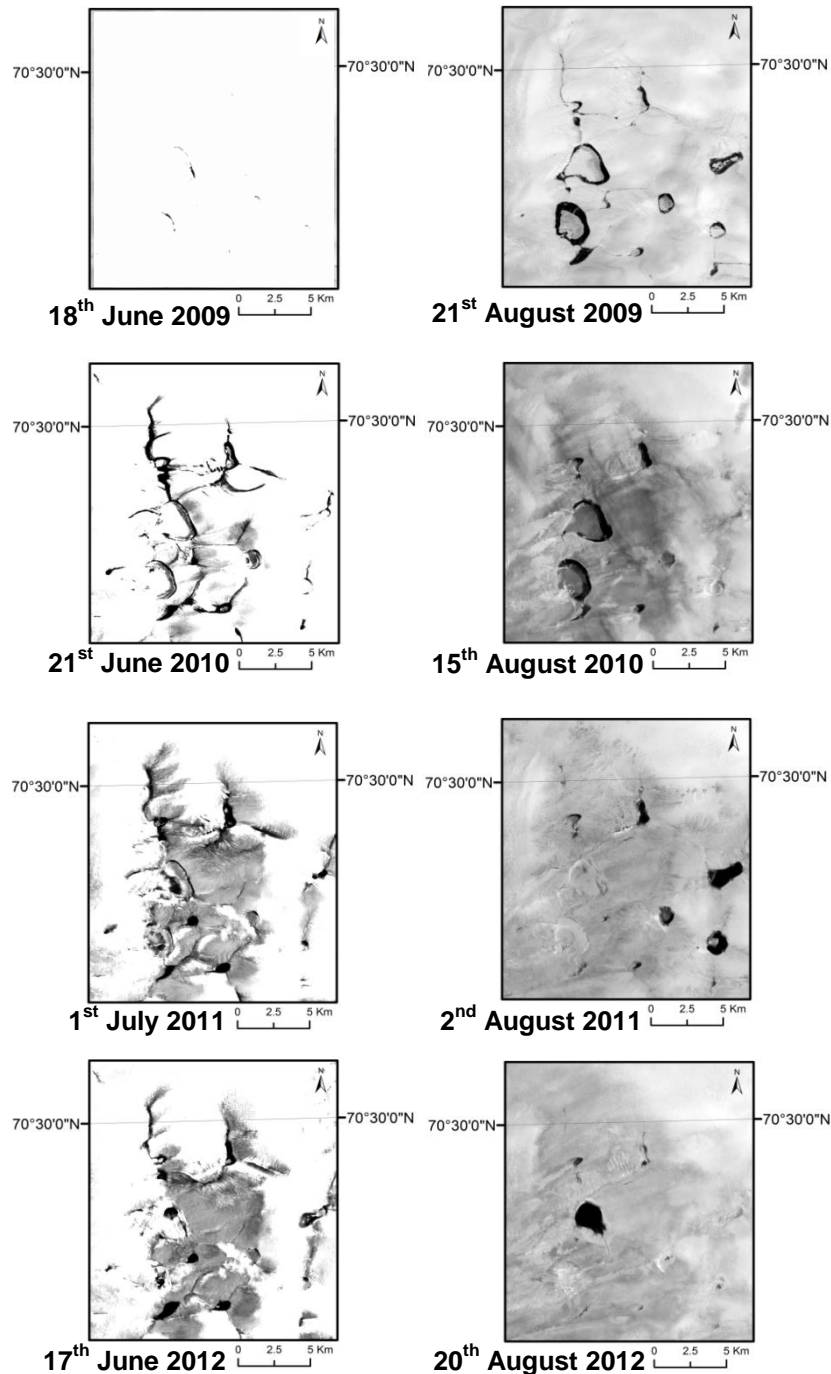


Figure 13: The evolution of the area outlined in figure 11(d) over the melt season between June/July and August for each year during the observation period 2009-2012 as identified in the Landsat-7 image acquisitions. They reveal highly contrasting morphologies at different stages of evolution for each melt season.

Two example areas are selected at both Store and Rink to demonstrate the range of contrast at both glaciers. At Store (fig.11), (c) identifies typical well-formed, circular lakes with progressively increasing depths towards the centre, up to 8 m in depth. In contrast, the lakes identified in (d) have a highly contrasting morphology to those in (c). They are a cluster of wispy linear features with much shallower depths overall relative to the lakes in (c) (1-3 m). Furthermore, there is no distinct progressive depth change as in (c) (however note how the output image is impacted by the choice of threshold causing data loss in very shallow areas to compensate for more accurate results across the catchment overall). Upon further investigation in other imagery, this area is also shown to evolve significantly throughout the melt season each year (fig.13). In all cases, the wispy linear features form in the same locations each year. However, by August, they transform into discrete individual lakes. This therefore presents a distinct contrast to the evolution of the lakes observed in (b) lower in the catchment, where they take on the same or similar forms each year.

Compared to Store, the range of lake morphologies observed at Rink is less extreme, with no particularly prominent differences between lakes within the catchment. Aside from evidence of pooling within the crevasses on the main glacier trunk at elevations of 200-400 m, lakes forming in regions further inland at higher elevations do not contrast to the same degree as at Store. In figure 12, (c) identifies the most prominent lake observed within Rink's catchment reaching maximum depth of 8.6 m. Like the lakes identified in (c) at Store, this lake also exhibits progressively increasing depth towards the centre of the lake. The lakes in (d) are much smaller than the lake in (c), and are less-well established with shallower depths overall (~2 m). However, in terms of general lake morphology, there is no distinct contrast as is the case at Store, with no prominent change in morphology identified throughout the observation period (however once again, note how the output is impacted by the choice of threshold causing some data loss in very shallow areas to compensate for more accurate results across the catchment overall).

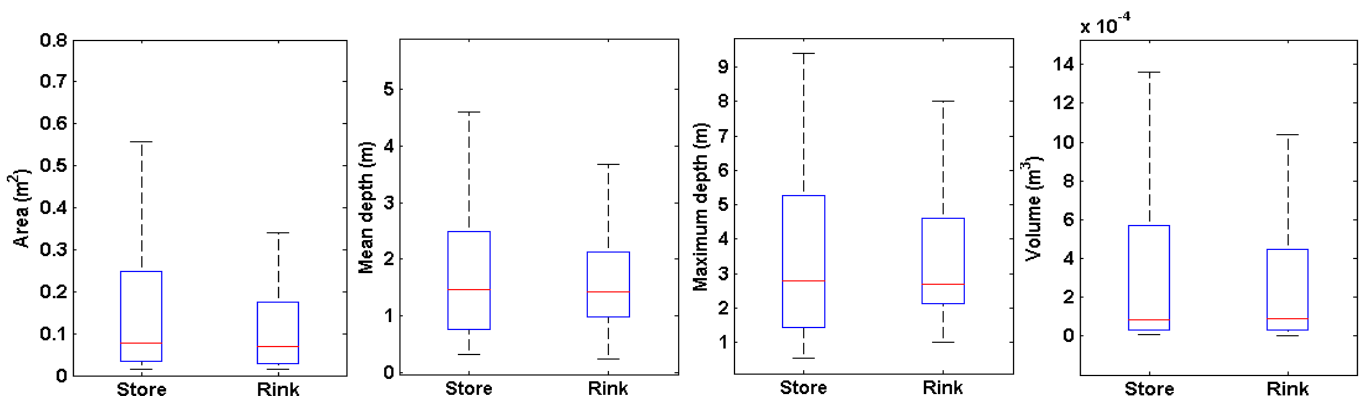


Figure 14: Boxplot diagrams comparing the same outputs in figure 11 and 12 for Store and Rink. For both glaciers, boxplots are shown for lake area (m²), mean lake depth (m), maximum lake depth (m), and lake volume (km³). In order for better visualisation of the data, outliers are removed, therefore extreme values either above or below the maximum and minimum values identified in each box plot are excluded from the data.

The boxplots in figure 14 identify the distributions of four parameters for the same images in figures 11 and 12; any outliers have been removed for better visualisation of the data. For all parameters, Store has a much wider range of lake type than Rink, particularly with regards to lake area and maximum lake depth. However, despite the deepest lakes at Store being deeper than those at Rink, the shallowest lakes at Rink are deeper than Store's shallowest lakes overall, for both mean and maximum depths. For lake volume, the smallest volumes are of similar magnitudes for both Store and Rink however the largest volumes at Store are greater than those at Rink.

3.1.3 Lake system evolution at Store and Rink

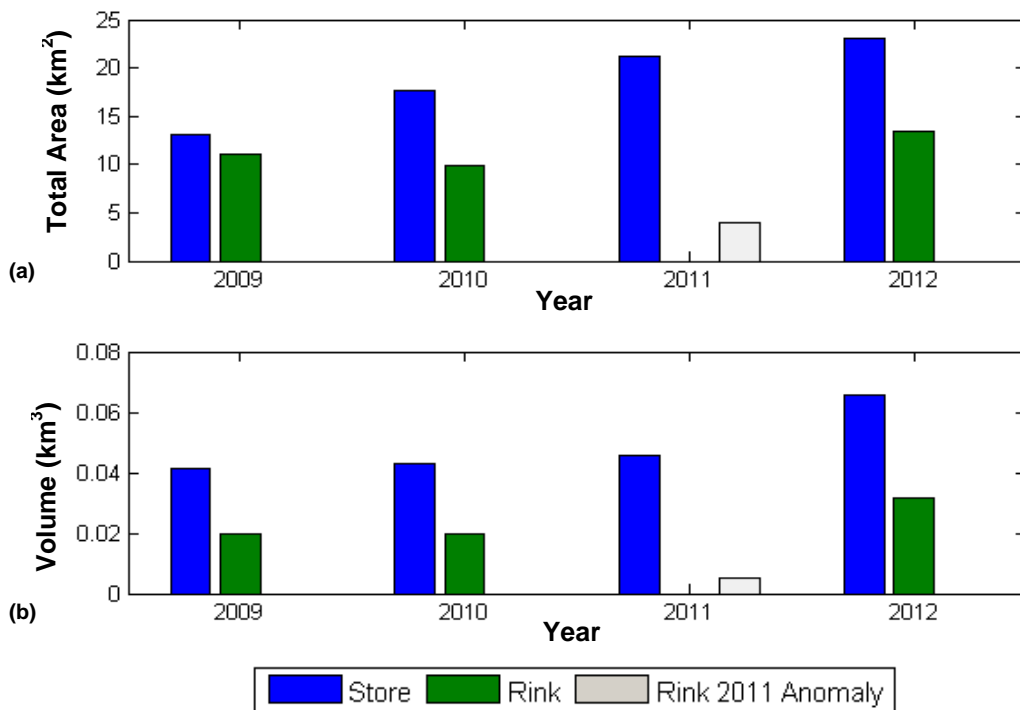


Figure 15: (a) Comparison between the trends in total lake areas (km²) at Store (blue) and Rink (green) (b) Comparison of total lake volume (km³) at Store (blue) and Rink (green) over the observation period 2009-2012. Each year represents a mean value for the total lake area and total lake volume of all suitable image acquisitions. The data for Rink in 2011 is in grey to highlight it as an anomaly due to insufficient data throughout the melt season.

Figure 15 compares changes in mean total lake area (a) and mean total lake volume (b) for Store (blue) and Rink (green) for all image acquisitions. The results for Rink in 2011 are also shown (grey), however clearly represent anomalous results due to poor temporal coverage and will therefore not be considered. Overall, Store has a greater mean total area and mean total volume than Rink for all years; this contrast is most significant in 2010 for both parameters where Store's mean total area is 1.79 times that of Rink, and mean total volume is 2.21 times that of Rink.

For both parameters, Store exhibits a clear increasing trend, particularly for mean total area, increasing from 13.1 km² in 2009 to 23.0 km² in 2012, and mean total volume, increasing 0.041 km³ in 2009 to 0.066 km³ in 2012. Rink also experiences an increase in both parameters between 2009 and 2012, with total area increasing from 11.0 km² to 13.4 km² and total volume increasing from 0.020 km³ to 0.032 km³. However, these numbers suggest a more significant trend at Store overall. Indeed, it is also apparent that at Rink, mean total lake area and mean total lake volume decrease between 2009 and 2010, with a -10.5% decrease in area, and a -0.46% decrease in volume. This contrasts greatly to Store, where Store experiences an increase in total lake area of +34%, and an increase in total lake volume of +4.6%.

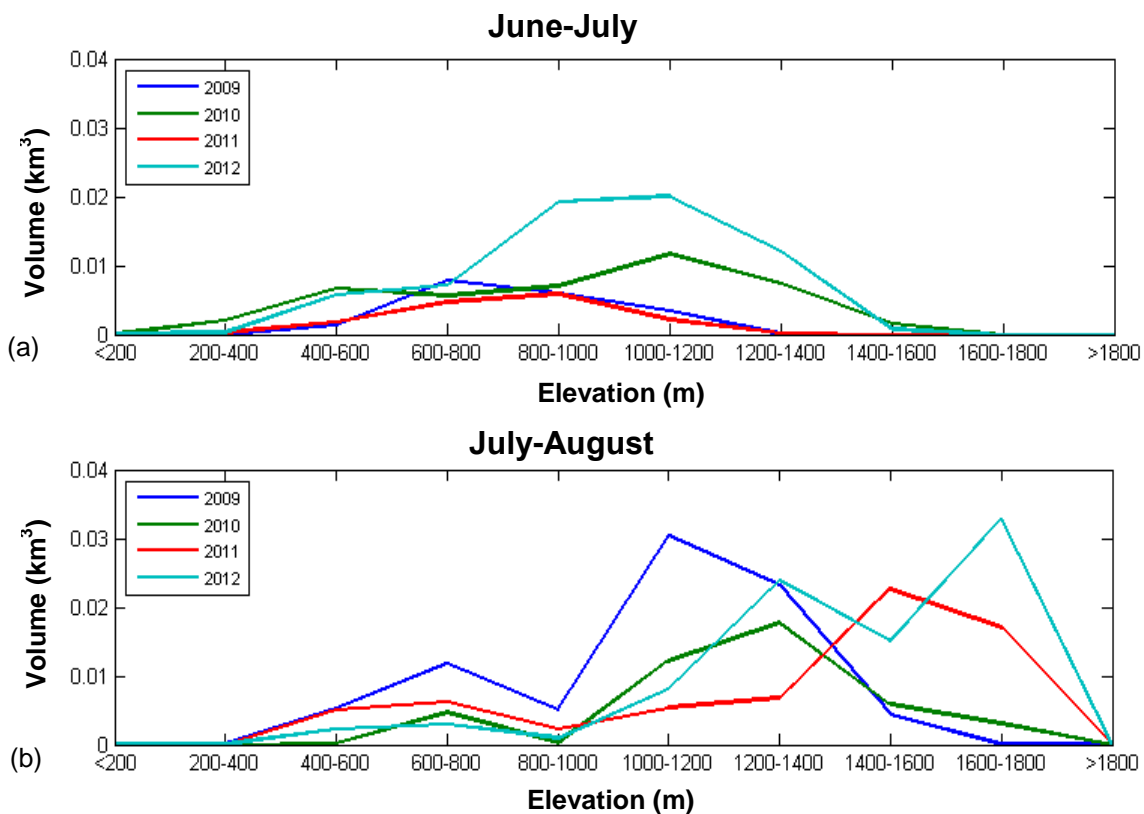


Figure 16: Comparing total lake volume (km³) identified within 200m elevation bands at Store 2009-2012 for the first half (a) and second half (b) of the melt season for 2009 (dark blue), 2010 (green), 2011 (red), and 2012 (light blue). Elevation is based on the GIMP DEM data (Howat *et al.*, 2010). Due to temporal coverage restrictions of the data, the two halves of the melt season are relatively ambiguous, taking mean values for data in June where appropriate and the first half of July in (a), and August and the second half of July in (b), using the most appropriate data possible.

To assess the distribution of total lake volume with elevation at different portions of the melt season at both glaciers, mean volume within 200 m elevation bands was estimated for the first half of the melt season (June and the first half of July), and the second half of the melt season (August and the second half of July). Figure 16 displays the results of this trend for Store where a distinct difference in lake volume distribution with elevation is identified. In the first half of the melt season (a), most volume is generally contained within

400-1200 m elevation bands. For years 2009 and 2011, the peaks occur at 600-800 m in 2009 (0.0079 km^3), and 800-1000 m in 2011 (0.059 km^3). However, for 2010 and 2012, peak volumes shift towards higher elevations peaking at 1000-1200 m in 2010 (0.012 km^3) and 2012 with an almost doubling of volume magnitude (0.02 km^3). For the second half of the melt season (b), there is a very distinct shift in the distribution of total lake volume towards higher elevations overall, with the peak volume occurring at higher elevations progressively each year. In 2009, the peak of 0.018 km^3 occurs at 1000-1200 m, in 2010 the peak of 0.012 km^3 occurs at 1200-1400 m, in 2011 the peak of 0.023 km^3 occurs at 1400-1600 m, and in 2012 the peak of 0.03 km^3 occurs at 1600-1800 m.

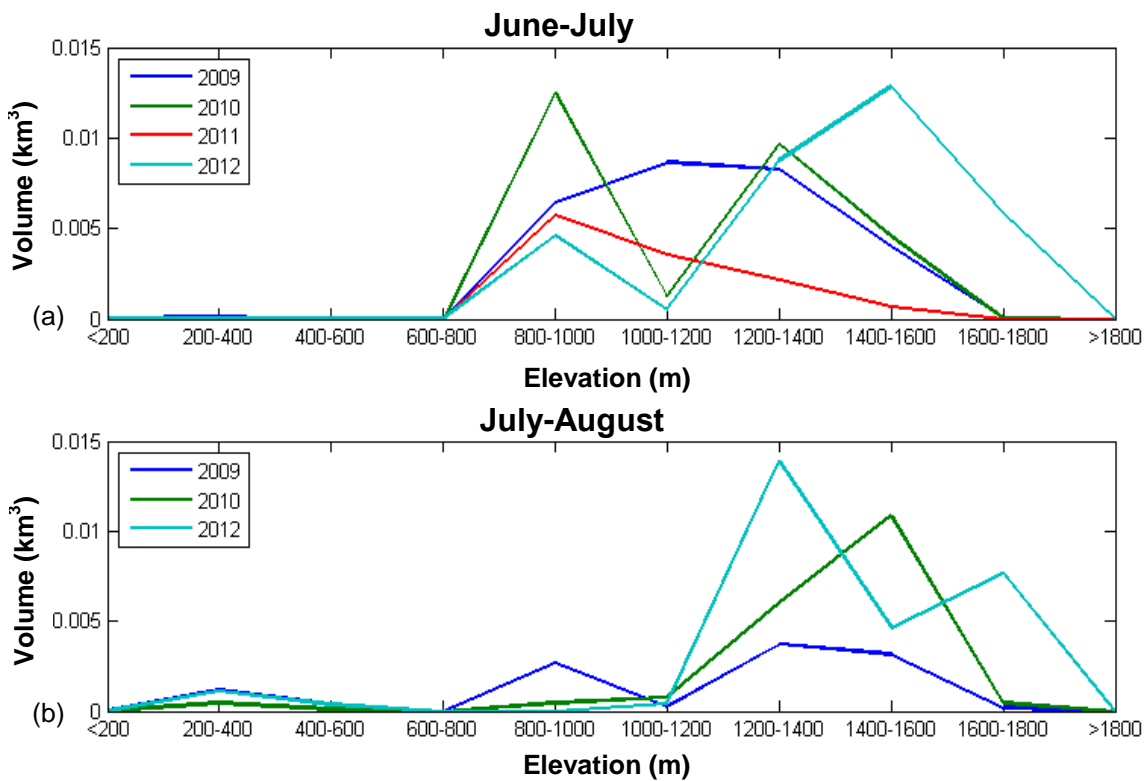


Figure 17: Comparing total lake volume (km^3) identified within 200m elevation bands at Rink 2009-2012 for the first half (a) and second half (b) of the melt season for 2009 (dark blue), 2010 (green), 2011 (red), and 2012 (light blue). Elevation is based on the GIMP DEM data (Howat *et al.*, 2010). Similarly to Store, due to temporal coverage restrictions of the data, the two halves of the melt season are relatively ambiguous, taking mean values for data in June and the first half of July in (a), and August and the second half of July in (b), using the most appropriate data possible. Fortunately, suitable 2011 data is available for the first half of the melt season (albeit in May) however there is no available data for the second half.

Contrasting to Store, the trend at Rink is far less pronounced (fig.17). For 2009 and 2010, there is a slight trend of the peak total lake volume shifting towards higher elevation bands between the first and second half of the melt season. In 2009, peak lake volume occurs at 1000-1200 m (0.0087 km^3) in the first half of the melt season, and a peak at 1200-1400 m (0.0037 km^3) in the second half of the melt season. In 2010, the peak lake volume increases from elevations of 800-1000 m in the first half of the melt season (0.012 km^3), to a peak at 1400-1600 m in the second half of the melt season (0.011 km^3). For 2010 in

particular, there is a distinct decrease in total lake volume within the 800-1000 m elevation band between the first and second half of the melt season, with a decrease of 0.012 km^3 . For 2012, the vast majority of lake volume is concentrated between 1000-1800 m in both the first half and second half of the melt season marking a different trend to observations in previous years. However, the elevation band at which peak volume occurs decreases between the first and second half of the melt season, with a decrease from 1400-1600 m (0.013 km^3) in the first half, to 1200-1400 m (0.014 km^3) in the second half, although there is still a high quantity of volume occurring at 1600-1800 m in the second half (0.008 km^3) pertaining to the vast majority being contained between 1000-1800 m elevations throughout the 2012 melt season.

3.1.4 Supraglacial lake drainage events

Store

Year	Number of events	Total volume drained (km^3)	Mean volume drained per drainage event (km^3)
2009	26	0.024	0.00092
2010	28	0.030	0.0011
2011	33	0.040	0.0013
2012	41	0.059	0.0014

Table 3: A summary of supraglacial lake drainage events identified at Store 2009-2012. For each year, the number of events, total volume drained (km^3), and mean volume drained (km^3) are shown.

Rink

Year	Number of events	Total volume drained (km^3)	Mean volume drained per drainage event (km^3)
2009	30	0.026	0.00087
2010	24	0.024	0.0011
2011	N/A	N/A	N/A
2012	26	0.035	0.0013

Table 4: A summary of supraglacial lake drainage events identified at Rink 2009-2012, however excluding 2011 due to insufficient temporal coverage. For each year, the number of events, total volume drained (km^3), and mean volume drained (km^3) are shown.

Tables 3 and 4 summarise drainage events identified at Store and Rink respectively over the observation period. The number of drainage events identified at both glaciers is relatively similar in the first half of the observation period, with 26 and 30 events identified in 2009, and 28 and 24 events in 2010 at Store and Rink respectively. However, in 2012 this trend changes significantly, where 41 drainage events are identified at Store, compared to only 26 events at Rink. The total volume drained at Store is also generally greater than that at Rink for all years, with Rink having a maximum total drainage volume of 0.035 km^3 in 2012 relative to 0.059 km^3 at Store also in 2012 (apart from 2009 where

Rink experiences marginally more drainage (0.026 km^3) than Store (0.024 km^3), although with fewer drainage events overall). The mean volume drained per event is very similar between the two glaciers for all years, however this is despite a greater number of drainage events occurring at Store overall. 2012 is a particularly prominent example where there is double the number of drainage events at Store relative to Rink despite both glaciers having very similar mean drainage volumes that year.

In terms of temporal progression, Store shows a distinct pattern of increasing number of drainage events, and increasing drainage event magnitude each year. There is a prominent contrast between 2009 and 2012 in particular, whereby in 2009, 26 lakes drain 0.024 km^3 , compared to 41 lakes draining 0.059 km^3 in 2012, indicating a +146% increase in drainage volume magnitude between these years. At Rink, there is no distinct trend in number of drainage events or total drainage volume throughout the observation period (although this is impacted by no available data for 2011). However, similarly to Store there is a distinct increase in the number of drainage events and total volume drained between 2009 and 2012, increasing from 30 lakes draining 0.026 km^3 in 2009 to 26 lakes draining 0.035 km^3 in 2012. However, proportionately this is a far less significant trend than at Store, with only a +34% increase in total volume drained between 2009 and 2012, compared to +146% at Store.

Upon assessment of all available Landsat imagery, lakes are identified to form and drain in the same locations each year at both glaciers. To demonstrate this, prominent examples at both glaciers are selected, comparing images acquired before and after lake drainage has occurred (figs.18-19). At Store (fig.18), three areas are highlighted to demonstrate lake formation and drainage in the same location each year. The red circle demarcates two particularly significant lakes. The lake nearer the terminus is identified to form and drain every year and is also one of the larger lakes in terms of lake volume, peaking at 0.0068 km^3 on 3rd July 2011. The second lake located ~3 km up-ice is another lake identified to form in the same location each year, however with drainage only captured in 2010 and 2012. The lakes outlined by the green box also drain recurrently, however they appear to have a far less cyclical nature than the first lakes identified, with full drainage only occurring in 2012. The lakes outlined by the blue box are also shown to drain recurrently each year.

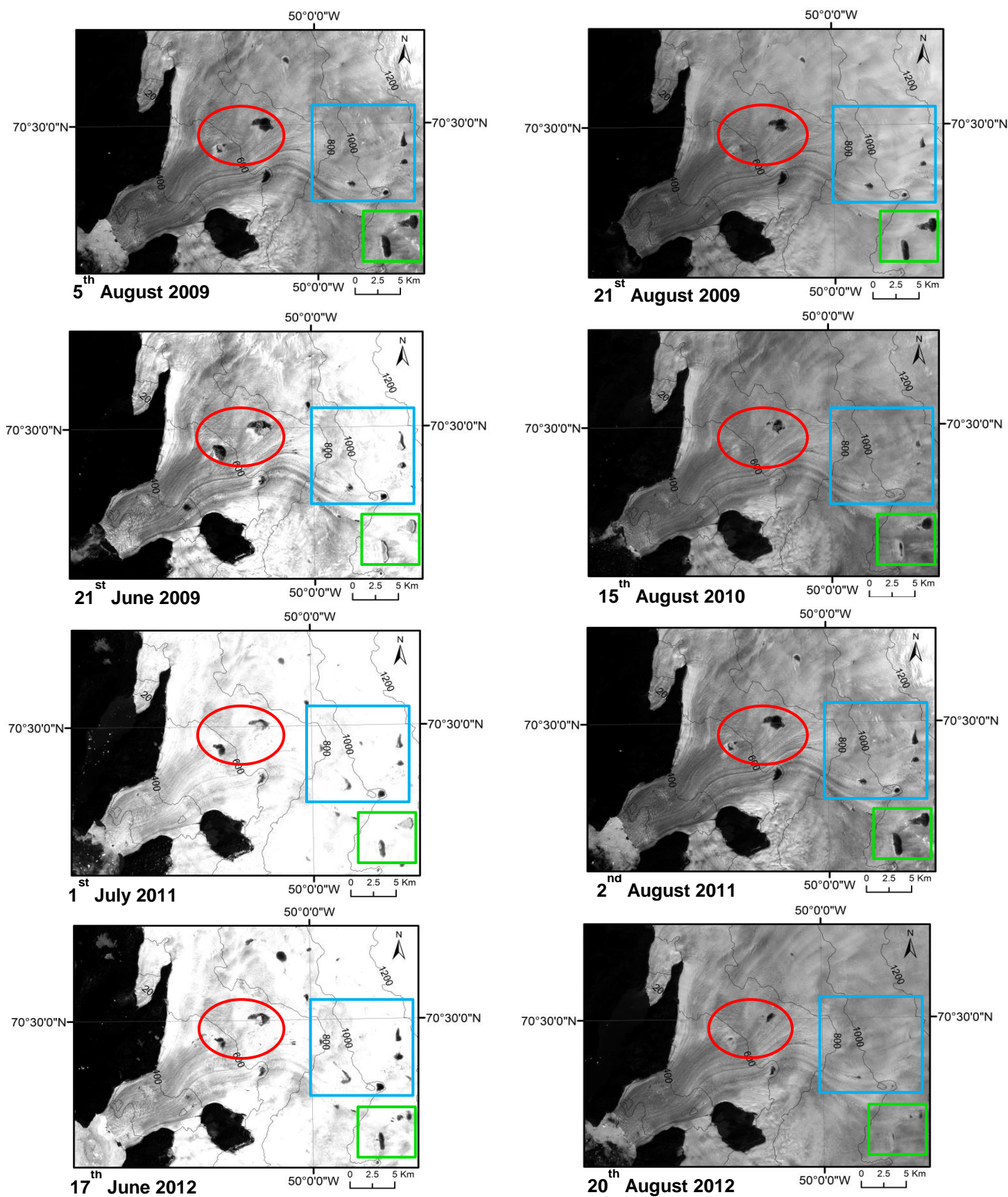


Figure 18: Examples of significant drainage events at Store near the terminus for all years as can be ascertained from the available Landsat imagery. Three key areas are highlighted by the red circle and green and blue boxes, for specific lakes identified to drain within the catchment, with their relative significances discussed in the text.

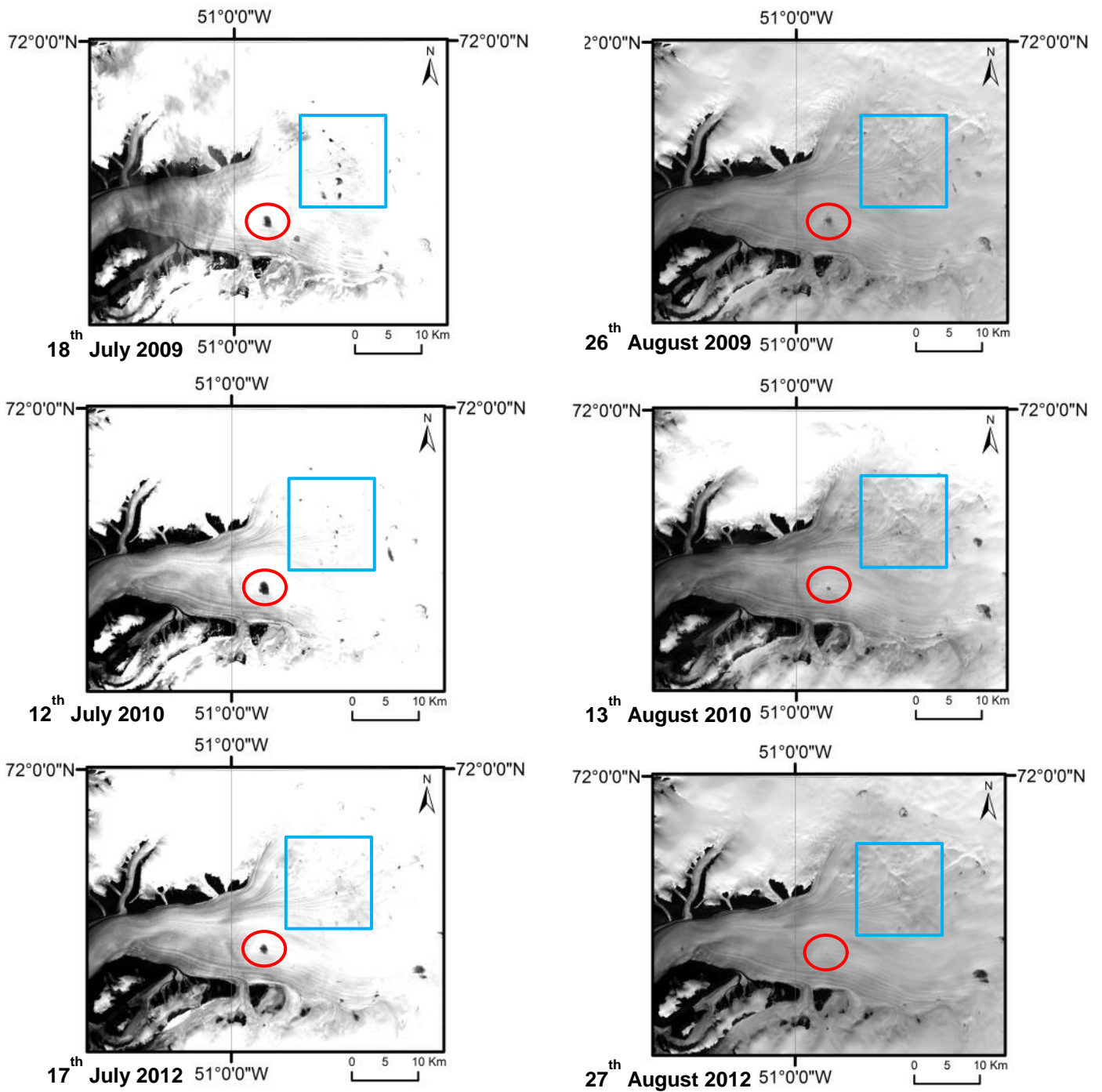


Figure 19: Examples of significant drainage events at Rink for available Landsat imagery 2009, 2010, and 2012. Two key areas are highlighted for specific lakes identified to drain within the catchment, with their relative significances discussed in the text.

Regions of recurrent lake drainage at Rink are also identified in figure 19. Of particular note is the lake outlined by the red circle, the same lake identified in figure 12 (c). For all years, this lake is shown to either fully or partially drain in the same location each year. Furthermore, this lake represents one of the largest lakes identified at both Store and Rink, with a maximum volume of 0.012 km^3 , and the largest estimated drainage event for both glaciers of 0.011 km^3 between 12th July and 13th August 2010. The lakes identified by the

blue box form in the same locations each year, and either fully or partially drain in 2009 and 2010 (with possible drainage in 2011 and 2012, however they are obscured by snow during these years). In terms of drainage volume however, these lakes are far smaller than the first lake, with volumes ranging 0.0005-0.008 km³.

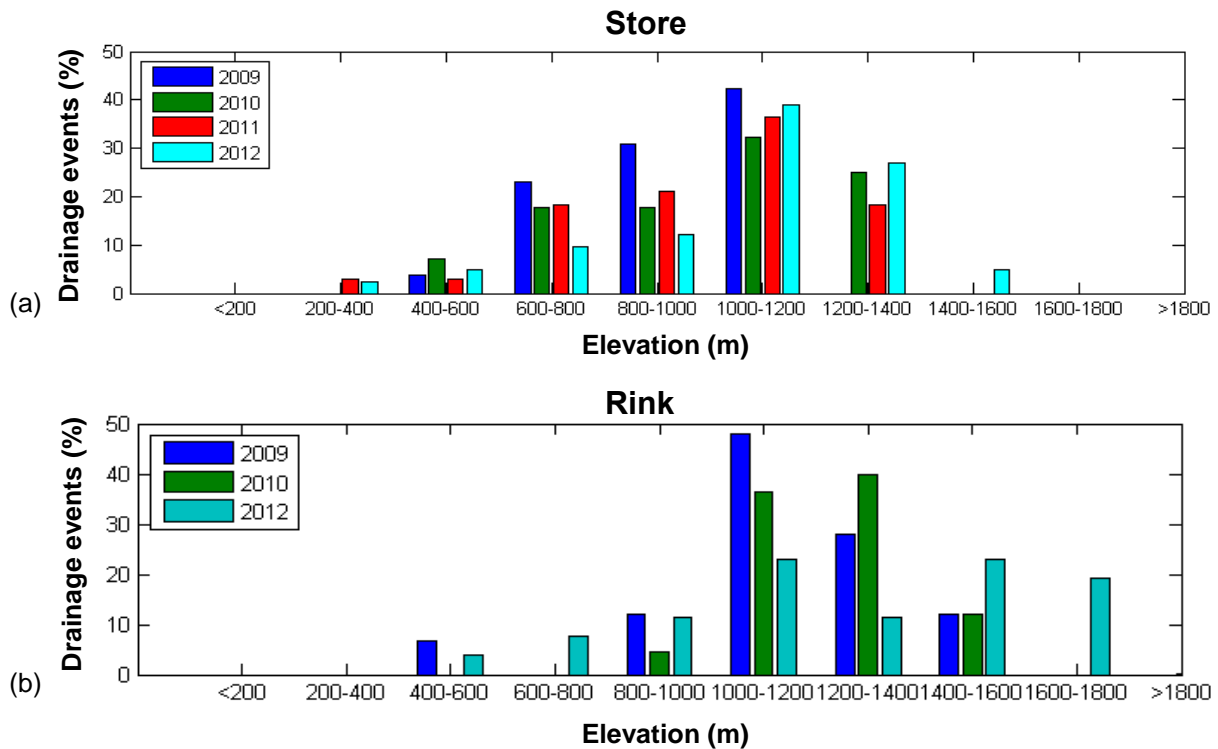


Figure 20: Bar graphs showing the percentage of the total number of drainage events identified each year 2009-2012 (2009 in dark blue, 2010 in green, 2011 in red, 2012 in light blue) occurring at different elevations within each glacial catchment for Store (a) and Rink (b). 200m elevation bands are used, using data from the GIMP DEM elevation data (Howat *et al.*, 2014). Due to insufficient temporal coverage at Rink in 2011, no data is included for 2011.

To indicate how lake drainage event occurrence varies with elevation between years, figure 20 quantifies the percentage of drainage events occurring within the same elevation bands as in figures 16 and 17 for each year 2009-2012 (excluding 2011 at Rink due to insufficient temporal coverage). The range of elevations at which drainage occurs at Store is generally skewed to higher elevations at Rink overall, ranging between 200-1600 m at Store, compared to 400-1800 m at Rink. For Store (fig.20 (a)), the peak in drainage event number occurs at 1000-1200 m for all years. However, there is still a noticeable trend of drainage events generally occurring at progressively higher elevations between years; the maximum elevation with drainage identified increases from 1000-1200 m in 2009, to 1200-1400 m in 2010 and 2011, and finally 1400-1600 m in 2012. For Rink (fig.20 (b)), drainage events tend to occur at higher elevations than Store overall, with only 2009 having its peak at a lower elevation between 1000-1200 m, whereas the peak in 2010 is 1200-1400 m and

the peak in 2012 is 1400-1600 m. Incidentally, there is also drainage identified to occur at 1600-1800 m elevations in 2012 which is not the case for Store for any year.

3.2 Seasonal change in ice flow

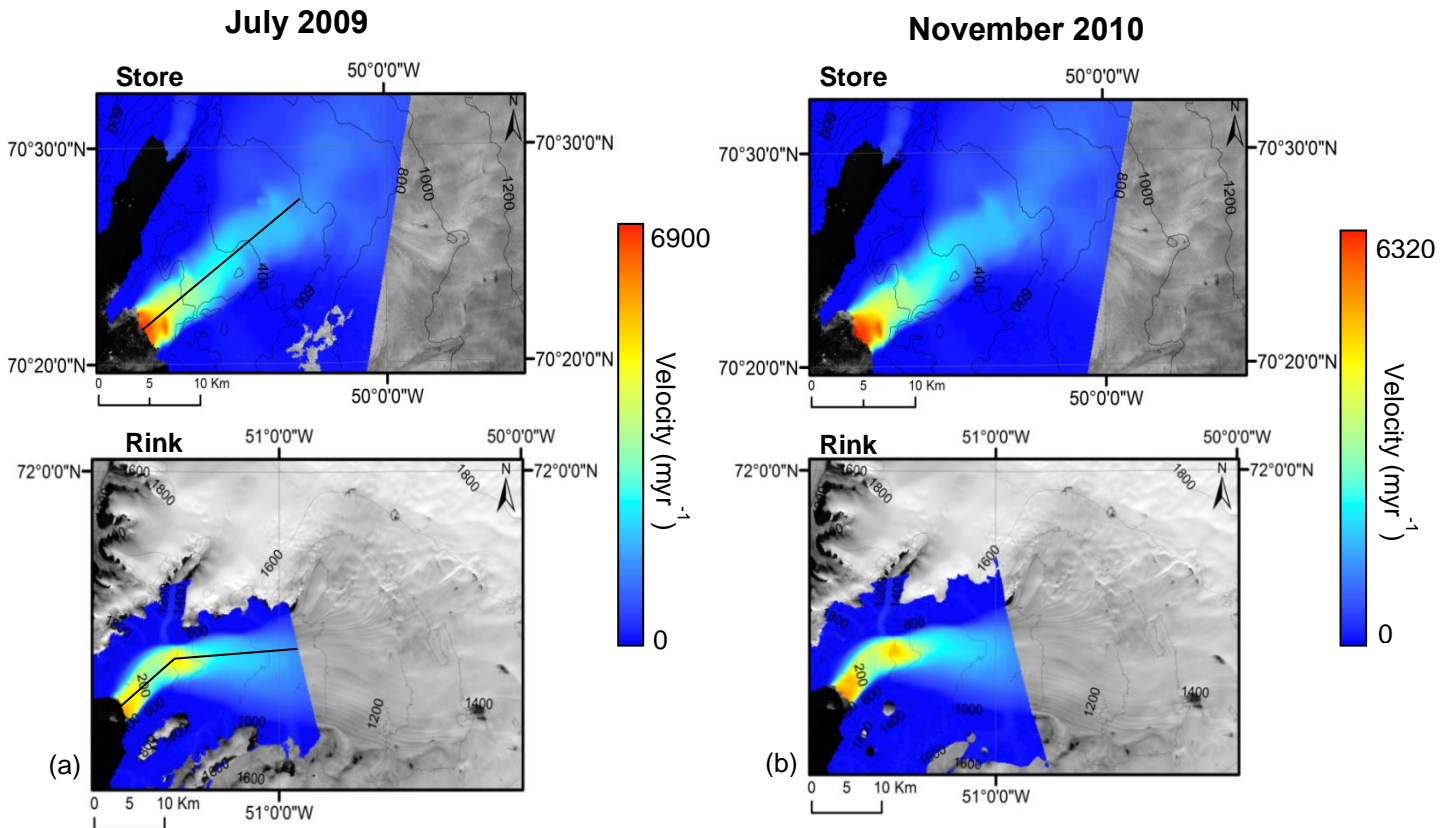


Figure 21: Examples of absolute velocity (myr^{-1}) on one day at Store (2nd July) and Rink (9th July) for summer 2009 (a) and winter 2010 (21st November at Store; 27th November at Rink) (b), using InSAR velocity data courtesy of the MeASUREs programme (Joughin *et al.*, 2011). Note that the scales on the colour bars differ. Elevation data is extracted from the GIMP DEM (Howat *et al.*, 2014). (The black lines on the July InSAR maps represent the flow-line transects used to find representative mean values for velocity in each acquisition, used for later analysis in figure 26.)

Store and Rink generally flow at similar rates to each other throughout the year (fig.21) although Store's maximum velocity is slightly higher than Rink in the examples in figure 21. Store's highest velocities are concentrated near the terminus, whilst at Rink this occurs further up the main trunk up to ~15 km from the terminus. Figure 21 also illustrates that absolute velocity is higher in summer (a) than winter (b) at both glaciers, with Store's peak velocity at 6900 myr^{-1} in July and 6320 myr^{-1} in November, whilst Rink's peak velocity is 5520 myr^{-1} in July, and 5499 myr^{-1} in November.

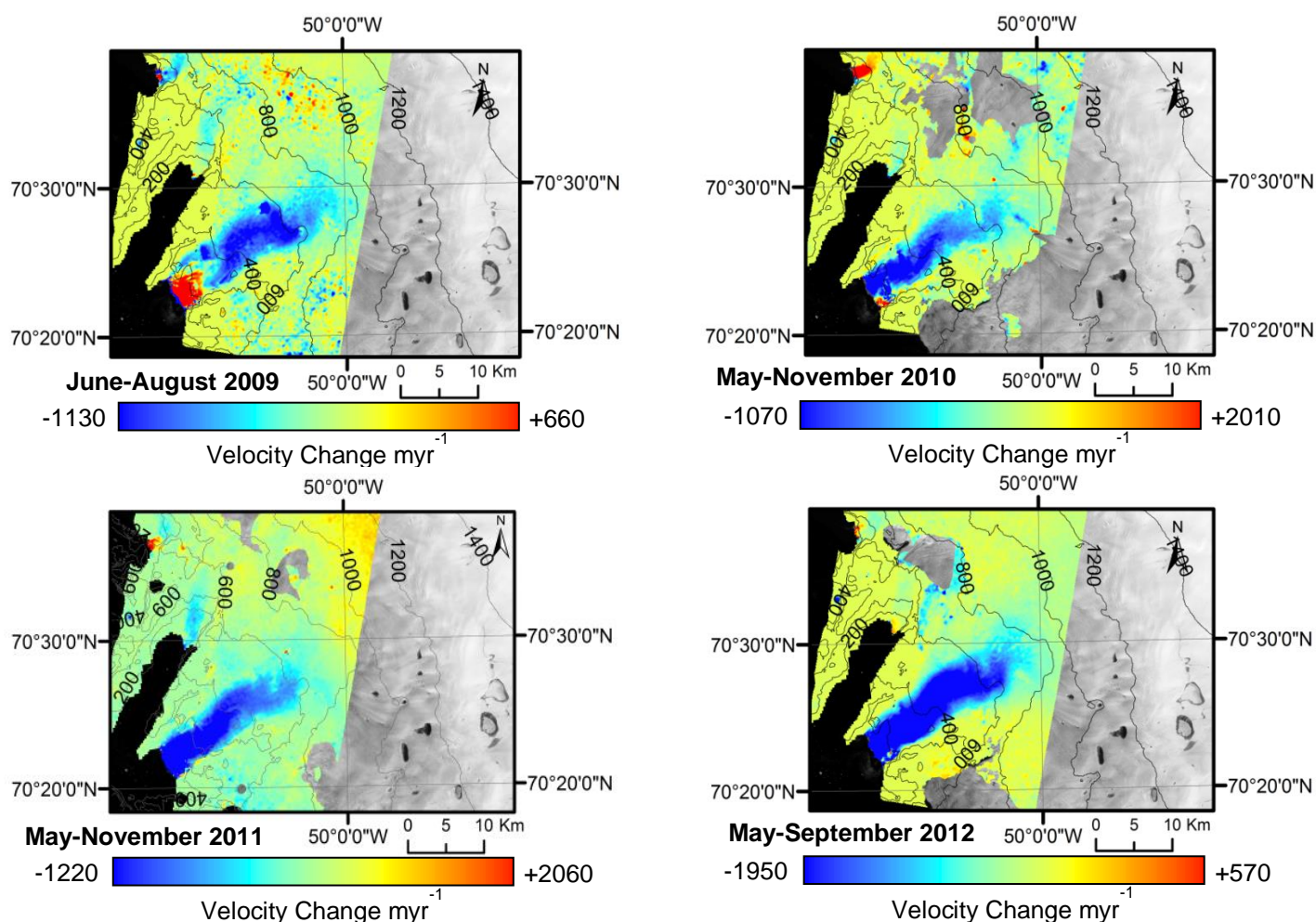


Figure 22: Velocity difference maps for the summer at Store 2009-2012 showing the net change in velocity over the summer months at Store (with selected months dependent on data availability), as indicated by the colour bars representing the change in velocity (myr^{-1}) each year. Blue colours signify net velocity decrease whilst red colours signify net velocity increase. Note that the scales on the colour bars differ. Data is InSAR velocity data courtesy of the MeASURES programme (Joughin *et al.*, 2011), whilst the elevation contours are courtesy of GIMP DEM data (Howat *et al.*, 2014).

Figures 22 and 23 identify net velocity change over the summer 2009-2012 (with coverage ranging April to November depending on InSAR acquisitions) at Store and Rink. Over the summer, Store (fig.22) exhibits net velocity decrease for all years, with the magnitude of this change varying between years; 2012 exhibits the greatest maximum change (-1950 myr^{-1}), and 2010 the smallest (-1070 myr^{-1}). The spatial trend reveals concentrated velocity decrease along main glacier trunk (in blue), most prominent in 2012. There is also evidence of velocity increase at the glacier terminus. In addition, there is evidence of velocity decrease occurring in patches at higher elevations for all acquisitions, generally illustrated by localised of high velocity decrease (dark blue) surrounded by lower velocity decrease (light blue). In addition to velocity decrease, there is also evidence of increase to the northeast in 2009 and 2011 contrasting to the general trend of velocity decrease.

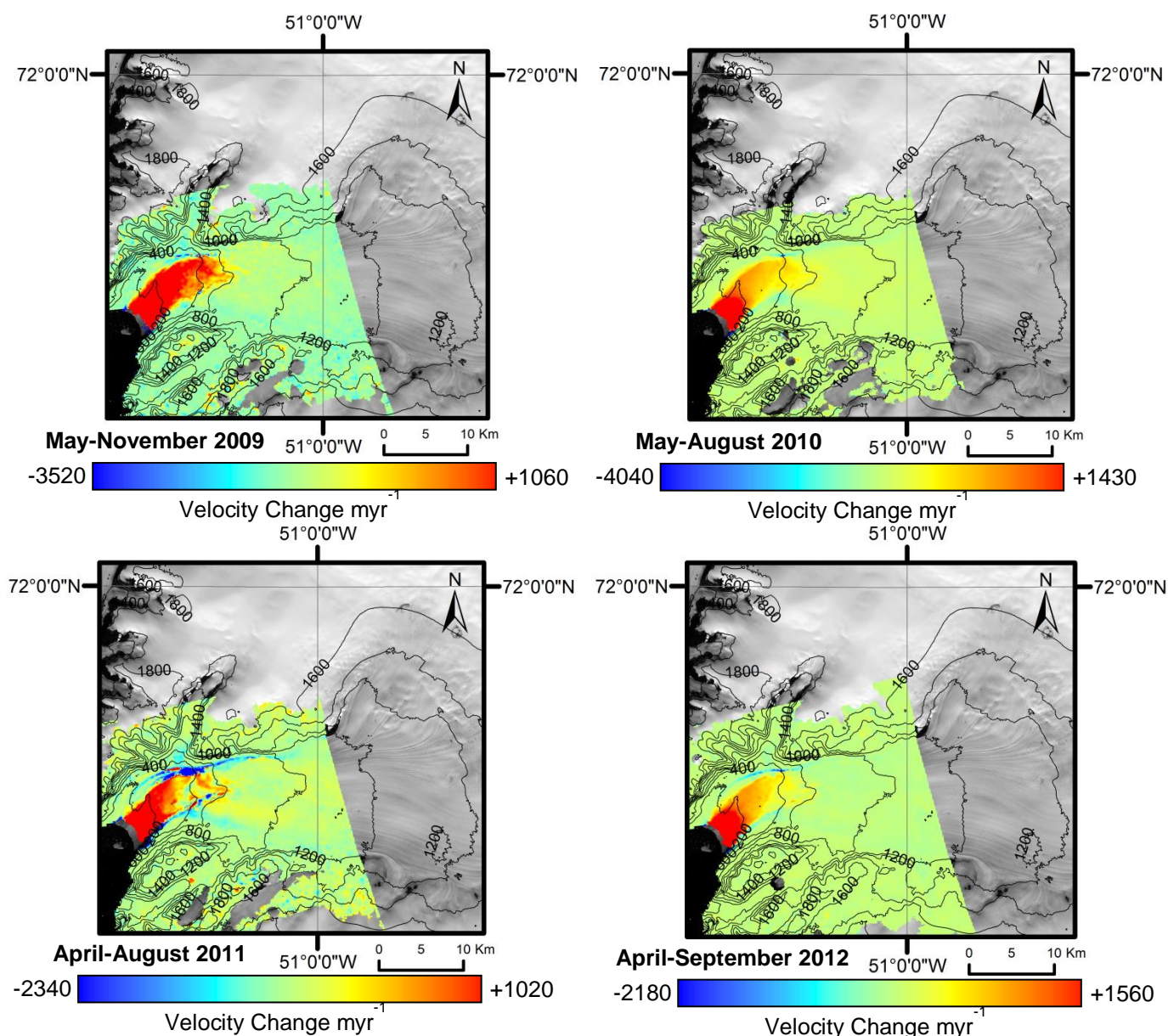


Figure 23: Velocity difference maps for the summer at Rink 2009-2012 showing the net change in velocity over the summer months at Rink (with selected months dependent on data availability), as indicated by the colour bars representing the change in velocity (myr^{-1}) each year. Blue colours signify net velocity decrease whilst red colours signify net velocity increase. Note that the scales on the colour bars differ. Data is InSAR velocity data courtesy of the MeASUREs programme (Joughin *et al.*, 2011), whilst the elevation contours are courtesy of GIMP DEM data (Howat *et al.*, 2014).

Contrasting to Store, the summer trend at Rink indicates a net increase in velocity (fig.23). The magnitude of this change varies each year, with 2012 experiencing the greatest maximum change ($+1560 \text{ myr}^{-1}$), and 2011 the lowest ($+1020 \text{ myr}^{-1}$). Once again, velocity increase is most prominent along the main glacier trunk. However, due to limited spatial coverage, it is not possible to identify velocity change at regions further inland. Contrasting to Store, there velocity decrease occurs at the lateral margins of Rink for all years with minimal evidence of velocity decrease elsewhere, and some decrease on the main glacier trunk in 2009 and 2011, however to a lesser extent.

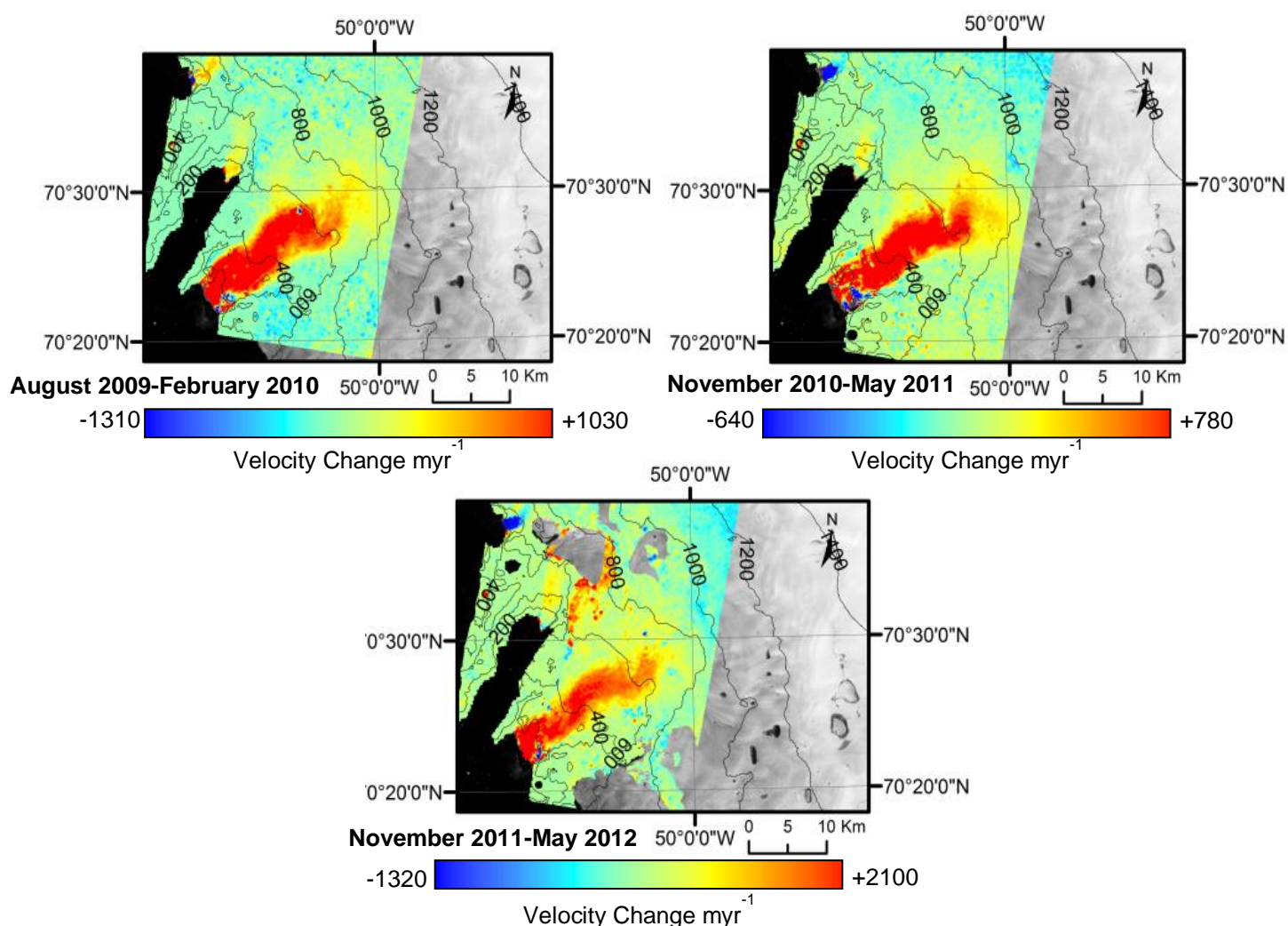


Figure 24: Velocity difference maps for the winter at Store 2009-2012 showing the net change in velocity over the winter months at Store (with selected months dependent on data availability), as indicated by the colour bars representing the change in velocity (myr^{-1}) each year. Blue colours signify net velocity decrease whilst red colours signify net velocity increase. Note that the scales on the colour bars differ. Data is InSAR velocity data courtesy of the MeASUREs programme (Joughin *et al.*, 2011), whilst the elevation contours are courtesy of GIMP DEM data (Howat *et al.*, 2014).

In comparison with summer velocity change, figures 24 and 25 illustrate winter velocity change for Store and Rink for the three winter periods 2009-2012 (with coverage ranging November to May depending on InSAR acquisitions). At Store (fig.24), there is an overall trend of net velocity increase similar to Rink's summer velocity change, concentrated along the main glacier trunk. There is generally less patchy velocity change identified further inland relative to summer, aside from a prominent zone of velocity increase to the north of Store's trunk during winter 2011-2012. 2011-2012 indicates the greatest maximum change for all winters ($+2100 \text{ myr}^{-1}$), whilst 2010-2011 has the lowest ($+780 \text{ myr}^{-1}$).

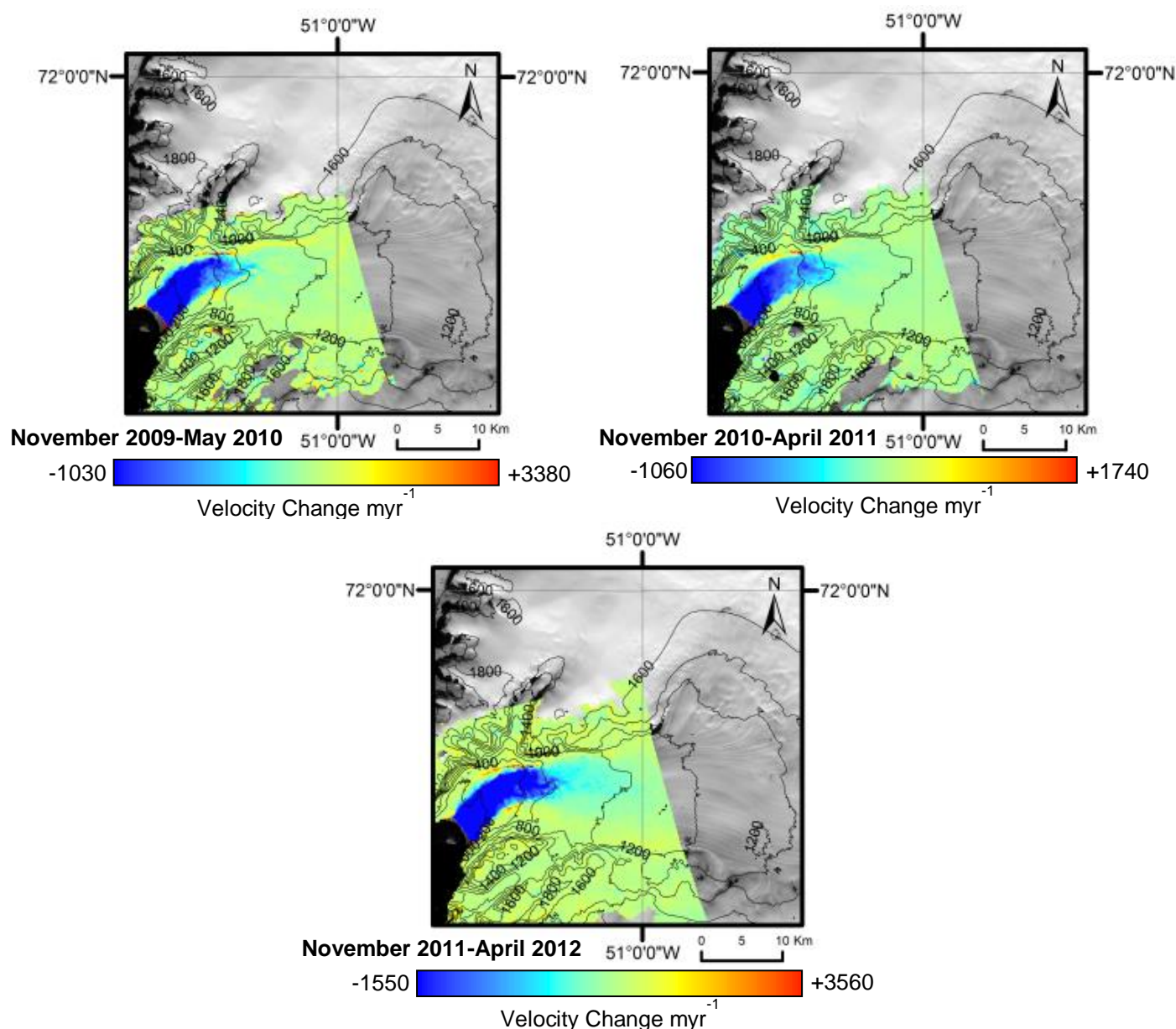


Figure 25: Velocity difference maps for the winter at Store 2009-2012 showing the net change in velocity over the winter months at Store (with selected months dependent on data availability), as indicated by the colour bars representing the change in velocity (myr⁻¹) each year. Blue colours signify net velocity decrease whilst red colours signify net velocity increase. Note that the scales on the colour bars differ. Data is InSAR velocity data courtesy of the MeASUREs programme (Joughin et al., 2011), whilst the elevation contours are courtesy of GIMP DEM data (Howat et al., 2014).

In contrast to Store, Rink shows a distinct net velocity decrease during the winter for all years (fig.25), similar to Store's summer velocity change (fig.24). Once again, this change is most prominent along the main glacier trunk with minimal evidence elsewhere. The largest change occurs 2011-2012 (-1550 myr⁻¹) and the smallest change occurs 2009-2010 (-1030 myr⁻¹). In further contrast to the summer, the lateral margins appear to show a net velocity increase over the winter, however a less prominent trend than the summer decrease.

3.3 Supraglacial lakes and velocity change

3.3.1 Trends through time

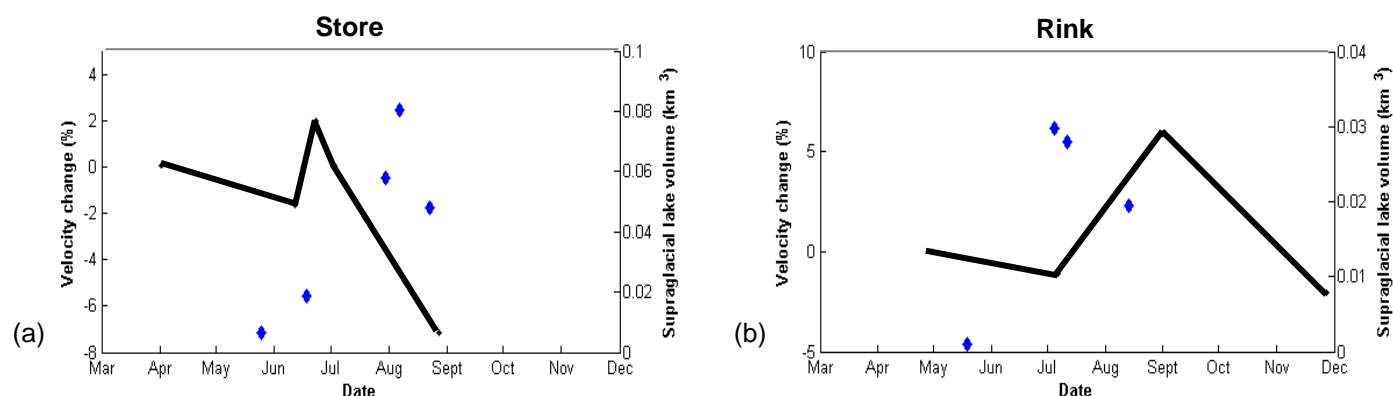


Figure 26: Percentage change in mean velocity for each InSAR acquisition (black line) compared to absolute total supraglacial lake volumes (km³) acquired using the lake detection algorithm for 2009 at Store (a) and 2010 at Rink (b) (blue diamonds). Mean velocity was acquired for each acquisition using velocity values along the flow-line transect in figure 21. These years were chosen due to containing the highest numbers of data points for both data sets, providing most effective comparison.

At Store, whilst total lake volumes increase throughout the melt season (Table 1), there is a net decrease in velocity overall (fig.22). This trend is broadly shown in figure 26 (a) comparing absolute lake volumes to percentage change in mean velocity acquired along a flow-line transect at each MeASURES InSAR acquisition in 2009 (fig.21), the year with the highest number of data points (however, caution must be taken with these results due to very limited data points masking potential changes in velocity and lake volume). In figure 26 (a), despite velocity increasing at the beginning of the melt season with increasing lake volumes, the highest magnitude increase in lake volume (+0.039 km³ between 18th June and 29th July) corresponds with significant velocity decrease (-7.1% 3rd July-27th August). Lake volumes are also shown to decrease (5th-21st August) with velocity decrease 3rd July-27th August however this occurs after the onset of velocity decrease on 22nd June.

In contrast, at Rink, with total lake volumes increasing over the summer period (Table 2), velocity is shown to increase as well (fig.23). Figure 26 (b) compares absolute lake volumes to percentage change in mean velocity acquired along a flow-line transect at Rink for each MeASURES InSAR acquisition in 2010 (fig.21), the year with the highest number of data points. In figure 26, the overall trend of velocity increase corresponds with lake volume increase. However, despite lake volumes decreasing after 5th July, velocity continues to increase until at least 31st August before velocity decrease over winter. However once again, the reliability of these trends is affected by the limited data points preventing significant comparisons from being made.

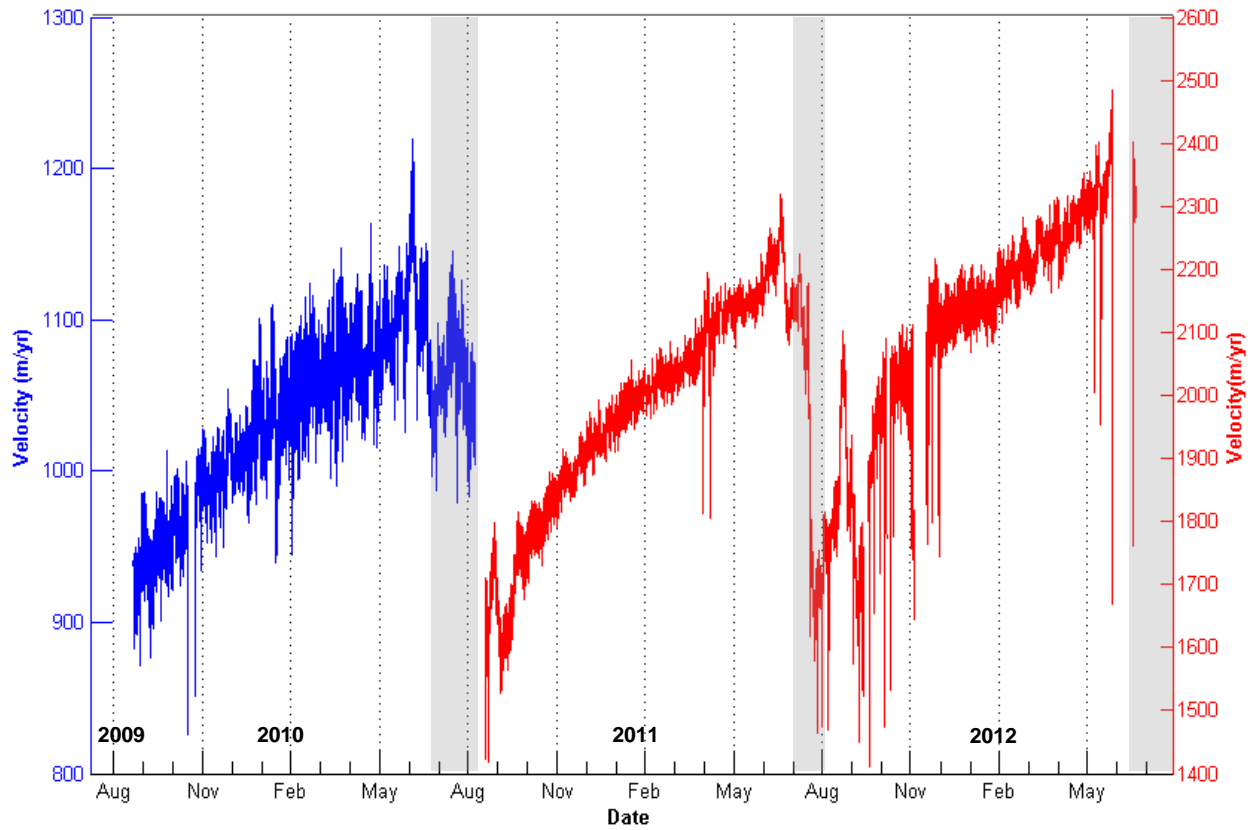


Figure 27: The occurrence of drainage events identified in figure 18 compared to velocity (m/yr) derived using *in situ* GPS at Store (Ahlstrøm *et al.*, 2013). The blue data corresponds to the left y-axis and the red data to the right y-axis for better visualisation of the data. Grey bars indicate the period of time before and after drainage of lakes in figure 18 based on available Landsat imagery.

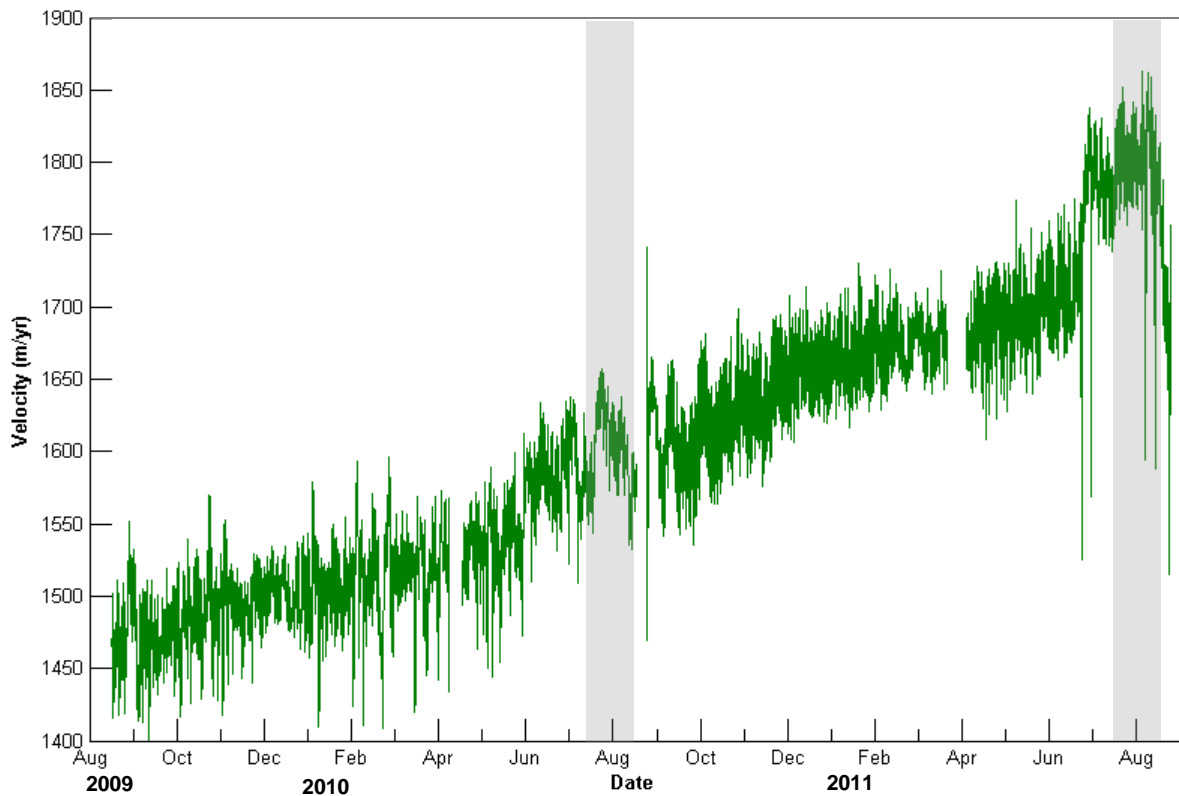


Figure 28: The occurrence of drainage events identified in figure 19 compared to velocity (m/yr) derived using *in situ* GPS at Rink (Ahlstrøm *et al.*, 2013). Grey bars indicate the period of time before and after drainage of lakes in figure 19 based on available Landsat imagery.

Although the *in situ* GPS data has been subject to severe advection effects (particularly at Rink) (fig.27; fig.28) (Ahlstrøm *et al.*, 2013), it demonstrates a relationship between supraglacial lake drainage and a midsummer slowdown at Store, with pre-and post-drainage image acquisitions outlining the period of drainage (grey bars) (fig.27). Therefore, the data are presented for both glaciers. At Store (fig.27), the GPS velocity data correspond well with the trends inferred by the InSAR velocity difference maps (fig.22; fig.24), with a net velocity decrease in summer and a net increase in winter. Although it is not possible to ascertain exactly when drainage occurred, it is clear that the likely period of lake drainage (between image acquisitions pre and post drainage) coincides with a distinct velocity decrease all years 2010-2012. At Rink (fig.28), drainage events do not correspond with a similar magnitude of summer velocity change as is the case at Store; however, these results must be treated with caution as the *in situ* GPS data for Rink do not correspond well with the InSAR velocity difference maps (fig.23; fig.25), indicating no decline in velocity over the winter, thus questioning the reliability of this comparison.

3.3.2 Trends through space

Due to various limitations affecting the reliability of the comparisons between lake volume, lake drainage, and velocity through time, it is more beneficial to compare the relationship between these variables in space. Therefore, the locations and magnitudes of individual supraglacial lake drainage events are superimposed onto summer InSAR velocity difference maps for all years at both glaciers to assess the relationship between lake drainage and velocity in space (figs.29-32).

Away from the main glacier trunk at Store (fig.29), there is some correspondence between drainage event locations and velocity decrease (purple boxes). This trend is particularly prominent in 2010 to the north of the main glacier trunk, where some of the largest identified drainage events occur (0.004-0.005 km³). A similar observation is made for 2009 where a region of slowdown occurs at the same location as a drainage event to the south of the main glacier trunk. However, there are also regions of velocity decrease where there is no evidence for lake drainage (pink boxes), particularly prominent in 2011 and 2012. In 2011, there is also evidence of widespread velocity increase (green box) not identified in other years, occurring in the same location as a group of 10 identified drainage events despite extensive drainage events occurring here.

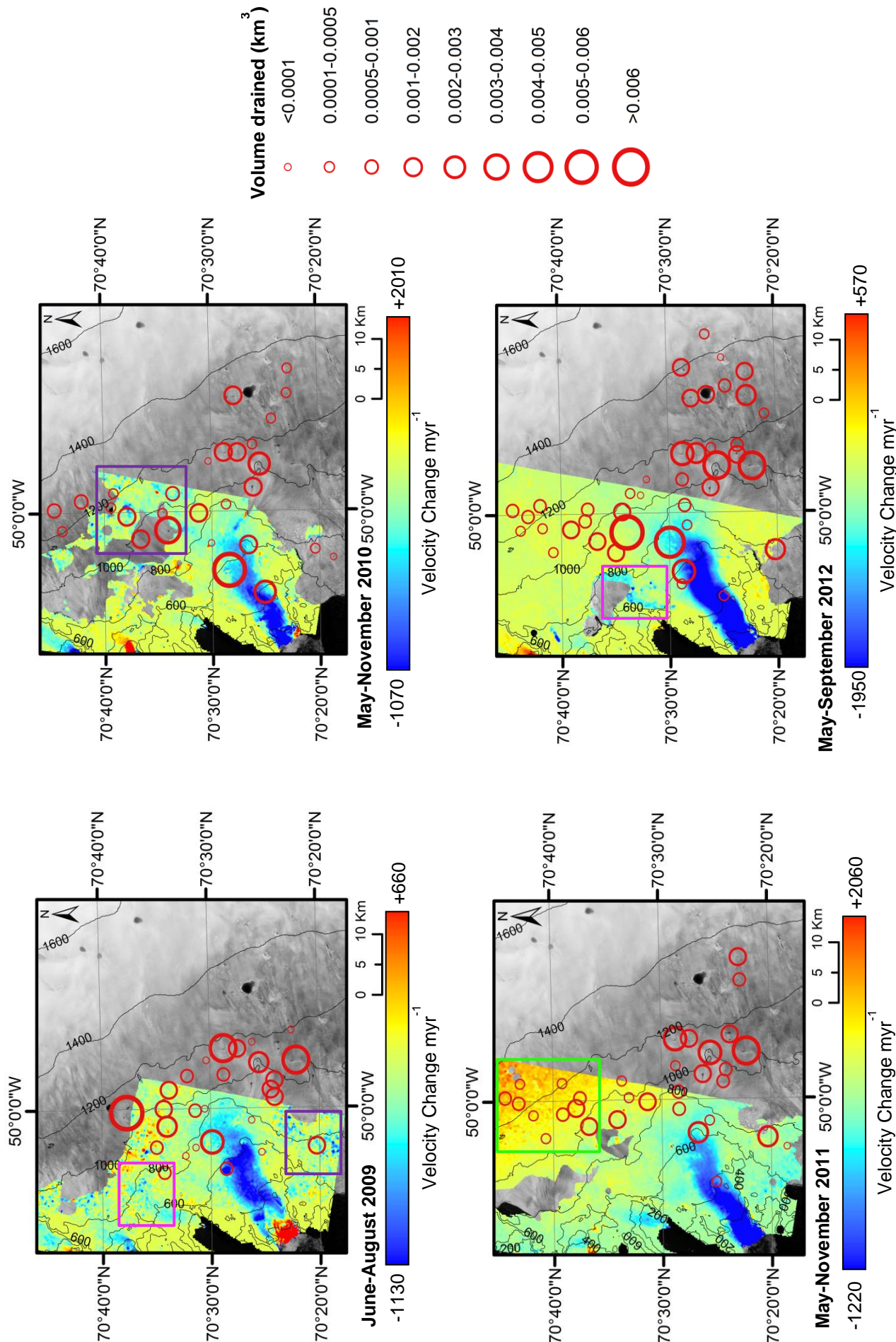


Figure 29: Summer velocity difference maps at Store (the same as in figure 22) using MeASURES InSAR velocity data (Joughin *et al.*, 2011) with identified lake drainage events superimposed according to their location (red circles). Red colours on the velocity maps indicate net velocity increase and blue colours indicate net velocity decrease. Lake drainage events are presented as graduated symbols in terms of estimated lake drainage volume (km³) between imagery throughout the melt season in 2009-2012 (see figure key). Note that the scales on the colour bars differ. Key areas of interest are outlined by coloured squares, with their significance discussed in the text. The elevation contours are elevation data extracted from the GIMP DEM data (Howat *et al.*, 2014).

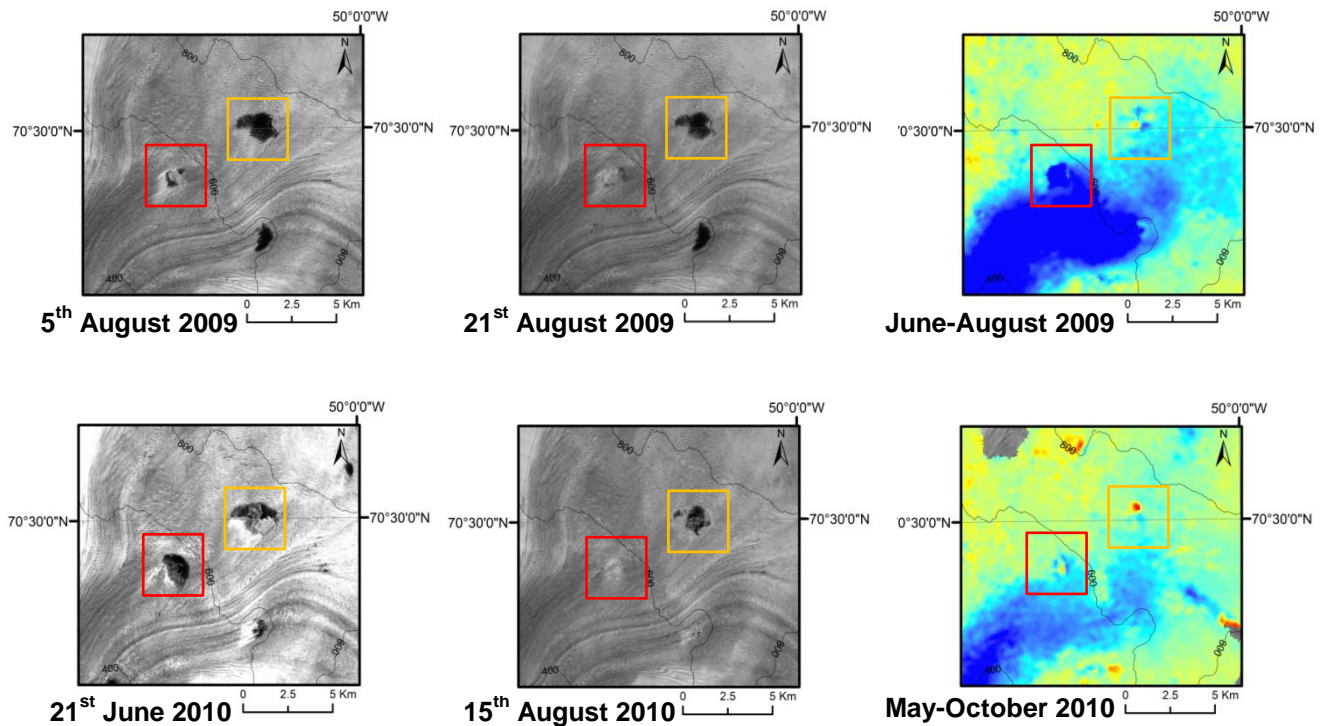


Figure 30: Specific examples of drainage events identified at Store identified to coincide with net change in velocity over the equivalent summer period using MeASUREs velocity data for 2009 and 2010 (Joughin *et al.*, 2011). Both lakes in the red and orange boxes are the same lakes identified to drain in figure 18. The colours on the velocity maps are equivalent to the colour bar values in figure 31.

On the main glacier trunk, there are localised points of significant velocity change identified to correspond with the locations of two larger drainage events (with maximum estimated drainage volumes of 0.054 km^3), particularly in 2009, and 2010 (fig.30). In 2009, the two lakes identified are superimposed over localised velocity change. The lake in the red box, shown to drain all observed melt seasons in figure 18, corresponds with a region where velocity decreases by $\sim 800 \text{ myr}^{-1}$. However, despite this high magnitude velocity decrease, this lake does not have a significantly high drainage volume (0.00024 km^3). In 2010, the same lake has a higher drainage volume than 2009 (0.0053 km^3), also occurring in a location of velocity decrease as in 2009, however with lower velocity change overall. There is also evidence of velocity increase in the same locality. The second lake (orange box) also corresponds with localised velocity decrease in 2009 showing a similar pattern to that observed by the first lake in 2010. In 2010, the second lake drains where high velocity increase is observed amongst net velocity decrease. In terms of drainage magnitude, this lake is estimated to drain 0.0029 km^3 in 2009, however only 0.00004 km^3 in 2010, representing a lower magnitude drainage event.

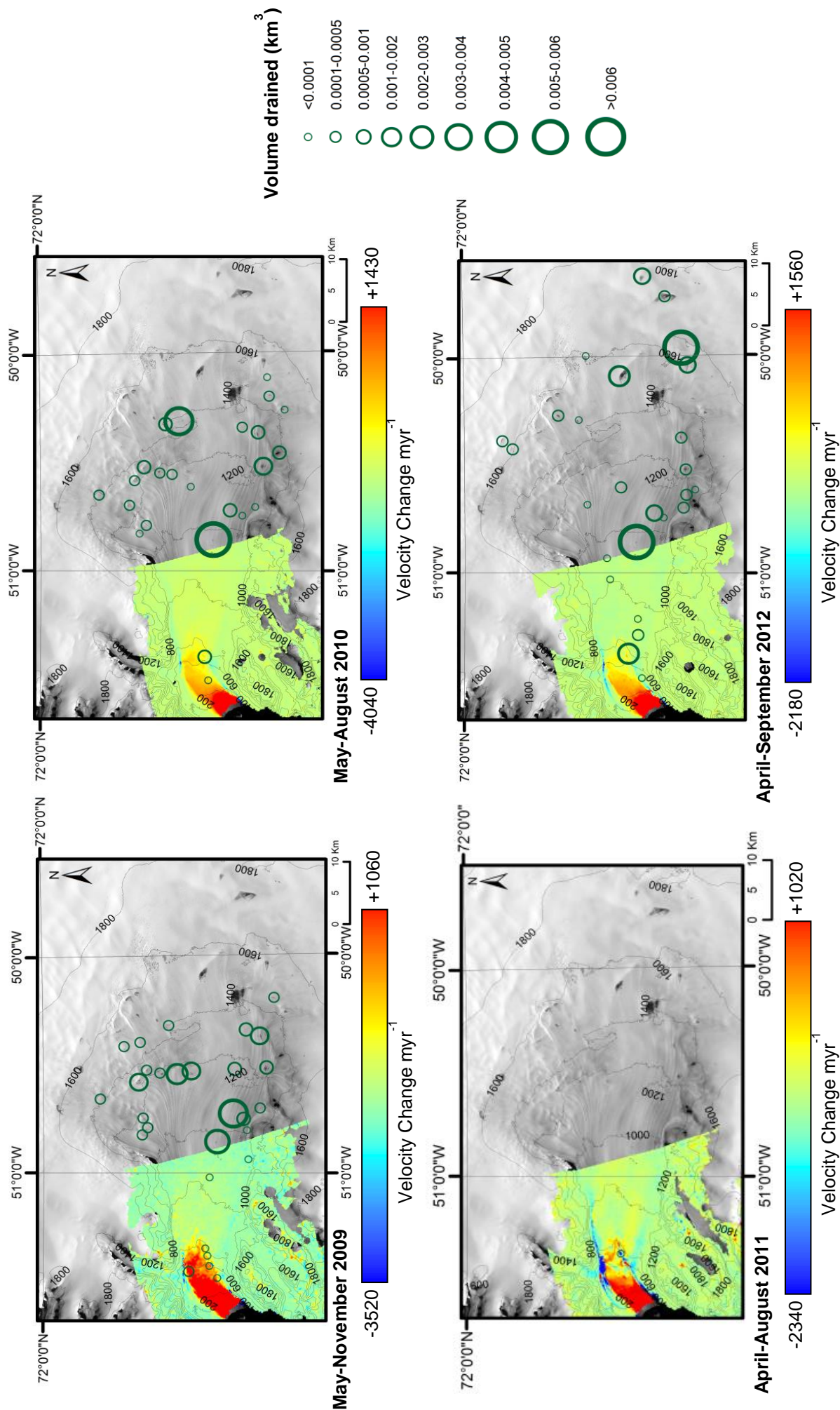


Figure 29: Summer velocity difference maps at Rink (the same as in figure 23) using MeASURES InSAR velocity data (Joughin *et al.*, 2011) with identified lake drainage events superimposed according to their location (green circles). Red colours on the velocity maps indicate net velocity increase and blue colours indicate net velocity decrease. Lake drainage events are presented as graduated symbols in terms of estimated lake drainage volume (km³) between imagery throughout the melt season in 2009-2012 (see figure key). Note that the scales on the colour bars differ. The elevation contours are elevation data is extracted from the GIMP DEM data (Howat *et al.*, 2014).

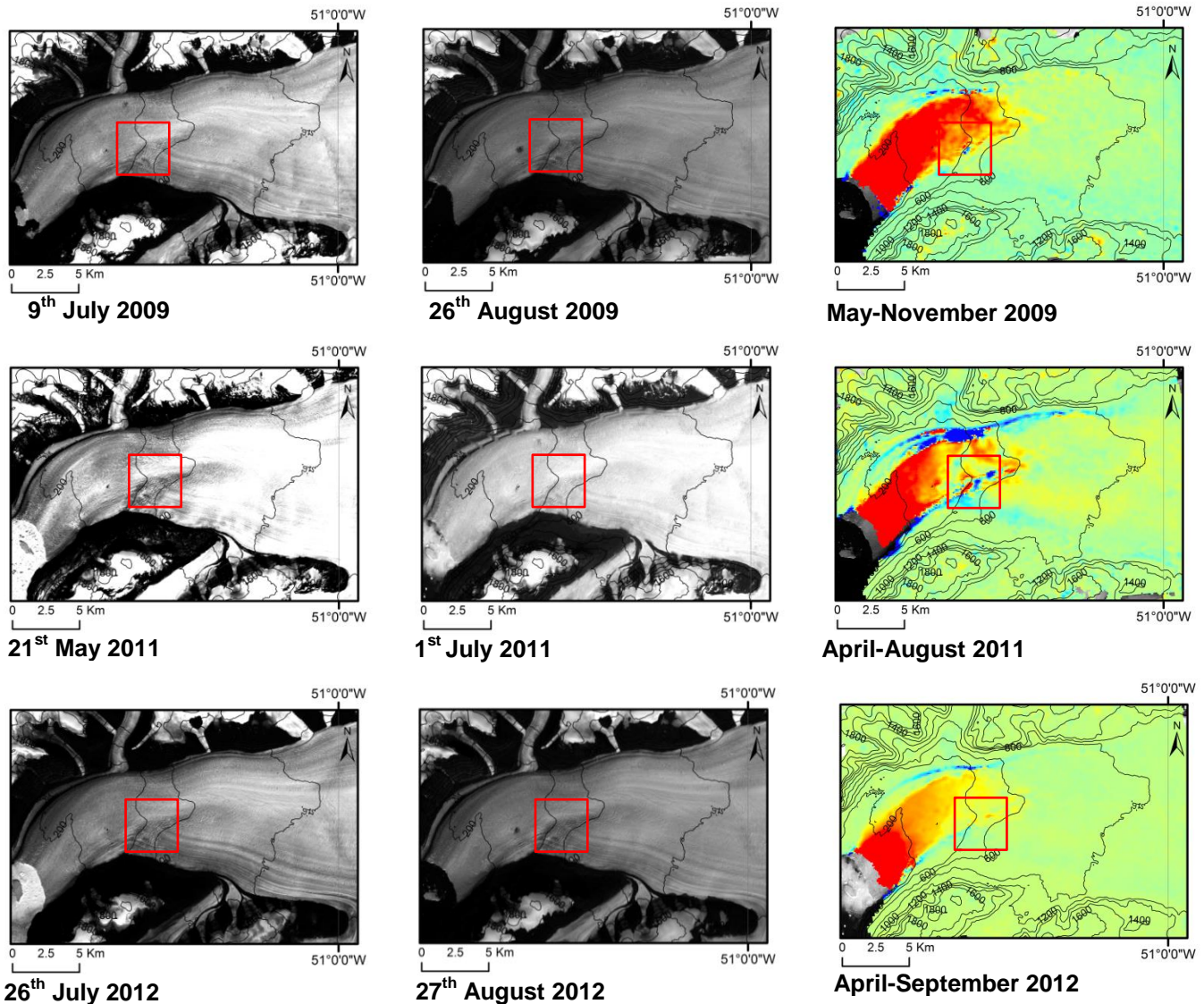


Figure 32: Specific examples of drainage events identified at Rink (in this case water-filled crevasses) identified to coincide with net change in velocity over the equivalent summer period using MeASURES velocity data for 2009, 2011, and 2012 (Joughin *et al.*, 2011). The colours on the velocity maps are equivalent to the colour bar values in figure 31. Although they are not clearly visible from the Landsat imagery, the lake detection algorithm clearly identify a change in lake number and volume at these locations in the form of water-filled crevasses between image acquisitions.

Unfortunately for Rink, the InSAR acquisitions do not have sufficient spatial coverage to cover most drainage events identified between 2009 and 2012 (fig.31) allowing for less detailed comparisons than at Store. However, from the drainage events that do, there is some possible evidence for supraglacial lake drainage events coinciding with localised velocity change (fig.32). In 2009 and 2011, there is evidence to suggest that drainage of the water-filled crevasses between 400-600 m elevations corresponds to localised velocity decrease. The lakes identified to drain are shallow water-filled crevasse lakes and although they are not clearly visible on the Landsat imagery, there is evidence of possible drainage due to their reoccurrence and drainage each year identified using the lake detection algorithm corresponding to some small evidence of pooling in the Landsat

imagery. These drainage events range in magnitude between 0.000048 km³ in 2010 to 0.0015 km³ in 2012 and therefore represent relatively low magnitude drainage events. However, for 2011 in particular, it is unclear whether this velocity decrease is instead a continuation of velocity decrease along the lateral margins of the glacier trunk rather than as isolated patches. Contrasting to 2009 and 2011, in 2012, in the same location drainage of the same lakes coincides with velocity increase; this is also the year where the drainage volume at this location was greatest (0.015 km³). However, this is a relatively minor increase in velocity (+220 myr⁻¹), compared to maximum increases of +1560 myr⁻¹.

3.4 Results summary

3.4.1 Supraglacial lake evolution

At both glaciers lakes form and drain in the same locations each year, with Store producing more lakes overall. The supraglacial lake system at Store is more diverse than at Rink, with a wider range of lake morphologies and volumes, however generally Rink's shallowest lakes are deeper than Store's shallowest lakes. At lower elevations, lakes form and drain earlier and exhibit little change overall whilst lakes at higher elevations evolve at slower rates.

Total supraglacial lake volume and drainage volume increases each year at both glaciers, with Store experiencing more drainage events overall with a greater volume drained. Store also experiences a much greater change in drainage between in 2012 relative to 2009, with a +146% increase in drainage volume compared to Rink's +34% increase.

Two lakes are identified to drain on an annual basis at Store, and one lake at Rink, with some of the larger magnitude drainage events identified. Every year at both glaciers, the percentage of total volume drained each year progressively increases to higher elevations, reaching higher maximum elevations at Rink than Store, with lakes at Rink generally draining at higher elevations overall.

3.4.2 Velocity change

Store and Rink exhibit opposite trends in inter-seasonal velocity change, with a net decrease in summer and a net increase in winter at Store, but a net increase in summer and net decrease in winter at Rink.

3.4.3 Supraglacial lake drainage and velocity

Through time, Store's velocity decreases with increasing total lake volume, however Rink's velocity increases with lake volume increase, however continues to increase after total lake volume decreases. Relating velocity trends through time with supraglacial lake drainage, drainage at Store coincides with sharp midsummer velocity decrease, with no significant trend observed at Rink.

Through space, patches of velocity decrease at Store often correspond to drainage events, although with no correlation to drainage event magnitude. However, there are also regions where velocity decrease does not coincide with lake drainage. The two identified drainage events indicate a relatively strong correspondence to localised velocity change overall in 2009, and 2010. Widespread velocity increase is also observed inland in 2011, coinciding with 10 identified drainage events. At Rink, due to restricted spatial coverage, it is not possible to make the same detailed comparisons, however where water-filled crevasses drain near the terminus, there is some possible evidence of localised velocity change in 2009, 2011, and 2012.

4.0 Discussion

4.1 Comparing the supraglacial lake systems at Store and Rink

Both glaciers demonstrate increasing lake formation at progressively elevations each year reflecting recent trends elsewhere (e.g. Howat *et al.*, 2013). Surface runoff is identified to be a key factor in determining lake formation and evolution by providing the available melt for lake pooling (Leeson *et al.*, 2014). Coinciding with temperature increases by 2°C in this region over the past two decades with higher temperatures associated with increased runoff production (Howat *et al.*, 2010) both glaciers demonstrate increasing total lake volume and total lake area over the observation period (fig.15) thus reflecting this relationship (McMillan *et al.*, 2007; Fitzpatrick *et al.*, 2014). Howat *et al.* (2013) have attributed this trend at varying portions of the GrIS to increasing elevations of the snowline over the past two decades, with snow melting at progressively higher elevations generating runoff increasingly at higher elevations (Braithwaite *et al.*, 1994), causing inland expansion of the lake line.

However, with higher elevations experiencing a more prolonged melt season due to summer lapse rates, lakes in these regions tend to form later in the melt season with lower rates of temperature rise and therefore more prolonged evolution (Lüthje *et al.*, 2006),

demonstrated by the lakes in figure 13 (Abdalati and Steffen, 2001). This therefore corresponds to lakes at lower elevations being found to form earlier in the melt season and experience little change in morphology, representing more intense warming here (McMillan *et al.*, 2007).

A more specific comparison can be made for both glaciers between high and low melt years. 2009 and 2011 were relatively cold and thus identified as low melt years whilst 2010 and 2012 are considered to be high melt years (Hanna *et al.*, 2014; Fitzpatrick *et al.*, 2014). Between 2009 and 2012, total supraglacial lake volume drained at Rink increased by +34%, likely relating to the difference between low and high melt years, whilst at Store, there was an increase of +146%. Additionally, the percentage of total drainage events within 200 m is at a maximum at higher elevations in 2010 and 2012 than in 2009 and 2011 at both glaciers, indicating a further relationship. It is therefore likely that lakes are able to reach sufficient volumes for drainage at higher elevations during high melt years with the possibility of an intensified 'slow fill fast drain lake cycle' at these elevations (Fitzpatrick *et al.*, 2014).

However, compared to Store, lake evolution and drainage trends at Rink are far less distinct, with only 2012 exhibiting a significant difference relative to previous years (figs.16-19). Furthermore, during June-July 2010, the warmest part of the observation period (Fitzpatrick *et al.*, 2014) the proportional area covered by lakes is 0.0059% at Store, almost double that of Rink (0.0035%) indicating lower lake coverage overall (figs.11-12). It is also apparent that Store has a more diverse lake system than Rink, with a wider range of lake sizes and morphologies (figs.11-12; fig.14). Furthermore it has already been identified that Rink experiences only a +34% increase in lake drainage volume relative to Store's +146% increase between a low melt (2009) and high melt (2012) year indicating a stronger trend at Store overall. Indeed, at Rink, the total number of identified drainage events appears to decrease over the period, despite an overall increase in total volume drained.

Surface runoff has been identified as one of the primary factors in determining lake evolution and morphology (Liang *et al.*, 2012). However, due to Store and Rink's relative proximity (with only ~150km north-to-south between them), the volume of surface runoff per unit area is unlikely to vary enough to cause this significant difference in supraglacial lake systems (McMillan *et al.*, 2007; Abdalati and Steffen, 2001). Indeed, lakes generally form at higher elevations at Rink than Store despite being further north which is usually

indicative of cooler conditions; therefore, differences in absolute air temperature variations are unlikely to play a role (figs.16-17) (Steffen and Box, 2001). However, with Store's wider ablation area, a higher quantity of surface runoff will be generated overall for lake formation (McMillan *et al.*, 2007); certainly, lakes only make up 0.0035% of Rink's catchment relative to 0.0059% at Store with deeper lakes at Store overall (fig.14). This suggestion is accounted for by the results of Liang *et al.* (2012) in a remote sensing study, revealing greater lake formation with higher overall melt volume in West Greenland.

Surface topography also provides a primary control on lake formation, so steeper topography at Rink relative to Store is therefore likely to impact lake formation and evolution (Echelmeyer *et al.*, 1991); indeed Store has a far greater range of lake sizes, whilst Rink's shallowest lakes are deeper than Store's shallowest lakes, indicating far greater capacity for lake formation across the catchment at Store (fig.13). This suggestion is supported by Howat *et al.* (2013) in a remote sensing study, identifying that lakes on the East coast do not form at progressively higher elevations with increasing elevation of the snow line to the same extent as the West, attributing this to steeper topography in the East providing a lower capacity for lake formation.

Therefore, Store's wider ablation area and lower hypsometry provides a surface for a more progressive and diverse lake system (McMillan *et al.*, 2007). Consequently, these suggestions can explain the peak in lake volumes before the end of the melt season each year at Rink, whereby Rink experiences net lake drainage, rather than formation at progressively higher elevations (Table 2; fig.16 (b)), whilst at Store volumes continually increase and at higher elevations (Table 1; fig.16 (a)). The lack of sensitivity of Rink to increasing runoff between cold and warm years pertaining to its differing geometry to Store therefore demonstrates the key role of glacier shape in determining response to surface runoff increase (Echelmeyer *et al.*, 1991).

The lack of lake evolution at Rink therefore raises the question of what happens to unaccounted for surface runoff. Fitzpatrick *et al.*, (2014) suggest that in a warming climate, rather than lake number and volume increasing in high melt years, drainage event frequency increases instead, intensifying the 'slow fill rapid drain' lake cycle. Therefore, with more melt, lakes fill earlier and drain earlier, at increasingly high elevations throughout the melt season, with lakes at lower elevations usually draining first (McMillan *et al.*, 2007). However, due to the temporal constraints of the data, it is not possible to assess the extent of this intensification. Additionally, another more likely possibility is surface runoff

percolating slowly through cracks in the ice rather than rapid lake drainage (Danielson and Sharp, 2013). However, it is not possible to draw any significant conclusions without higher temporal resolution data.

4.2 Hydrological controls on the flow of marine-terminating outlet glaciers

4.2.1 Hydrology and ice flow at Store

The inter-seasonal trends in velocity change at Store (figs.22 and 24) are suggestive of the 'alpine-style' response with varying basal water pressures (Iken and Bindshadler, 1986; Schoof, 2010), a process recently suggested to explain seasonal velocity trends at marine-terminating outlet glaciers (Moon *et al.*, 2014; Howat *et al.*, 2010). In summer, there is a net decrease in velocity, indicative of a switch from inefficient to efficient basal drainage with increased melt; as meltwater inputs exceed the capacity of the inefficient drainage system, conduit widening occurs via dissipative heating, reducing basal sliding (Bartholomew *et al.*, 2012; Schoof, 2010). This therefore corresponds with the high variability in summer velocity at Store in 2002 and 2005 (Howat *et al.*, 2010).

In contrast, during winter, velocity experiences a net increase (fig.24) occurring most prominently along the main glacier trunk. This observation can also be explained by varying basal water pressures, with a resultant transition to inefficient drainage at the end of the melt season once meltwater availability wains, lowering the capacity of the drainage system and producing an inefficient distributed system (Schoof, 2010; Bartholomew *et al.*, 2011). Indeed, the patches of velocity increase may relate to a switch to inefficient drainage here after drainage either by lake drainage or surface runoff (Bartholomew *et al.*, 2011).

Therefore, both the summer and winter trends represent analogous evidence for the 'alpine-style' response previously identified at land-terminating portions of the GrIS (e.g. van de Wal *et al.*, 2008), and increasingly at marine-terminating portions (e.g. Moon *et al.*, 2014; Sundal *et al.*, 2013). The same trends are also apparent from figure 27 (Ahlstrøm *et al.*, 2013), where extreme velocity variability illustrated by increasing velocity during the winter, followed by higher rates of velocity increase at the onset of the melt season until midsummer when there is a sharp decline in velocity.

Relating areas of velocity decrease to supraglacial lake drainage events, there appears to be a relationship. Velocity is identified to decrease where lake drainage occurs (purple boxes, fig.29), and if this velocity change relates to hydrological processes, it may relate to

subsequent transition to efficient basal drainage (Schoof, 2010) after lake drainage injects a high volume of water to the bed via the mechanisms previously described (Bartholomaeus *et al.*, 2008; Das *et al.*, 2008). Indeed, Csatho *et al.* (2014) suggested that widespread trends in ice thickness observations up-glacier at Store were suspected to relate to hydrological processes occurring over widespread areas, representing a similar pattern to the patchy velocity changes identified. Indeed, with no evidence for velocity change diminishing gradually inland, which is expected when relating velocity changes to terminus position (Thomas, 2004), this provides further evidence for a more widespread process being responsible.

The two drainage events identified to drain on an inter-annual basis exhibit a particularly strong correspondence with velocity change (fig.30), however the type of velocity change varies. Observed net increases in velocity here could be related to processes associated with hydrofracture causing localised velocity increase (Das *et al.*, 2008), which is likely due to both lakes exceeding Krawczynski *et al.*'s (2009) critical lake dimension for hydrofracture (250-500 m across, 2-5 m deep). However due to temporal constraints of the data it is not possible to accurately determine this process; although, a critical volume threshold has yet to be determined (e.g. Danielson and Sharp, 2013), despite the existence of one being suspected (e.g. Banwell *et al.*, 2012).

Regardless of the possible interpretations of figures 27 and 30, drainage of these lakes has previously been identified to correspond to midsummer velocity decline by Howat *et al.* (2010) in 2002 and 2005 (figure 9 in Howat *et al.*, 2010); figure 27 therefore indicates a similar pattern for 2010, 2011, and 2012 as in 2002 and 2005 for the same lakes, identifying the significance of their drainage on Store's flow. Although it is not possible to assess whether this process occurs in other years due to the short observation period, the close correspondence with the data of Howat *et al.* (2010) certainly suggests a likely significant trend. Although only two significant lakes are identified, previous research indicates that there are rarely more than two events distinctly identified to impact summer velocity (Hoffman *et al.*, 2011), therefore providing a realistic case for their drainage having a significant impact on Store's flow.

However, there are also lake drainage events coinciding with regions of velocity increase, most notably in 2011 (green box, fig.29). Cowton *et al.* (2013) suggest that velocity increase can still occur after a transition to efficient drainage if meltwater continually enters the system at high volumes to overcome the capacity of the efficient network, a process

observed at higher elevations at Leverett Glacier, a land-terminating glacier in Southwest Greenland; this may therefore explain the trends observed here. However, this would be restricted towards the end of the melt season, whilst figures 22, 26 and 27 indicate an overall net decrease in velocity throughout the summer.

Alternatively, borehole observations far inland at a land-terminating region in the west, suggest that there may be an inland limit for where efficient drainage is able to develop of (~35 km) (Meierbachtol *et al.*, 2013); indeed, the velocity increases noted at Store in 2011 occur between 30-40 m inland. Therefore, velocities would be expected to continually increase under a constant inefficient subglacial drainage network. Meierbachtol *et al.* (2013) explain this by the shallower slopes further inland reducing hydraulic potential relative to steeper down-glacier regions, preventing conduit widening, demonstrating how glacier shape can impact glacier response (Enderlin *et al.*, 2013).

Regardless of the potential relationships between supraglacial lake drainage and ice flow, there are multiple areas where velocity change does not correspond well with drainage (pink boxes, fig.29). Additionally, drainage volume magnitude does not correlate well with velocity change. Both could be a function of temporal sampling restrictions using Landsat imagery, with lakes possibly forming and draining between image acquisitions, whilst volumes represent minimum estimates (Fitzpatrick *et al.*, 2014). However, a likely possibility is due to influence from daily surface runoff not accounted for. Only a small proportional quantity of surface runoff is stored within supraglacial lakes (Chu, 2013), indicating the potential the vast majority of surface runoff not contained within lakes draining to the bed as well. Although daily surface runoff will not cause the same high magnitude meltwater pulses to the bed as lake drainage events (Das *et al.*, 2008), previous research has found strong relationships between daily surface runoff and ice flow at land-terminating portions of the ice sheet (e.g. Sundal *et al.*, 2011; Sole *et al.*, 2011; Palmer *et al.*, 2011), and more recently at marine-terminating portions (Moon *et al.*, 2014). Indeed, velocity changes associated with drainage are relatively rare overall (Hoffman *et al.*, 2011; van de Wal *et al.*, 2008). Therefore, despite the ability for lake drainage events to transport high volume meltwater pulses to the bed at high rates, surface runoff is likely to account for much of the observed trend.

4.2.2 Hydrology and ice flow at Rink

Rink exhibits an opposite trend to Store, with a net increase in velocity over summer, followed by a net decrease in winter (fig.23, and 25). Consequently, this suggests there is

no switch to efficient drainage in summer, despite lake drainage generating high inputs of meltwater to the bed (Schoof, 2010). Although it is not possible to assess the relationship between lake drainage and velocity change higher up in the catchment due to limited spatial coverage of the MeASURES data, regardless of possible localised effect of drainage higher up in the catchment, this velocity change is clearly not translated to the main glacier trunk, unlike at Store, indicating a different sensitivity to varying basal water pressures.

A noticeable feature at Rink is the annual drainage of water-filled crevasses near the terminus (fig.32). Although they contain relatively small volumes of runoff, these events may occur earlier in the melt season at a particularly inefficient bed causing disproportionate velocity change, similar to observations at Belcher glacier, a marine-terminating outlet glacier in Canada (Danielson and Sharp, 2013). However, although there is possible evidence for velocity change corresponding with their drainage (fig.32), these observations most likely relates to a continuation of velocity decrease at the lateral margins.

Previous research has identified Rink's velocity to coincide more strongly with terminus position ("type 1" in fig.2 (Moon *et al.*, 2014)), with no identified midsummer deceleration in flow (Howat *et al.*, 2010), in a similar manner to Jakobshavn Isbrae (Joughin *et al.*, 2008a, 2008b). However, with supraglacial lakes shown to be actively draining to the bed during each melt season over the observation period (figs.31-32; table 4), additional meltwater should interact with the basal boundary conditions at Rink to some extent (Sundal *et al.*, 2013), with summer velocity increase suggesting increasingly inefficient basal drainage (van der Veen *et al.*, 2011) and no transition to efficient channelisation (Schoof, 2010). With efficient drainage dependent on a steep hydraulic potential, as well as high basal discharge for conduit widening with dissipative heating (Bartholomew *et al.*, 2012; Bartholomew *et al.*, 2008; Schoof, 2010), despite the steeper hypsometry at Rink likely promoting a steeper hydrological potential in favour of conduit widening, it is likely that factors specific to Rink which not in operation at Store may be preventing the development of efficient drainage. Three key factors are highlighted to possibly be causing this effect:

1. Lake drainage volume and rate

Schoof (2010) identify the need for a critical drainage threshold to be reached for efficient drainage development. Indeed, when considering total surface runoff, Palmer *et al.* (2011) identified a strong positive correlation between ice flow change and surface runoff. Whilst

Rink is unlikely to have sufficiently less surface runoff than Store per unit area, the total volume reaching the bed via lake drainage is much lower at Rink relative to Store overall (tables 3 and 4). This is suspected to be a function of Rink experiencing fewer drainage events due to topographic restrictions preventing additional lake formation at higher elevations in warmer years and lower quantities of surface runoff overall despite similar volumes per unit area (Echelmeyer *et al.*, 1991; Arnold *et al.*, 2014), unlike at Store where there is a distinct trend of progressively increasing lake volumes 2009-2010, and 2011-2012 in particular (fig.15). This pertains to Rink's much narrower ablation area and steeper hypsometric profile, providing less potential for wider lake formation (Echelmeyer *et al.*, 1991). Indeed, it has also been suggested that steeper slopes complicate ice flow response to surface melt by adding an additional dynamic to the system (Sundal *et al.*, 2011; Schoof, 2010) suggesting that this may impact the effectiveness of drainage pulses to the bed on influencing Rink's basal drainage.

However, observations at Leverett glacier have revealed the importance of duration and rate of meltwater volume delivery to the subglacial drainage network, rather than simply absolute volume, with the rate of drainage governing ice dynamic response (Bartholomew *et al.*, 2012; McMillan *et al.*, 2007). If meltwater inputs to the bed via lake drainage are sporadic over wide temporal intervals, steady-state water pressure at the bed of a glacier is unlikely to be maintained preventing a transition to efficient drainage (Rothlisberger, 1972). Consequently, drainage rate and duration will be just as crucial as total volume drained, suggesting the observations at Leverett may also apply to marine-terminating outlet glaciers.

The rate of drainage depends on how individual lakes drain (Krawczynski *et al.*, 2009; Hoffman *et al.*, 2011), whether by hydrofracture, whereby drainage occurs over a few hours resulting in rapid high magnitude influxes, or by overspill over the ice surface into nearby moulins and crevasses, occurring over multiple days (Danielson and Sharp, 2013). Although temporal restrictions of the data prevent classification of rapid or slow draining lakes, Krawczynski *et al.* (2009) conclude that only lakes 250-800 m across and 2-5 m deep will contain sufficient water volumes for hydrofracture to the bed at the GrIS; with draining lakes at Rink exceeding these parameters (fig.31; table 2), it is probable that lakes at Rink drain via hydrofracture. Instead, the duration and rate of drainage overall will also be impacted by the number of drainage events, with fewer events likely yielding greater disparity of meltwater pulses. Consequently, with fewer lakes draining at Rink

overall, consistently high volumes generated at the bed is unlikely to be maintained, thus preventing a transition to efficient drainage (Schoof, 2010; Bartholomew *et al.*, 2011).

2. Ice thickness

With the greater ice-overburden pressure introduced by thicker ice, it is thought that thicker ice promotes conduit closure indicating higher rates of creep closure than conduit-wall melting (fig.1), preventing a switch to efficient drainage (Hoffman *et al.*, 2011; Schoof, 2010; Bartholomew *et al.*, 2011). Additionally, it is also possible that with thicker ice, water draining from the surface may freeze at intermediate depths, particularly with insufficient crevasse propagation, preventing full drainage to the bed (McGrath *et al.*, 2011). These factors may therefore impact the effectiveness of lake drainage melt fluxes on influencing ice flow (Sundal *et al.*, 2013).

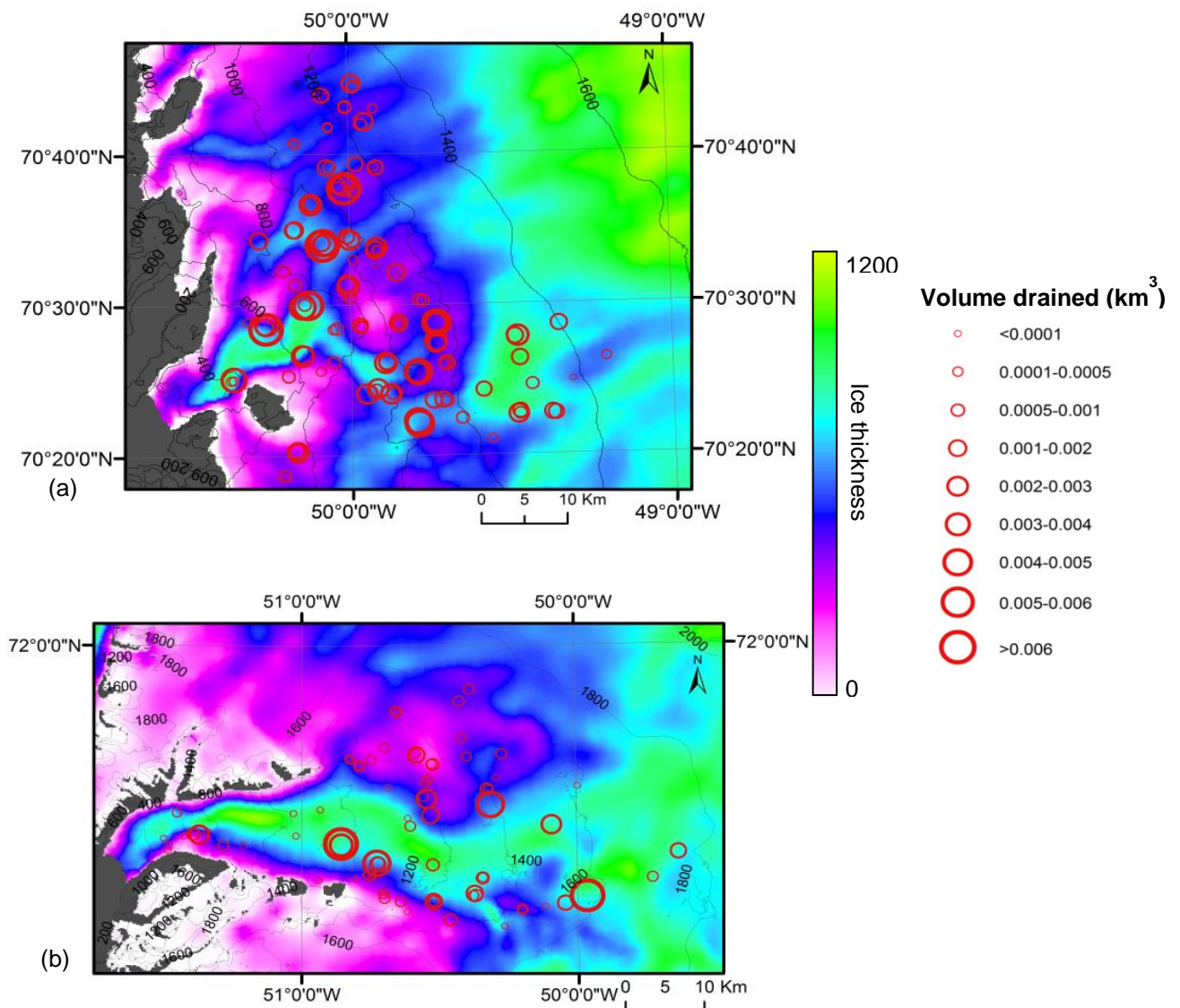


Figure 33: Supraglacial lake drainage events at Store (a) and Rink (b) as graduated symbols (red circles) according to drainage volume as can be ascertained from available Landsat imagery throughout the observation period as compared to changes in ice thickness (m). Pink and white regions indicate low ice thickness, whilst green indicates high ice thickness (m). Ice thickness data are from IceBridge Bedmachine version 2 (2015) downloaded at <http://nsidc.org/data/docs/daac/icebridge/idbmq4/index.html> courtesy of Morlighem *et al.* (2014).

Analysis of the relationship between lake drainage with ice thickness is presented in figure 33, figure 34 and table 5. In figure 33, the ice at Rink is generally much thicker across the catchment. Relating ice thickness to supraglacial lake drainage (fig.33-34), all drainage events $>0.003 \text{ km}^3$ at Rink drain in locations where ice is thicker than 800 m. However, for drainage volumes at Store, these lakes drain at much thinner ice overall ($\sim 500 \text{ m}$) with a greater spread of high magnitude drainage events at thinner ice. Indeed, Rink's largest drainage event (0.011 km^3 in 2009) (fig.19), drains through ice $>1180 \text{ m}$ thick, potentially impacting the influence of this high magnitude drainage event on the basal drainage network.

Store			Rink		
Minimum (m)	Maximum (m)	Mean (m)	Minimum (m)	Maximum (m)	Mean (m)
348	1309	776	300	1313	765

Table 5: Minimum, maximum, and mean ice thickness (m) at centroid the location of drainage events throughout the observation period (figure 33) using ice thickness data from Icebridge BedMachine version 2 (Morlighem *et al.*, (2014)).

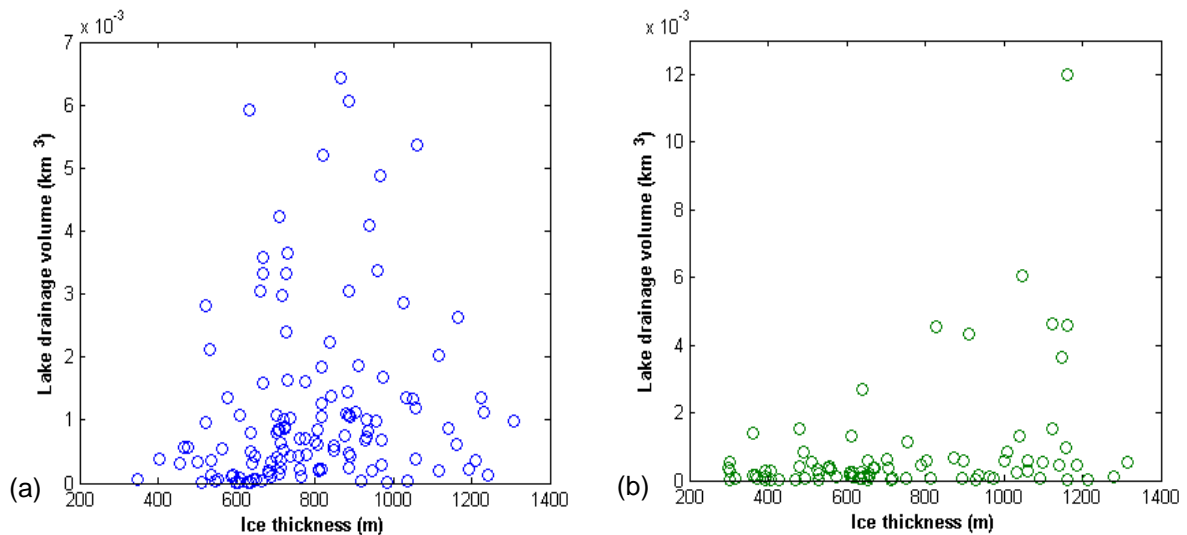


Figure 34: Scatter plots indicating how ice thickness (m) at the centroid locations of supraglacial lake drainage events compares with the volumes of each supraglacial lake drainage event (km^3) for Store (a) and Rink (b) over the observation period. Ice thickness data from Icebridge BedMachine version 2 (Morlighem *et al.*, (2014)) is used.

However, table 5 indicates that for all drainage events, the ice tends to be thinner at Rink overall, with lower mean and minimum ice thickness at the locations of drainage events. Nevertheless, with many drainage events occurring along the margins of the main glacier trunk, a possible explanation could be hydrological routing to regions beneath the very thick glacier trunk where thicker ice here is likely to promote greater rates of

overdeepening with flow into a steep fjord (Iken, 1981) thus directing water flow beneath regions of thicker ice, promoting conduit closure.

Regardless of the possible connection between ice thickness and conduit closure (Bartholomew *et al.*, 2011), numerical modelling by Meierbachtol *et al.* (2013) suggests that ice thickness may not be so crucial in determining the evolution of basal drainage. They identified similar rates of conduit widening near the margins and inland, despite thicker ice in the ice sheet interior, suggesting that ice thickness is unlikely to have such an influence basal drainage evolution (Hoffman *et al.*, 2011). Instead, they propose that a stronger influence on efficient drainage production is surface slope gradient influencing the hydraulic gradient, with the ice sheet interior being relatively flat compared to the margins. However, this cannot explain the contrasting responses of Store and Rink, with Store having lower slope gradients relative to Rink with a lower hypsometry, which would suggest that the basal drainage at Store would in fact be more unlikely to switch to efficient channelisation (Schoof, 2010).

3. Basal conditions

A final possibility is the influence of basal conditions on glacier response to varying basal water pressure. Basal conditions readily impact how glaciers flow, for example through impacting the relative contributions of basal sliding (e.g. Kamb, 1987) and subglacial deformation (e.g. Boulton and Hindmarsh, 1987). They have also been identified to impact how glaciers respond to varying basal water pressures (Iken, 1981; Iken and Bindschadler, 1986), prompting the need for suitable conditions at the bed to allow for channelisation to develop. Recent work by Joughin *et al.* (2013) at a land-terminating portion of the GrIS suggests that in order for efficient drainage to develop, bed topography should be well-aligned with ice flow to enhance the hydraulic potential. Consequently, if Rink's bed topography is not well aligned with the direction of ice flow, this may be a cause for limited evidence of a transition to efficient subglacial drainage. However, this research was conducted at a land-terminating portion of the ice sheet far inland, with no similar research conducted at marine-terminating outlet glaciers, and may therefore not be analogous at marine-terminating outlet glaciers. Regardless, with the steep gradient of flow at Rink, it is likely that the bed is well aligned with ice flow, and thus this observation is unlikely to correspond here.

Another possibility is the suggestion of marine-terminating outlet glaciers being less sensitive to variations in basal water pressure due to a continuous supply of water to the

bed with faster ice flow generating efficient drainage before the melt season (Iken, 1981; van der Veen *et al.*, 2011). This occurs due to higher rates of frictional heating at the bed with faster ice flow generating more melt, possibly desensitising marine-terminating outlet glaciers to varying basal water pressures (Joughin *et al.*, 2008a). However, this is unlikely to be a significant influencing factor at Rink due to Store also likely experiencing the same process with similarly high velocities (fig.21).

Therefore, a final possibility is the effect of intense lateral resistive stresses generated by flow through a thin fjord at Rink keeping its bed at melting point all year round and generating a continuous supply of meltwater to the bed (Iken, 1981). Indeed, there is evidence of strong lateral resistive stresses with bands of velocity decrease at the lateral margins of Rink over the summer in figure 23 transitioning to faster flow in the winter once the velocity of the main glacier trunk begins to decrease as glacier flow eases (fig.25), with no evidence of the same process at Store (fig.22). Furthermore, research by van der Veen *et al.* (2011) indicate that a higher ratio of lateral to basal resistive stress near the terminus has a strong impact on how marine-terminating outlet glaciers respond to basal sliding mechanisms based on modelling at Jakobshavn Isbrae by generating higher water content at the glacier bed.

With the interaction of the above processes, the net increase in ice flow observed over summer may be in response to sufficient melt pulses entering an already efficient drainage network, exceeding the capacity of the efficient network to enhance basal sliding, but insufficient volumes for further channel widening (Cowton *et al.*, 2013). However, the chances of these precise conditions occurring each year of the observation period are minimal, suggesting that these suggestions are unlikely to explain the velocity increase in summer (van der Veen *et al.*, 2011). Furthermore, regardless of an efficient bed at the onset of the melt season, the total volume estimated to drain to the bed each year is relatively low suggesting it to be unlikely that the capacity of an efficient drainage system could be exceeded to cause velocity increase.

4.3 Reconciling contrasting flow regimes of Store and Rink

This analysis has revealed contrasting seasonal velocity changes at Store and Rink to varying basal water pressures with supraglacial lake drainage, despite being subject to the same environmental conditions in Uummannaq Bay. Store exhibits a switch to efficient basal drainage in summer coinciding with supraglacial lake drainage and enhanced surface runoff represented by a net decrease in ice velocity, transitioning to inefficient

drainage in winter as drainage wains causing velocity increase (Howat *et al.*, 2010). In contrast, Rink experiences a net increase in velocity over summer thus inferring increasing efficiency throughout the summer despite active supraglacial lake drainage (van der Veen *et al.*, 2011). The cause of Rink's unapparent switch to efficient drainage have been attributed to three possible causes relating to lake drainage magnitude and frequency, ice thickness, and basal conditions. These suggestions therefore indicate how glacier-specific factors can greatly influence the response of marine-terminating outlet glaciers in the same locality to the same mechanism (Meier and Post, 1987; Carr *et al.*, 2013).

All explanatory factors pertain directly to the contrasting shapes of Rink and Store, thus demonstrating how important glacier shape is in determining response to different mechanisms (Enderlin *et al.*, 2013). Rink's steeper hypsometry and narrower fjord, contributing to stronger lateral resistive stresses will possibly generate higher rates of meltwater production with frictional heating at the bed generating melt all year round (Iken, 1981; van der Veen *et al.* 2011). Variable ice thicknesses are less of a product of hypsometry and geometry, however further indicate how glacier-specific factors may influence the role of enhanced summer meltwater input (Enderlin *et al.*, 2013). However, arguments against both these factors have been presented, due to limited available knowledge of basal conditions at the bed with Store likely exhibiting similar processes, and the unlikely influence of greater ice thicknesses promoting conduit closure with sufficient research suggesting efficient drainage is possible at >1 km thick ice (e.g. Bartholomaeus *et al.*, 2008).

Therefore, the most likely explanation pertains to the volume and rate of drainage at Rink relative to Store with supraglacial lake drainage events over the melt season. Hypsometry and ablation area size have a direct influence on the areal coverage of lakes, and the potential size of each lake basin (Echelmeyer *et al.*, 1991; Arnold *et al.*, 2014). Rink's lake system is less diverse with weaker evolutionary trends, with only half of Store's equivalent proportional areal catchment, suspected to be due to Rink's steeper hypsometry and narrower ablation area. Consequently, Rink experiences a lower number of drainage events, and smaller drainage volumes having a direct impact on the quantity and rate of meltwater pulse intrusion to the bed. This therefore attests to the hypothesis suggesting that *"Due to Store's lower hypsometric profile and wider ablation area, Store develops a more extensive and dynamic supraglacial lake network with a higher volume and frequency of drainage events, increasing Store's sensitivity to varying basal water pressures."*

However, regardless of the possible influence of supraglacial lake drainage in determining marine-terminating outlet glacier response to varying basal water pressures, it is not reasonable to present a thorough conclusion, due to inferring basal conditions based on surface processes alone, whether it be the basal drainage regime (Schoof, 2010), or the rate of meltwater generation with frictional heating (Iken, 1981). Consequently, although the evidence presented possibly corresponds to efficient drainage at Store and inefficient drainage at Rink in summer, it is not possible to draw absolute conclusions due to no direct observation at the bed; indeed, the ‘alpine-style’ response is only an analogue for Greenland based on observations elsewhere (Andersen *et al.*, 2011). However, since previous research has also been restricted to surface observations drawing similar conclusions (e.g. Palmer *et al.*, 2011; Sundal *et al.*, 2011) it is likely that these observations pertain to similar processes.

Despite the possible influence of varying basal water pressures at the bed of Rink, however, past work has suggested that Rink’s velocity is more influenced by terminus position controlled by calving rates (Moon *et al.*, 2014; Howat *et al.*, 2010; Ahlstrøm *et al.*, 2013). This therefore reflects earlier work by Joughin *et al.* (2008a) whereby a survey of glaciers on the western flank of the ice sheet revealed minimal influence of basal sliding on velocity change with a stronger influence of terminus position with reduced backstress (Howat *et al.*, 2007), with similar observations at Jakobshavn Isbrae despite evidence of drainage (Sundal *et al.*, 2013; Joughin *et al.*, 2008b; van der Veen *et al.*, 2011). Indeed, recent work at Store has also demonstrated a strong influence of terminus position on flow, controlled by the seasonal cycle of the sea ice melange (Todd and Christoffersen, 2014), and much of the long term trends in ice flow observed at marine-terminating outlet glaciers correlating with terminus position (Rignot and Kanagaratnam, 2006). Therefore, regardless of the possible influence of supraglacial lake drainage on ice flow at either glacier, other factors will also operate to influence ice flow at different timescales, pertaining to the highly dynamic system of marine-terminating outlet glacier stability (Meier and Post, 1987).

5.0 Study limitations

5.1 Theoretical

Previous work has mostly considered the daily input of surface runoff to the bed in relation to ice flow, identifying significant relationships between surface runoff and velocity (e.g. Zwally *et al.*, 2002; Palmer *et al.*, 2011; Moon *et al.*, 2014; Sundal *et al.*, 2011; van de Wal

et al., 2008; Shepherd *et al.*, 2009). Therefore, with supraglacial lakes only containing a very small proportion of total surface runoff (Chu, 2013), lake drainage will account for minimal possible influence of surface runoff, excluding surface runoff percolating to the bed through cracks and moulins. However, the choice in this study to only focus on volumes of supraglacial lakes at both glaciers, rather than total surface runoff, is justified by supraglacial lake drainage providing the main mechanism for transporting high volumes of melt to the bed quickly (Das *et al.*, 2008), and thus likely having a strong relationship to ice flow (e.g. Hoffman *et al.*, 2011).

Furthermore, as already discussed, observation of surface processes alone is unlikely to yield clear representations of basal drainage. However, this is an inherent limitation of understanding such a transient process at the base of ~1 km thick ice (Schoof, 2010), restricting all observations to surface processes. Indeed, the 'alpine-style' response at the GrIS is only theoretical based on what is observed on the surface (Andersen *et al.*, 2011) with comparisons to alpine glacier processes (Iken and Bindshadler, 1986).

5.2 Methodological

5.2.1 Landsat-7

An overriding problem using Landsat-7 imagery is due to the scan line corrector failure in 2003 generating scan lines masking 22% of each acquisition. Consequently, even with effective interpolation methods (fig.6), lakes obscured by scan lines will be excluded from the results.

Landsat-7 also presents temporal restrictions when observing trends due to suitable acquisitions acquired at multi-week intervals, thus not accounting for the average 10-day life cycle of lakes (McMillan *et al.*, 2007). Furthermore, due to the method requiring suitable images for analysis, many images had to be rejected due to extensive cloud cover, impacting Rink in 2011 in particular. Consequently, observed lakes will not necessarily represent their maximum extents, thus all analysis represents minimum values. Additionally, lakes forming and draining between image acquisitions will not be accounted for. It is also not possible to ascertain the rates of lake drainage (e.g. Fitzpatrick *et al.*, 2014), which may have had an impact on the ice dynamic response to drainage (Danielson and Sharp, 2013; Poinar *et al.*, 2015).

Previous studies have overcome these problems using higher temporal resolution MODIS imagery whereby images are acquired at daily intervals allowing for more robust analysis

of lake evolution (e.g. Fitzpatrick *et al.*, 2014; Howat *et al.*, 2013; Liang *et al.*, 2012). However, Landsat-7 provides the advantage of higher spatial resolution allowing for more detailed analysis of lake morphology and extent (e.g. Banwell *et al.*, 2014; Arnold *et al.*, 2014). Landsat-7 has a spatial resolution of 30m allowing for lakes $>0.0009 \text{ km}^2$ to be captured. However, for MODIS imagery, the highest spatial resolution is 250m pixels only allowing for lakes $>0.0625 \text{ km}^2$ to be captured.

An additional temporal limitation relates to the short observation period (4 years), whereby observed trends will not necessarily pertain to longer term trends. However, with similar observations made in other studies over longer time periods (e.g. Howat *et al.*, 2013; Fitzpatrick *et al.*, 2014), it is reasonable to suggest they are significant and pertain to the same processes.

5.2.2 Lake detection algorithm

Classification of water-filled pixels depends directly on the reflectance ratio threshold chosen for each image. Selecting this value based on manual inspection with Landsat imagery therefore introduces a high level of subjectivity, impacting lake extent and number (Box and Ski, 2007); indeed figures 11 (c) and 12 (d) demonstrate how the choice of threshold impacts shallower areas for more accurate data across the catchment overall. Fortunately, the reflectance ratio threshold has a negligible impact on lake volume estimates, with only the shallowest pixels affected, having minimal impact on this study (Arnold *et al.*, 2014).

An additional source of misclassification is the influence of cloud cover and cloud shadows; if they have spectrally similar reflectance to that chosen for water-filled pixels, they will be incorrectly classified as lakes (Box and Ski, 2007; Fitzpatrick *et al.*, 2014). This is particularly evident for 15th August 2010 at Store, with 83 misclassified lakes due to cloud cover (table 1). Fortunately, this problem is resolved by comparing the output to original Landsat image and masking these areas from analysis in the lake detection algorithm.

In terms of lake depth estimation, the most significant limitation is the assumption of a homogenous bottom substrate (A_d) at each lake (Tedesco and Steiner, 2011), although it is an improvement on the original method whereby only one value for A_d was selected for each image (Banwell *et al.*, 2014; Sneed and Hamilton, 2007). Additional limitations include assumptions whereby inelastic scattering, and suspended and dissolved organic

and inorganic materials have a negligible impact on depth reflectance estimates, whilst lake surfaces are assumed to be flat with no disturbance from wind with surface waves (Sneed and Hamilton, 2007).

Floating ice at some lakes also presents an additional source of error. The presence of floating ice masks water-filled regions during image acquisitions, resulting in minimum estimates for lake volume and extent when ran through the lake detection algorithm (Fitzpatrick *et al.*, 2014; Banwell *et al.*, 2014). However, with this being an inherent limitation of remote-sensing approaches, the lake detection algorithm cannot effectively correct for this, aside from masking these areas as 'no data' values to avoid negative lake depths (Banwell *et al.*, 2014).

5.2.3 Hydrological catchment delineation

Three main limitations arise for the methods used to delineate the hydrological catchments at Store and Rink. Firstly, an inherent limitation is the possible unaccounted for influence of water piracy, whereby continuous ice deformation and bed modification will alter subglacial hydrological routing (van As *et al.*, 2012). Secondly, due to the surface DEM being at a higher resolution (90 m) than the bed DEM, it had to be resampled to match the spatial resolution of the bed DEM (150 m), possibly impacting the accuracy of the resultant hydraulic potential surface generated. However despite the lower resolution bed DEM, the Icebridge Bedmachine dataset represents the most recent and accurate bed data available for this portion of the GrIS (Morlighem *et al.*, 2014). Finally, the tools used in ArcGIS to generate the hydrological catchment have been criticised as being inaccurate over smooth surfaces such as ice, with infilled lakes also giving the impression of a flat surface (van As *et al.*, 2012), potentially impacting the accuracy of the output. However, due to both catchments taking account of the majority of the nearby lakes at each glacier, it is unlikely that the resultant output has a significant impact on the reliability of the data.

5.3 Velocity data

5.3.1 Temporal resolution

The most significant limitation of the MeASUREs data is temporal coverage, with few and irregular acquisitions. This problem arises due to limited suitable SAR image acquisitions, with images only acquired at 11 day intervals via TerraSAR-X. Therefore, the use of this data to observe temporal trends is limited (e.g. Sundal *et al.*, 2013), restricting the capability of assessing how supraglacial lake volume changes relate to velocity change.

Attempts have been made to overcome this via continuous *in situ* GPS velocity measurements at marine-terminating outlet glaciers (Ahlstrøm *et al.*, 2013; figs.27-28). However, despite containing a significant number of data points, this data is unsuitable for statistical analysis due to severe advection effects of the GPS receiver moving into faster regions of ice flow, particularly at Rink (Ahlstrøm *et al.*, 2013).

5.3.2 Spatial coverage

Although the 100 m spatial resolution of MeASUREs is sufficient, the spatial coverage of each selected glacier site restricts observations at elevations $\sim >1000$ m. This therefore impacts the extent to whether comparisons can be made between occurrences of lake drainage events to velocity change through space. Although the ice sheet wide velocity map would have provided the necessary coverage at these elevations (Joughin *et al.*, 2011), unfortunately this dataset only covers winter 2000-2009, thus excluding summer velocity change in relation to drainage. Indeed, this data is also at insufficient spatial resolution (500 m). Spatial coverage is also affected by gaps within the data, caused by insufficient data for velocity estimation, despite speckle-tracking (Joughin *et al.*, 2011; Joughin *et al.*, 2002).

The limitations arising from the available velocity data therefore demonstrates a significant need for greater InSAR data availability at more regular and frequent intervals throughout the year for more effective comparison between velocity and other processes, with InSAR being readily identified as having a particularly great impact in glaciological studies (Nathan-King, *unpublished*).

6.0 Conclusion

This study used remote sensing to assess the relationships between supraglacial lake volumes and ice flow at two marine-terminating outlet glaciers in west Greenland, Store and Rink, revealing relationships with wider implications for the stability of the GrIS. Regardless of the temporal constraints of Landsat-7 imagery, this is also the first comprehensive study of the lake systems at these glaciers, quantifying the evolution and drainage of lakes at both glacier catchments over the observation period 2009-2012, thus introducing a new set of data to be used in the realm of glaciological research in Greenland.

Previous studies have touched upon the asynchronous trends observed at neighbouring marine-terminating outlet glaciers, despite similar environmental controls, identifying the

likely importance of glacier-specific factors in controlling how glaciers respond to certain mechanisms. Therefore, Store and Rink were chosen due to previous work demonstrating their contrasting flow regimes despite both terminating into the same fjord. Most significantly, there has been little previous research on the response of marine-terminating outlet glaciers to hydrological mechanisms with surface runoff and supraglacial lake drainage due to most focus on the control of terminus position in modulating ice flow. However, more recent studies reveal a greater influence of hydrological mechanisms than previously thought (e.g. Moon *et al.*, 2014). Therefore, this study explained these differences in terms of the lake systems at Store and Rink, with the wider ablation area and lower hypsometry at Store pertaining to a more expansive and active lake drainage system than Rink.

Indeed, one of the most prominent conclusions to be drawn from this study is the contrasting supraglacial lake systems observed at Store and Rink over the observation period. Store develops a more expansive network of lakes with a greater range of volumes and morphologies compared to Rink, with greater areal coverage and higher volumes overall. Furthermore, drainage events at Store are on the whole much greater in number and volume than at Rink, suggesting that Store responds more readily to increasing air temperatures and surface runoff despite being subject to similar environmental controls. This contrast can therefore be explained in terms of the different geometries of Store and Rink, with Store providing a more suitable environment for lake formation due to its shallower hypsometry and wider ablation area, pertaining to the primary controls of surface topography and surface runoff on supraglacial lake evolution.

A second prominent conclusion is the revelation of contrasting velocity changes observed at Store and Rink for the summer and winter periods, with Store exhibiting a response analogous to observations at alpine glaciers and more recently at land-terminating portions of the GrIS. This trend is a switch to efficient drainage in summer followed by inefficient drainage in winter, represented by a net decrease and a net increase in ice velocity respectively. However, Rink exhibits opposite trends with no switch to efficient drainage in summer with a net increase in summer velocity. Consequently, Rink's lack of efficiency has been explained in terms of the less expansive and dynamic supraglacial lake system at Rink relative to Store thus having less of an impact on the subglacial drainage regime. Two additional factors also highlighted as possible explanations are thicker ice at the locations of larger drainage events at Rink, and unsuitable basal conditions with higher rates of perennial meltwater production. However, due to previous work indicating no

significant influence of ice thickness on subglacial drainage (e.g. Meierbachtol *et al.*, 2013), and with no observations of basal conditions at Rink or Store, the hypothesis regarding the evolution of supraglacial lakes at Store and Rink is considered most relevant, representing the most significantly contrasting factor between both glaciers overall pertaining to glacier shape.

If hydrological mechanisms are responsible for the contrasting modes of ice flow at Store and Rink, this identifies a much stronger influence of hydrological mechanisms on marine-terminating outlet glaciers than previously thought. Therefore, the impacts of surface runoff and supraglacial lake drainage should be considered in equal measure with the modulating effects of terminus position, particularly in terms of short term velocity change. However, regardless of the conclusions drawn, Rink's lack of response to hydrological mechanisms has previously been explained in terms of the modulating influence of terminus position suggesting its possible overriding control likely pertaining to glacier-specific factors. Consequently, this research therefore further emphasises the importance of considering the influence of glacier-specific factors when assessing response of different glaciers to the same processes despite flowing under the same environmental conditions, revealing the dynamic nature of marine-terminating outlet glacier flow and stability.

6.1 Future research

The results of this study reveal the potential significance of hydrological mechanisms in modulating ice flow at marine-terminating outlet glaciers, however the evidence is only analogous based on research elsewhere and surface processes, with minimal research on the subglacial conditions at marine-terminating outlet glaciers. This therefore highlights the need to develop knowledge on basal conditions at the GrIS to assess the extent to which alpine processes can be applied to the GrIS. Supraglacial lake remote sensing studies are also impacted by the subjectivity of lake classification, and therefore classification methods need to be improved for more objective results overall and more accurate data. Furthermore, there should be continued focus on improving temporal and spatial coverage of InSAR velocity data, to allow more effective comparisons between ice flow and other processes. Finally, with this study building upon previous observations by Howat *et al.* (2010), the lakes at Store should be continually monitored in relation to ice flow.

Reference list

- Abdalati, W., Steffen, K (2001) Greenland ice sheet melt extent: 1979-1999. *Journal of Geophysical Research*. 106, doi: 10.1029/2001JD900181
- Ahlstrøm, A.P., Andersen, S.B., Andersen, M.L., Machguth, H., Nick, F.M., Joughin, I., Reijmer, C.H., van de Wal, W., Merryman Boncori, J.P., Box, J.E., Citterio, M., van As, D., Fausto, R.S., Hubbard, A. (2013) Seasonal velocities of eight major marine-terminating outlet glaciers of the Greenland ice sheet from continuous in situ GPS instruments. *Earth Systems Science Data*, 5, 277-287.
- Alley, R.B., Dupont, T.K., Parizek, B.R., Anandakrishnan, S (2005) Access of surface meltwater to beds of subfreezing glaciers: preliminary insights. *Annals of Glaciology* 40, p.8-14.
- Amundson, J.M., Fahnestock, M., Truffer, M., Brown, J., Luthi, M.P., Motyka, R.J. (2010) Ice melange dynamics and implications for terminus stability, Jakobshavn Isbrae, Greenland. *Journal of Geophysical Research*. 115, F01005, doi:10.1029/2009JF001405.
- Andersen, M.L., Nettles, M., Elosegui, P., Larsen, T.B., Hamilton, G.S., Stearns, L.A. (2011) Quantitative estimates of velocity sensitivity to surface melt variations at a large Greenland outlet glacier. *Journal of Glaciology*. 57 (204), p.609-620.
- Andersen, M. L., Larsen, T. B., Nettles, M., Elosegui, P., van As, D., Hamilton, G. S., Stearns, L. A., Davis, J. L., Ahlstrøm, A.P., de Juan, J., Ekström, G., Stenseng, L., Khan, S. A., Forsberg, R., and Dahl-Jensen, D. (2010) Spatial and temporal melt variability at Helheim Glacier, East Greenland, and its effect on ice dynamics. *Journal of Geophysical Research*., 115, F04041, doi:10.1029/2010JF001760,
- Arnold, N.S., Banwell, A.F., Willis, I.C (2014) High-resolution modelling of the seasonal evolution of surface water storage on the Greenland Ice Sheet. *The Cryosphere*. 8, 1149-1160.
- Banwell, A.F., Caballero, M., Arnold, N.S., Glasser, N.F., Cathles, L.M., MacAyeal, D.R. (2014) Supraglacial lakes on the Larsen B ice shelf, Antarctica, and at Paakitsoq, West Greenland: a comparative study. *Annals of Glaciology*. 55(66) doi: 10.3189/2014AoG66A049

- Banwell, A.F., Willis, I., Arnold, N. (2013) Modelling subglacial water routing at Paakitsoq, West Greenland. *Journal of Geophysical Research – Earth Surface*. 118, doi:10.1002/jgrf.20093
- Banwell, A.F., Arnold, N.S., Willis, I.C., Tedesco, M., Ahlstrøm, A.P. (2012) Modelling supraglacial water routing and lake filling on the Greenland Ice Sheet. *Journal of Geophysical Research*. 117, F04012, doi:10.1029/2012JF002393
- Bartholomew, T., Anderson, R.S., Anderson, S. (2008) Response of glacier basal motion to transient water storage. *Nature Geoscience*. 1, p.33-37.
- Bartholomew, I., Nienow, P., Sole, A., Mair, D., Cowton, T., King, M (2012) Short-term variability in Greenland Ice Sheet motion forced by time-varying meltwater drainage: Implications for the relationship between subglacial drainage system behaviour and ice velocity, *Journal of Geophysical Research* 117, F03002, doi:10.1029/2011JF002220, 117, F03002, doi:10.1029/2011JF002220.
- Bartholomew, I., Nienow, P., Sole, A., Mair, D., Cowton, T., Palmer, S., Wadham, J. (2011) Supraglacial forcing of subglacial drainage in the ablation zone of the Greenland ice sheet. *Geophysical Research Letters*. 38, L08502, doi:10.1029/2011GL047063
- Bartholomew, I., Nienow, P., Mair, D, Hubbard, A., King, M.A., Sole, A (2010), Seasonal evolution of subglacial drainage and acceleration in a Greenland outlet glacier, *Nature Geoscience*, 3(6), p.408-411.
- Benn, D.I., Warren, C.R., Mottram, R.H. (2007) Calving processes and the dynamics of calving glaciers. *Earth Science Reviews*. 82, p.143-179.
- Braithwaite, R J., Laternser, M., Pfeffer, W.T. (1994) Variations of near-surface firn density in the lower accumulation area of the Greenland ice sheet, Paakitsoq, West Greenland. *Journal of Glaciology* 40 (136), p.477-485.
- Boulton, G.S., Hindmarsh, R.C.A. (1987) Sediment deformation beneath glaciers: rheology and sedimentological consequences. *Journal of Geophysical Research*, 92, p.9059–9082.
- Box, J.E., Ski, K (2007) Remote sounding of Greenland supraglacial melt lakes: implications for subglacial hydraulics. *Journal of Glaciology*. 53(181) p.257-265.

- Carr, R.J., Stokes, C.R., Vieli, A. (2013) Recent progress in understanding marine-terminating Arctic outlet glacier response to climatic and oceanic forcing: Twenty years of rapid change. *Progress in Physical Geography*. DOI: 10.1177/0309133313483163
- Chander, G., Markham, B.L., Helder, D.L (2009) Summary of current radiometric calibration coefficients for Landsat MSS, TM, ETM+, and EO-1 ALI sensor *Remote Sensing Environmen.*,113(5), p.893–903
- Chandler, D.M., Wadham, J.L., Lis, G.P., Cowton, T., Sole, A., Bartholomew, I., Telling, J., Nienow, P., Bagshaw, E.B., Mair, D., Vinen, S., Hubbard, A (2013) Evolution of the subglacial drainage system beneath the Greenland Ice Sheet revealed by tracers. *Nature Geoscience*. 6, p.195-198
- Chauché, N., Hubbard, A., Gascard, J.C., Box, J.E., Bates, R., Koppes, M., Sole, A., Christoffersen, P., Patton, H. (2014) Ice-ocean interaction and calving front morphology at two west Greenland tidewater outlet glaciers. *The Cryosphere*. 8, p.1457-1468.
- Christoffersen, P., Mugford, R.I., Heywood, K.J., Joughin, I., Dowdeswell, J.A., Syvitski, J.P.M., Luckman, A., Benham, T.A. (2011) Warming of waters in an East Greenland fjord prior to glacier retreat: mechanisms and connection to large-scale atmospheric conditions. *The Cryosphere*. 5, p.701-714.
- Chu, V.W. (2013) Greenland ice sheet hydrology: A review. *Progress in Physical Geography* DOI: 10.1177/0309133313507075
- Cowton, T., Nienow, P., Sole, A., Wadham, J., Lis, G., Bartholomew, I., Mair, D., Chandler, D. (2013) Evolution of drainage system morphology at a land-terminating Greenlandic outlet glacier. *Journal of Geophysical Research: Earth Surface*. 118, (1), p.29-41.
- Csatho, B.M., Schenk, A.F., van der Veen, C.J., Babonis, G., Duncan, K., Rezvanbehbahani, S., van den Broeke, M.R., Simonsen, S.B., Nagarajan, S., van Angelen, J.H. (2014) Laser altimetry reveals complex pattern of Greenland Ice Sheet Dynamics. *Proceedings of the National Academy of Sciences*. 111 (52), 18478=18483.

- Cuffey, K.M., Paterson, W.S.B. (2010) *The Physics of Glaciers*. 4th Edition, Academic Press, Amsterdam.
- Danielson, B., Sharp, M. (2013) Development and application of a time-lapse photograph analysis method to investigate the link between tidewater glacier flow variations and supraglacial lake drainage events. *Journal of Glaciology*. 59 (214), p.287-302.
- Das, S.B., Joughin, I., Behn, M.D., Howat, I.M., King, M.A., Lizarralde, D., Bhatia, M.P. (2008) Fracture propagation to the base of the Greenland ice sheet during supraglacial lake drainage. *Science*. 320 (5877), p778-781.
- Doyle, S.H., Hubbard, A.L., Dow, C.F., Jones, G.A., Fitzpatrick, A., Gusmeroli, A., Kulesa, B., Lindback, K., Pettersson, R., Box, J.E. (2013) Ice tectonic deformation during the rapid in situ drainage of a supraglacial lake on the Greenland ice sheet. *The Cryosphere*. 7, p.129-140.
- Echelmeyer, K., Clarke, T.S., Harrison, W.D. (1991), Surficial glaciology of Jakobshavn Isbræ, West Greenland: Part 1. Surface morphology, *Journal of Glaciology*, 37(127), p.368–382
- Echelmeyer, K., Harrison, W.D. (1990) Jakobshavns Isbræ, West Greenland: seasonal variations in velocity – or lack thereof. *Journal of Glaciology*, 36(122), p.82–88.
- Enderlin, E.M., Howat, I.M., Vieli, A. (2013) High sensitivity of tidewater outlet glacier dynamics to shape. *The Cryosphere*, 7, p.1007-1015.
- Ettema, J., vanden Broeke, M.R., van Meijgaard, E., van de Berg, W.J., Bamber, J.L., Box, J.E., Bales, R.C. (2009) Higher surface mass balance of the Greenland ice sheet revealed by the high-resolution climate modelling. *Geophysical Research Letters* 36, L12501, p.1-5.
- Fitzpatrick, A.A.W., Hubbard, A.L., Box, J.E., Quincey, D.J., van As, D., Mikkelsen, A.P.B., Doyle, S.H., Dow, C.F., Hasholt, B., Jones, G.A. (2014) A decade (2002-2012) of supraglacial lake volume estimates across Russell Glacier, West Greenland. *The Cryosphere*. 8, p.107-121.
- Hanna, E., Fettweis, X., Mernild, S. H., Cappelen, J., Ribergaard, M. H., Shuman, C. A., Steffen, K., Wood, L., Mote, T. L. (2014), Atmospheric and oceanic climate forcing of

the exceptional Greenland ice sheet surface melt in summer 2012. *International Journal of Climatology*, 34 p.1022–1037.

Hoffman, M.J., Catania, G.A., Neumann, T.A., Andrews, L.C., Rumrill, J.A. (2011) Links between acceleration, melting, and supraglacial lake drainage of the western Greenland Ice Sheet. *Journal of Geophysical Research*. 116, F04035, doi:10.1029/2010JF001934

Holland, D.M., Thomas, R.H, De Young, B, Ribergaard, M.H., Lyberth, B. (2008) Acceleration of Jakobshavn Isbrae triggered by warm subsurface ocean waters. *Nature Geoscience*. 1, p.659-654.

Howat, I.M., Negrete, A., Smith, B.E. (2014), The Greenland Ice Mapping Project (GIMP) land classification and surface elevation datasets, *The Cryosphere*, 8, p.1509-1518, doi:10.5194/tc-8-1509-2014

Howat, I., de la Pena, S., van Angelen, J.H., Lenaerts, J.T.M., van den Broeke, M.R. (2013) Brief Communication: Expansion of meltwater lakes on the Greenland ice sheet. *The Cryosphere*. 7, p.201-204.

Howat, I.M., Box, J.E., Ahn, Y., Herrington, A., McFadden, E.M. (2010) Seasonal variability in the dynamics of marine-terminating outlet glaciers in Greenland. *Journal of Glaciology*. 56(198), p.601-613.

Howat, I.M., Joughin, I., Scambos, T.A. (2007) Rapid changes in ice discharge from Greenland outlet glaciers. *Science*, 315, p.1559-1561.

Iken, A. (1981) The effect of the subglacial water pressure on the sliding velocity of a glacier in an idealized numerical model. *Journal of Glaciology* 27(97), p.407–421.

Iken, A., Bindschadler, R.A. (1986) Combined measurements of subglacial water pressure and surface velocity of Findelengletscher, Switzerland: conclusions about drainage system and sliding mechanism. *Journal of Glaciology* 32(110), p.101–119

Iken, A., Rothlisberger, H., Flotron, Haeberli, W. (1983) The uplift of Unteraargletscher at the beginning of the melt season – a consequence of water storage at the bed? *Journal of Glaciology*. 29(101), p.28–47

Ingle, J.D., Crouch, S.R., (1988) Spectrochemical measurements. In: *Ingle JD and Crouch SR eds. Spectrochemical analysis*. Prentice Hall, Upper Saddle River, NJ.

- IPCC, 2013: Summary for Policymakers. In: Climate Change 2013: The Physical Science Basis. Contribution of Working Group I to the Fifth Assessment Report of the Intergovernmental Panel on Climate Change [Stocker, T.F., D. Qin, G.-K. Plattner, M. Tignor, S.K. Allen, J. Boschung, A. Nauels, Y. Xia, V. Bex and P.M. Midgley (eds.)] Cambridge University Press, Cambridge, United Kingdom and New York, NY, USA.
- Jenkins, A. (2011) Convection-driven melting near the grounding lines of ice shelves and tidewater glaciers. *Journal of Physical geography*. 41, p.2279-2294
- Joughin, I., Smith, B.E., Shean, D.E., Floricioiu, D. (2014) Brief communication: further summer speedup of Jakobshavn Isbrae. *The Cryosphere*. 8, p.209-214.
- Joughin, I., Das, S.B., Flowers, G.E., Behn, M.D., Alley, R.B., King, M.A., Smith, B.E., Bamber, J.L., vanden Broeke, M.R., van Angelen, J.H. (2013) Influence of ice-sheet geometry and supraglacial lakes on seasonal ice flow variability. *The Cryosphere*. 7, p. 1185-1192.
- Joughin, I., I. Howat, B. Smith, T., Scambos (2011) MEaSUREs Greenland Ice Velocity: Selected Glacier Site Velocity Maps from InSAR. Boulder, Colorado, USA: NASA DAAC at the National Snow and Ice Data Center. doi:10.5067/MEASURES/CRYOSPHERE/nsidc-0481.001
- Joughin, I. (2002) Ice-sheet velocity mapping: a combined interferometric and speckle-tracking approach. *Annals of Glaciology*. 34, p.195-201
- Joughin, I., Smith, B.E., Howat, I.M., Scambos, T., Moon, T. (2010) Greenland flow variability from ice-sheet-wide velocity mapping. *Journal of Glaciology*. 56, p.415-430.
- Joughin, I., Das, S.B., King, M.A., Smith, B.E., Howat, I.M., Moon, T. (2008a) Seasonal speedup along the western flank of the Greenland Ice Sheet. *Science*. 320, p.781-783.
- Joughin, I., Howat, I.M., Fahnestock, M., Smith, B., Krabill, W., Alley, R.B., Stern, H., Truffer, M. (2008b) Continued evolution of Jakobshavn Isbrae following its rapid speed up. *Journal of Geophysical Research*. 113, F04006, doi:10.1029/2008JF001023

- Joughin, I., Abdalati, W., Fahnestock, M. (2004) Large fluctuations in speed on Greenland's Jakobshavn Isbrae glacier. *Nature*. 432, p.608-610.
- Joughin, I., Tulaczyk, S., Fahnestock, M., Kwok, R. (1996) A mini-surge on the Ryder glacier, Greenland, observed by satellite radar interferometry. *Science*, 274, 5285, p.228-230
- Kamb, B. (1987) Glacier surge mechanism based on linked cavity configuration of the basal water conduit system. *Journal of Geophysical Research: Solid Earth*. 92, B9, p.9083-9100.
- Krawczynski, M.J., Behn, M.D., Das, S.B., Joughin, I. (2009) Constraints on the lake volume required for hydrofracture through ice sheets. *Geophysical Research Letters*. 36, L10501, doi:10.1029/2008GL036765.
- Leeson, A.A., Shepherd, A., Briggs, K., Howat, I., Fettweis, X., Morlighem, M., Rignot, E. (2014) Supraglacial lakes on the Greenland ice sheet advance inland under warming climate. *Nature Climate Change*. 5, p.51-55.
- Liang, Y.L., Colgan, W., Lv, Q., Steffen, K., Abdalati, W., Stroeve, J., Gallaher, D., Bayou, N. (2012) A decadal investigation of supraglacial lakes in West Greenland using a fully automatic detection and tracking algorithm. *Remote Sensing of Environment*. 123 (2012), 127-138.
- Lüthje, M., Pedersen, L.T., Reeh, N., Greuell, W. (2006) Modelling the evolution of supraglacial lakes on the West Greenland ice sheet margin. *Journal of Glaciology*. 52 (179), p.608-611.
- McGrath, D., Colgan, W., Steffen, K., Lauffenburger, P., Balog, J (2011) Assessing the summer water budget of a moulin basin in the Sermeq Avannarleq ablation region, Greenland Ice Sheet, *Journal of Glaciology* 57, p.954–964
- McMillan, M., Nienow, P., Shepherd, A., Benham, T., Sole, A. (2007) Seasonal evolution of supraglacial lakes on the Greenland ice sheet. *Earth and Planetary Science Letters*. 262 (2007), p.484-492.
- Meier, M.F., Post, A. (1987) Fast tidewater glaciers. *Journal of Geophysical Research*. 92(B9), p.9051-9058.

- Meierbachtol, T., Harper, J., Humphrey, N. (2013) Basal drainage system response to increasing surface melt on the Greenland Ice Sheet. *Science*. 341, p.777-779.
- Mobley, C.D. (1994) Light and water: radiative transfer in natural waters. Academic Press, San Diego.
- Moon, T., Joughin, I., Smith, B., van den Broeke, M.R., van de Berg, W.J., Noel, B., Usher, M. (2014) Distinct patterns of seasonal Greenland glacier velocity. *Geophysical Research Letters*. 41, p.7209-7216.
- Moon, T., Joughin, I. (2008) Changes in ice front position on Greenland's outlet glaciers from 1992-2007. *Journal of Geophysical Research*. 113, F02022, doi:10.1029/2007JF000927
- Morlighem, M., Rignot, E., Mouginot, J., Seroussi, H., Larour, E. (2014) Deeply incised submarine glacial valleys beneath the Greenland ice sheet. *Nature Geoscience*. 7, p.418-422
- Motyka, R.J., Truffer, M., Fahnestock, M., Mortensen, J., Rysgaard, S., Howat, I. (2011) Submarine melting of the 1985 Jakobshavn Isbrae floating tongue and the triggering of the current retreat. *Journal of Geophysical Research*. 116, F01007, doi:10.1029/2009JF001632
- Nathan-King, H. (2014, *unpublished*) Using examples, discuss the applications of imaging radar in polar environments, *MPhil Essay, Unpublished*.
- Nick, F.M., Vieli, A., Howat, I.M., Joughin, I. (2009) Large-scale changes in Greenland outlet glacier dynamics triggered at the terminus. *Nature Geoscience*. 2,p.110-114.
- O'Leary, M., Christoffersen, P. (2013) Calving on tidewater glaciers amplified by submarine frontal melting. *The Cryosphere*. 7, p.119-128.
- Palmer, S., Shepherd, A., Nienow, P., Joughin, I. (2011) Seasonal speedup o the Greenland ice sheet linked to routing of surface water. *Earth and Planetary Science Letters*. 302 (2011), p.423-428.
- Parizek, B.R., Alley, R.B. (2004) Implications of increased Greenland surface melt under global warming scenarios: ice sheet simulations. *Quaternary Science Reviews*. 29(2004), p.1013-1027.

- Pfeffer, W.T. (2007) A simple mechanism for irreversible tidewater glacier retreat. *Journal of Geophysical Research*. 112, F03S25, doi:10.1029/2006JF000590
- Philpot, W.D. (1989) Bathymetric mapping with passive multispectral imagery. *Applied Optics* 28(8), p.1569–1578
- Poinar, K., Joughin, I., Das, S.B., Behn, M.D., Lenaerts, J.T.M., van den Broeke, M.R. (2015) Limits to future expansion of surface-melt enhanced ice flow into the interior of western Greenland. *Geophysical Research Letters*. 42, doi:10.1002/2015GL063192.
- Rees, W.G. (2013) *Physical Principles of Remote Sensing*. 3rd Edition. New York, USA, Cambridge University Press.
- Rignot, E., Velicogna, I., van den Broeke, M.R., Monaghan, A., Lenaerts, J.T.M. (2011) Acceleration of the contribution of the Greenland and Antarctic ice sheets to sea level rise. *The Cryosphere*. 38, L05503, doi:10.1029/2011GL046583.
- Rignot, E., Box, J.E., Burgess, E., Hanna, E. (2008) Mass balance of the Greenland ice sheet from 1958-2007. *Geophysical Research Letters*. 35(20) L20502, doi:10.1029/2008GL035417.
- Rignot, E., Kanagaratnam, P. (2006) Changes in the velocity structure of the Greenland ice sheet. *Science*. 311, p.986-990.
- Rothlisberger, H. (1972) Water pressure in intra- and subglacial channels. *Journal of Glaciology*. 11(62), p.177- 203
- Schild, K.M., Hamilton, G.S. (2013) Seasonal variations of outlet glacier terminus position in Greenland. *Journal of Glaciology*. 59(216), p.759-770.
- Schoof, C. (2010) Ice-sheet acceleration driven by melt supply variability. *Nature*. 468, p.803-806.
- Seale, A., Christoffersen, P., Mugford, R.I., O’Leary, M. (2011) Ocean forcing of the Greenland ice sheet: Calving fronts and patterns of retreat identified by automatic satellite monitoring of eastern outlet glaciers. *Journal of Geophysical Research*. F03013, doi:10.1029/2010JF001847
- Shepherd, A., Hubbard, A., Nienow, P., King, M., McMillan, M., Joughin, I. (2009) Greenland ice sheet motion coupled with daily melting in late summer. *Geophysical Research Letters*. 36, L01501, doi:10.1029/2008GL035758

- Shreve, R.L., (1985) Esker Characteristics in terms of glacier physics, Katahdin esker system, Maine. *Geological Society of America Bulletin*, 96, p.639–646, doi: 10.1130/0016-7606(1985)96<639:ECITOG>2.0.CO;2.
- Sneed, W.A., Hamilton, G.S. (2011) Validation of a method for determining the depth of glacial melt ponds using satellite imagery. *Annals of Glaciology*. 52(59), p.15-22.
- Sneed, W.A., Hamilton, G.S. (2007) Evolution of melt pond volume on the surface of the Greenland Ice Sheet. *Geophysical Research Letters*. 34, L03501, doi:10.1029/2006GL028697
- Sole, A.J., Mair, D.W.F., Nienow, P.W., Bartholomew, I.D., King, M.A., Burke, M.J., Joughin, I. (2011) Seasonal speedup of a Greenland marine-terminating outlet glacier forced by surface melt-induced changes in subglacial hydrology. *Journal of Geophysical Research*. 116, F03014, doi:10.1029/2010JF001948
- Steffen, K., Box, J.S. (2001) Sublimation on the Greenland ice sheet from automated weather station observations. *Journal of Geophysical Research*. 106, D24, p.33965-33981.
- Straneo, F., Hamilton, G.S., Sutherland, D.A., Stearns, L.A., Davidson, F., Hammill, M.O., Stenson, G.B., Rosing-Asvid, A. (2010) Rapid circulation of warm subtropical waters in a major glacial fjord in East Greenland. *Nature Geoscience*. 3, p.182-186.
- Sundal, A.V., Shepherd, A., van den Broeke, M., van Angelen, J., Gourmelen, N., Park, J. (2013) Controls on short term variations in Greenland glacier dynamics. *Journal of Glaciology*. 59(217), p.883-892.
- Sundal, A.V., Shepherd, A., Nienow, P., Hanna, E., Palmer, S., Huybrechts, P. (2011) Melt-induced speed-up of Greenland ice sheet offset by efficient subglacial drainage. *Nature*. 469, p.521-524.
- Sundal, A.V., Shepherd, A., Nienow, P., Hanna, E., Palmer, S., Huybrechts, P. (2009) Evolution of supraglacial lakes across the Greenland ice sheet. *Remote Sensing of Environment*. 113(2009), 2164-2171.
- Tedesco, M., Steiner, N. (2011) In situ multispectral and bathymetric measurements over a supraglacial lake in western Greenland using a remotely controlled watercraft. *The Cryosphere*, 5, p.445-452.

- Thomas, R. H. (2004), Force-perturbation analysis of recent thinning and acceleration of Jakobshavn Isbrae, Greenland. *Journal of Glaciology*, 50, p.57-66.
- Todd, J., Christoffersen, P. (2014) Are seasonal calving dynamics forced by buttressing from ice melange or undercutting by melting? Outcomes from full-Stokes simulations of Store Gletscher, West Greenland. *The Cryosphere*. 8, p.3525-3561.
- United States Geological Survey (USGS) website (2013) SLC-off Products: Background. http://landsat.usgs.gov/products_slc_off_background.php Accessed: February 2014
- van As, D., Hubbard, A.L., Hasholt, B., Mikkelsen, A.B., van den Broeke, M.R., Fausto, R.S. (2012) Large surface meltwater discharge from the Kangerlussuaq sector of the Greenland ice sheet during the record-warm year 2010 explained by detailed energy balance observations. *The Cryosphere*. 6, p.199-209.
- Van de Wal, R.S.W., Boot, W., van den Broeke, M.R., Smeets, C.J.P.P., Reijmer, C.H., Donker, J.J.A., Oerlemans, J. (2008) Large and rapid melt-induced velocity changes in the ablation zone of the Greenland ice sheet. *Science*. 321, p.111-113.
- Van der Veen, C.J. (2007) Fracture propagation as means of rapidly transferring surface meltwater to the base of glaciers. *Geophysical Research Letters*. 34 (1), 10.1029/2006GL028385
- Van der Veen, C.J., Plummer, J.C., Stearns, L.A. (2011) Controls on the recent speed-up of Jakobshavn Isbrae, West Greenland. *Journal of Glaciology*. 57 (204), p. 770-782
- Vaughan, D.G., et al., (2013) *Observations: Cryosphere. Climate Change 2013: The Physical Science Basis*. Contribution of Working Group I to the Fifth Assessment Report of the Intergovernmental Panel on Climate Change. Cambridge University Press, Cambridge UK. 317–382.
- Vieli, A., Nick, F.M. (2011) Understanding and modelling rapid dynamic changes of tidewater outlet glaciers: Issues and implications. *Survey Geophysics*. 32, p.437-458.
- Vieli, A., Jania, J., Blatter, H., Funk, M (2004) Short-term velocity variations on Hansbreen, a tidewater glacier in Spitsbergen. *Journal of Glaciology*. 50(170), p.389-398
- Walter, J.I., Box, J.E., Tulaczyk, S., Brodsky, E.E., Howat, I.M., Ahn, Y., Brown, A. (2012) Oceanic mechanical forcing of a marine-terminating Greenland glacier. *Annals of Glaciology*. 53(60), p.181-192.

- Weertman, J. (1973). Can a water-filled crevasse reach the bottom surface of a glacier? *Union Geodesique et Geophysique Internationale. Association Internationale d'Hydrologie Scientifique. Commission de Neiges et Glaces. Symposium on the Hydrology of Glaciers, Cambridge, 7-13 September 1969*, p. 139-45.
- Weidick, A (1995) The Landsat images of Greenland: Satellite Image Atlas of Glaciers of the World: Greenland, edited by: Williams, R. S. and Ferrigno, J. G., *United States Geological Survey Professional Paper 1386-C, Washington*
- Weidick, A., Bennike, O. (2007) Quaternary glaciation history and glaciology of Jakobshavn Isbrae and the Disko Bugt region, West Greenland: a review. *Geological Survey of Denmark and Greenland Bulletin*. 14.
- Zwally, H.J., Abdalati, W., Herring, T., Larson, K., Saba, J., Steffen, K. (2002) Surface melt-induced acceleration of Greenland ice-sheet flow. *Science*. 297(5579), p.218-222.